Journal of Food Quality

Implications of Drying Techniques on the Bioactive Components and Quality of Food

Lead Guest Editor: R. Pandiselvam
Guest Editors: R. Kaavya and Anjineyulu Kothakota

Implications of Drying Techniques on the Bioactive Components and Quality of Food

Journal of Food Quality

Implications of Drying Techniques on the Bioactive Components and Quality of Food

Lead Guest Editor: R. Pandiselvam
Guest Editors: R. Kaavya and Anjineyulu Kothakota

Chief Editor

Associate Editors

Academic Editors

Contents

Hindawi
Journal of Food Quality
Volume 2023, Article ID 5799365, 13 pages
https://doi.org/10.1155/2023/5799365

Research Article

Mathematical Modelling, Drying Behavior, and Quality Investigation of the Turkey Berry in a Fluidized Bed Dryer

Barathiraja Rajendran,[1] **Ananthakumar Sudalaimani**,[2] **Thiyagaraj Jothi**,[3,4] **Ashokkumar Mohankumar**,[5] **Deepak Sampathkumar**,[6] **Mathanbabu Mariappan**,[5] **and Abdulkhader Mohaideen**[7]

[1]*Department of Mechanical Engineering, Einstein College of Engineering, Tirunelveli 627012, Tamil Nadu, India*
[2]*Department of Mechanical Engineering, Government College of Engineering, Tirunelveli 627007, Tamil Nadu, India*
[3]*Department of Mechatronics Engineering, Er.Perumal Manimekalai College of Engineering, Hosur 635117, Tamil Nadu, India*
[4]*Vellore Institute of Technology, Vellore, Tamilnadu, 632014, India*
[5]*Department of Mechanical Engineering, Government College of Engineering, Bargur, Krishnagiri-635104, Tamil Nadu, India*
[6]*Department of Mechanical and Automation Engineering, Agni College of Technology, Thalambur, Chennai 600 130, Tamil Nadu, India*
[7]*Department of Mechanical Engineering, Mai-Nefhi College of Engineering and Technology, Mai Nefhi, Eritrea*

Correspondence should be addressed to Abdulkhader Mohaideen; mohaideen22@gmail.com

Received 12 December 2022; Revised 29 May 2023; Accepted 12 August 2023; Published 20 September 2023

Academic Editor: Kaavya Rathnakumar

The dehydration behavior of turkey berries was analysed in a fluidized bed dryer at various inlet air velocities (0.8, 2.1, and 3.4 m/s) and temperatures (50, 60, and 70°C). The drying parameters and physiochemical values of fruits were extensively studied, as were the moisture content, rate of drying, moisture diffusivity of the sample, shrinking percentage, color variations, retention of vitamin C, β-carotene, antioxidant capacity, and total phenolic content. The activation energy varies between 36.82 and 45.63 kJ/mol under different bed conditions. According to the experimental results, it has been observed that the maximum moisture diffusion rate was 2.898×10^{-10} m^2/s and maximum retention rates of vitamin C, β-carotene, antioxidant capacity, and total phenolic content were 1.91 mg/100 g d.m, 184 μg/100 g d.m, 21.34 mg AAE/100 g d.m, and 513 mg GAE/100 g, during the drying of the sample at 70°C and 3.4 m/s. The minimum shrinkage (49.1%) and color variation ($\Delta E = 11.08$) were detected at 3.4 m/s and 70°C. The Midilli et al. model was fitted, which is the most preferable model for predicting the dehydration characteristics of turkey berries.

1. Introduction

Turkey berry, *Solanum torvum* (Solanaceae family), is a pharmaceutical plant that can be taken as a fresh or dried form. The vegetables are still used as traditional medicine by people in South India and other Asian countries, particularly in rural areas. This is an essential medicinal plant whose leaves, vegetables, and fruits are utilized as therapeutics for antihypertensive, viral fever, antioxidant, and antimicrobial purposes [1–3]. In addition, these fruits are also provided in addition to a regular diet. Nonetheless, they have a valuable supply of nutritious foods that will decay within a couple of days after harvesting, just like any other foodstuff. To prolong its lifespan, it must consequently be stored in a cold storage room or freezer or dried. Furthermore, dried foodstuffs are easier to move from one place to another and store in small places.

Dehydration of agro-food products in the open sun (OSD) is a simple and common process employed all around the world. However, there are other issues involved with drying in the OSD. The crop is harmed due to adverse weather conditions, agro-food product contamination from external elements, and degeneration caused by overheating

[4–6]. Furthermore, the drying rate is exceedingly low, which means that the drying period is substantially longer. As a result, the dehydration process must be practiced in a sustainable environment, as well as using a quick processing approach, in order to preserve its physical and biological qualities.

Many types of dryers were widely accessible in the food industry, including oven dryers, fluidized bed dryers, microwave dryers, drum dryers, freeze dryers, indirect solar dyers, and infrared radiation dryers. Among the different kinds of dehydration methods, fluidized bed dryers (FBDs) are employed all over the world for the dehydration of agro-food products [4, 7]. The FBD is known for its consistent dehydration as well as its effective heat and mass transfer phenomena, which effectively remove the moisture from foodstuffs within a short period of time. Furthermore, FBD is a convenient way to avoid overheating heat-sensitive fruits and vegetables [4, 8–13]. In addition, the FBD is the most popular type of dryer employed in various sectors, such as chemical industries, fertilizer industries, medicine industries, agricultural industries, and milk industries. In industries that handle particulates, FB dryers exhibit excellent evaporation rates. The advantages of FB dryers over traditional dryers include rapid drying with great product quality, minimal losses from nutrition, good air-stream interaction with the wet substances, significant heat transfer between the gas and wet substances, and suitable circulation rates. Several researchers have reported updated designs for FB dryers to improve the drying process while consuming the least amount of energy [9-15].

Numerous studies on the drying kinetics of various food products have been conducted, including Monukka seedless grapes [5], terebinth seeds [8], hawthorn fruit [14], soybean [15], and barberry [16]. Other key quality parameters of dried foodstuffs are shrinkage, color changes, vitamin C, β-carotene, antioxidant capacity, and total phenolic content; they also have a substantial impact on consumer acceptance and attractiveness. Shrinkage and color of several items such as soybean [15], hawthorn fruit [14], and terebinth seeds [8] as well as the physiochemical properties of several items such as blueberries [17], myrtle fruits [18], sea buckthorn fruits [19], and goji berries [20] have been reported in detail in the previous literature.

As per the review of extant literature, no research has been conducted on the mathematical modelling and minimum fluidization behavior of turkey berry in a FBD. With these considerations in mind, the current research was carried out to examine the dehydration parameters of the samples, like the minimum fluidization velocity, rate of drying, diffusivity of water molecules, amount of energy required for activation of water molecules, percentage of volumetric shrinkage, and overall color variation of the turkey berries at different bed conditions. In addition, other key bioactive properties like vitamin C, β-carotene, antioxidant capacity, and total phenolic content of turkey berries at different bed conditions were also studied. This research also revealed a befitting model for estimating the dehydration behavior of the turkey berry.

2. Materials and Methods

2.1. Sample Preparation. The fruits were procured from the vegetable market, and the damaged and immature samples were removed from the lot. Turkey berry samples of uniform size and unimpaired fruit were separated from the entire bunch of procurements, allowing for additional experimentation. The mean diameter of the samples was metered and recorded as 13.2 ± 0.8 mm, and one piece of the berry weight of 1.9 ± 0.3 g was utilized for the trials. According to the AOAC (1990) procedure [21], the initial water content of the sample was examined by employing 8 g of fresh fruit, and the mean value was found to be 5.22 ± 0.03 kg water/kg dry matter (dry basis). Before introducing the sample into the chamber, the sorted-out samples were chosen for the studies and held at $5 \pm 1^{\circ}$C.

2.2. Experimental Setup. The dehydration behavior and physiochemical quality of the sample were investigated using a batch type fluidized bed dryer (FBD), as illustrated in Figure 1. The FBD's primary features include a backward-type centrifugal blower with VFD, a controllable electric heater, and an air filter.

The whole setup as well as the drying chamber is fabricated by S.S (stainless steel) having a height of 0.85 m and an interior diameter of 0.14 m. The air circulated all over the bed by way of the punctured S.S plate, which has a hole with a dimension of 3.8 ± 0.02 mm and a trilateral space of 7.8 ± 0.03 mm with only $21 \pm 0.1\%$ open area. A hot wire anemometer was used to monitor the input air flow with a precision of 0.2 m/s. An electric heater heats the air before it is flown to the drying chamber. A pressure measuring instrument was used to record the pressure difference during the experiment.

2.3. Analysis of Minimum Fluidization Velocity and Drying Procedure. During the dehydration of samples, the pressure drop (Δp) and the inlet air velocity were determined, and the peak "Δp" point was detected as point B, as shown in Figure 2. The existence of bed conditions is defined in point B, which is referred to as the "minimum fluidization point/semifluidized bed" [22]. Two conditions, such as "A" and "C," were selected randomly from the chart, in such a way that the velocity of A is smaller than B and the velocity of C is higher than B. In addition, points A (0.8 m/s) and C (3.4 m/s) refer to the fixed bed and fluidized bed conditions, and point B (2.1 m/s) is equal to the condition of a semifluid bed.

Drying studies were performed at three inlet temperatures of 50–70°C and three velocities (A, B, and C) as well as keeping the sample weight at 250 g. Initially, by adjusting the inlet temperature and flow velocity of air, the dryer attained a steady-state mode; thereafter, the sample was introduced into the drying cabin. Every half hour, the entire sample was emptied from the bed, and the weight was recorded using an electronic weighing scale with a precision of 0.01 g. Following the weight recording, the fruits were loaded into the drying chamber for an additional 30 minutes to further reduce their moisture content. The fruits were loaded till the

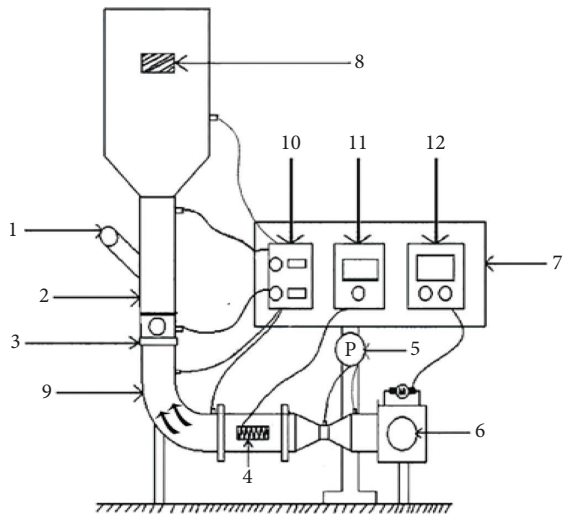

Figure 1: Schematic diagram of the fluidized bed dryer.

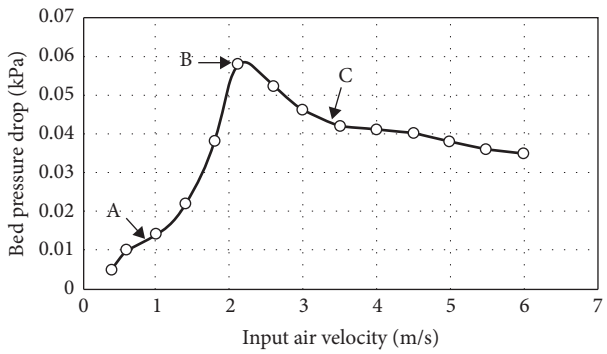

A - 0.8 m/s
B - 2.1 m/s
C - 3.4 m/s

Figure 2: Fluidization curve of turkey berry.

moisture level was less than 0.14 ± 0.05 g water/kg dry matter (d.b). Three investigations were carried out for each experimental condition to establish the reproducibility of the analysis.

2.4. Drying Curves. The weight loss of a product as a function of time is used to evaluate drying parameters systematically. The water content of berries was calculated on a dry basis (d.b) by the following equation [4, 23]:

$$M_{\mathrm{db}} = \left(\frac{W_{\mathrm{st}} - W_{\mathrm{dry}}}{W_{\mathrm{dry}}}\right). \tag{1}$$

The moisture ratio (MR) of the berry during the dehydration process in a fluidized bed is determined by the following formula:

$$\mathrm{MR} = \left(\frac{M_{\mathrm{st}} - M_{\mathrm{eq}}}{M_{\mathrm{in}} - M_{\mathrm{eq}}}\right). \tag{2}$$

Equation (2) is changed in the form of $\mathrm{MR} = M_{\mathrm{st}}/M_{\mathrm{in}}$, and the moisture ratio is a nondimensional unit. The experiment data were transformed into a moisture ratio and correlated to the different kinds of drying models reported in the literature which are described in Table 1. The various empirical drying models that were employed in this analysis were intended to find a reliable model for the drying performance of turkey berries. The drying rate (D.R) of the berry in the time of drying was estimated by the following equation [5]:

$$\mathrm{D.R} = \left(\frac{M_{s,t_1} - M_{s,t_2}}{t_2 - t_1}\right). \tag{3}$$

2.5. Computation of Effective Moisture Diffusivity (D_{eff}). Fick's second law of diffusion equation was employed to examine drying kinetic parameter and predict D_{eff} of the materials with spherical geometry:

$$\frac{\partial M}{\partial t} = D_{\mathrm{eff}} \frac{\partial^2}{\partial t}. \tag{4}$$

Considering that the sample of the turkey berry is almost spherical and the phenomenon of moisture migration occurs solely through diffusion, the MR can be determined by the following equation [5–8]:

$$\mathrm{MR} = \frac{M_{\mathrm{st}} - M_{\mathrm{eq}}}{M_{\mathrm{in}} - M_{\mathrm{eq}}} = \frac{6}{\pi^2} \sum_{n=1}^{\infty} \frac{1}{n^2} \exp\left(\frac{-D_{\mathrm{eff}} n^2 \pi^2 t}{R_p^2}\right). \tag{5}$$

During the dehydration periods where the moisture ratio seems to be beyond 0.6, the first part of their sequence of equations is evaluated, and equation (5) can thus be reformulated as

$$\mathrm{MR} = \left(\frac{6}{\pi^2}\right) \exp\left(\frac{-D_{\mathrm{eff}} \pi^2 t}{{R_p}^2}\right). \tag{6}$$

Using natural log on both left and right hand sides of equation (6), the first-degree equations such as linear equations are formed and rewritten as

$$\ln \mathrm{MR} = \ln\left(\frac{M_{\mathrm{st}} - M_{\mathrm{eq}}}{M_{\mathrm{in}} - M_{\mathrm{eq}}}\right) = \ln\left(\frac{6}{\pi^2}\right) - \left(\frac{D_{\mathrm{eff}} \pi^2 t}{{R_p}^2}\right). \tag{7}$$

By graphing the drying time against natural logarithmic of moisture ratio data of ln (MR), linear slope S_1 was obtained:

$$S_1 = \left(\frac{D_{\mathrm{eff}} \pi^2}{{R_p}^2}\right). \tag{8}$$

2.6. Determination of Activation Energy (E_{act}). The Arrhenius relationship is used to define E_{act} which communicates the interrelationship with D_{eff} and the supply air temperature (T_{in}) as shown in the following equation [5, 8–13]:

Table 1: Name of the different drying models.

Name of model	Model equation
Newton	$MR = \mathrm{Exp}(-k_1 t)$
Page	$MR = \mathrm{Exp}(-k_1 t^m)$
Henderson and Pabis	$MR = a_1 \mathrm{Exp}(-k_1 t)$
Logarithmic	$MR = a_1 \mathrm{Exp}(-k_1 t) + b_1$
Midilli et al.	$MR = a_1 \mathrm{Exp}(-k_1 t^m) + b_1 t$
Logistic	$MR = a_1/(1 + b_1 \mathrm{Exp}(k_1 t))$

a_1, b_1, k_1, and m are mathematical model coefficients.

$$D_{\mathrm{eff}} = D_c \exp\left(-\frac{E_{\mathrm{act}}}{R_{\mathrm{Ug}} T_{\mathrm{in}}}\right). \quad (9)$$

Using natural log on both left and right hand sides of equation (9), the upcoming findings are derived:

$$\ln(D_{\mathrm{eff}}) = \ln(D_c) - \left(\frac{E_{\mathrm{act}}}{R_{\mathrm{Ug}} T_{\mathrm{in}}}\right). \quad (10)$$

By graphing the inverse inlet temperature of air ($1/T_{\mathrm{in}}$) against natural logarithmic of moisture diffusivity values of $\mathrm{Ln}(D_{\mathrm{eff}})$, linear slope S_2 was obtained:

$$S_2 = \frac{E_{\mathrm{act}}}{R_{\mathrm{Ug}}}. \quad (11)$$

2.7. Analysis of the Quality

2.7.1. Computation of the Volumetric Shrinkage (VS_p). The berry dimensions were determined using a digitized Vernier caliper to compute their initial volume. Furthermore, the sample was measured multiple times along the relevant axis. After dehydration of the sample, select any three samples from each test and measure their dimensions. With the help of equation (12), the change in volume percentage was calculated as a ratio of the volume of dehydrated berries (V_{fi}) to the volume of raw berries (V_{in}) [8, 14].

$$\mathrm{VS}_p = \left(\frac{V_{\mathrm{in}} - V_{\mathrm{fi}}}{V_{\mathrm{in}}}\right) \times 100. \quad (12)$$

2.7.2. Computation of Total Color Change. A tristimulus colorimeter (Model: VT-10) was measured to assess the skin color of turkey berries under a D65 light lamp at a 10° camera angle. On the Hunter scale, color values were expressed as L—ranging from brightness to darkness (100–0), "a"—ranging from redness to greenness (positive to negative), and "b"—ranging from yellowish color to blueness (positive to negative), with the subscripts "fi" and "in" denoting final and initial intensity of color. For every sample, three data points were measured in three distinct locations, and the mean reading was calculated. Total color difference (ΔE) values were determined from the variables "L," "a," and "b" [13, 23, 24]:

$$\Delta E = \sqrt{(L_{\mathrm{fi}} - L_{\mathrm{in}})^2 + (a_{\mathrm{fi}} - a_{\mathrm{in}})^2 + (b_{\mathrm{fi}} - b_{\mathrm{in}})^2}. \quad (13)$$

2.7.3. Determination of Vitamin C and β-Carotene. According to AOAC No. 967.21 [25], vitamin C, also known as ascorbic acid (AA), was identified using the analytical discoloration of 2,6-dichlorophenolindophenol. In order to compare the amounts of vitamin C in fresh and dried turkey berries, 5.0 ± 0.1 g of each sample was crushed and diluted in 1 L of distilled water. The amount of vitamin C was given as mg AA/100 g d.m. Similarly, β-carotene content was determined with the help of the spectrophotometric method, modified from López et al. [26]. Hexane, acetonitrile, and ethanol were used to extract the β-carotene, which was then measured at wavelengths of 503 nm and 480 nm, respectively. Each test was made three times.

2.7.4. Determination of Total Phenolic Content and Antioxidant Activity. According to Chen et al. [27], the Folin–Ciocalteu method was modified to estimate the extract's total phenolic content (TPC). Two 0.5 mL aliquots of the turkey berry extract solution, made with 100% ethanol, were thoroughly combined in a vortex with 0.5 mL of the Folin–Ciocalteu reagent and 2 mL of 20% Na_2CO_3 solution. After 15 minutes of incubation at room temperature, 10 mL of ultra-pure water was added, and the layer of precipitate that had developed was removed by spinning for 5 minutes at 4,000 × g. At 725 nm, the absorbance was detected in a spectrophotometer to be compared to a curve that was calibrated for gallic acid equivalent (GAE). The findings were expressed as mg GAE per 100 g of d.m. Three measurements were taken for each test.

The phosphomolybdenum technique was used to assess the turkey berries' overall antioxidant capability [28]. 1 mL of the reagent solution (0.6 M sulfuric acid, 28 mM sodium phosphate, and 4 mM ammonium molybdate) was added to 2 mL of the extract. Each of the tubes was sealed and heated to 50°C (boiling water bath) for 90 minutes. Using a spectrophotometer, the absorbing capacity of all the solutions was detected at 695 nm against a blank of the reagent after the samples had cooled to ambient temperature. The findings were expressed as ascorbic acid equivalent (AAE) in AAE mg per gram d.m. Three measurements were taken for each test.

2.8. Statistical Evaluation of the Equations. The six mathematical models are listed in Table 1, and these models were applied to turkey berry drying data (MR vs. time). MATLAB software (MathWorks Inc.) was employed to build mathematical models for MR of the product.

Three indicators, namely, sum of squared errors, root mean square error, and square of coefficient of correlation (R^2), were applied for choosing the appropriate model to symbolize the dehydration behavior of the sample and their equations as described in equations (14)–(16) [7, 15, 23, 27–29]. A suitable model can be chosen on the basis of the indicator value such as the maximum values of R^2 as well as the minimum values of SSE and RMSE observed from the analysis results.

$$\mathrm{SSE} = \sum_{j=1}^{M} \frac{\left(\mathrm{MR}_{\mathrm{test},j} - \mathrm{MR}_{\mathrm{pre},j}\right)^2}{M-n}, \tag{14}$$

$$R^2 = \frac{\sum_{j=1}^{M}\left(\mathrm{MR}_{\mathrm{test},j} - \mathrm{MR}_{\mathrm{test}}\right)\left(\mathrm{MR}_{\mathrm{pre},j} - \mathrm{MR}_{\mathrm{pre}}\right)}{\left[\sum_{j=1}^{M}\left(\mathrm{MR}_{\mathrm{test},j} - \mathrm{MR}_{\mathrm{test}}\right)^2 \sum_{j=1}^{M}\left(\mathrm{MR}_{\mathrm{pre},j} - \mathrm{MR}_{\mathrm{pre}}\right)^2\right]^{1/2}}, \tag{15}$$

$$\mathrm{RMSE} = \left[\frac{1}{M}\sum_{j=1}^{M}\left(\mathrm{MR}_{\mathrm{test},j} - \mathrm{MR}_{\mathrm{pre},j}\right)^2\right]^{1/2}, \tag{16}$$

where $\mathrm{MR}_{\mathrm{test},j}$ is the experimental moisture ratio of j^{th} data point, $\mathrm{MR}_{\mathrm{pre},j}$ is the predicted moisture ratio of j^{th} data point, M is the total number of occurrences, and n is the number of constants in the model equation.

2.9. Statistical Evaluation of the Quality Analysis. At each experimental condition, three trials were conducted, and the mean values were evaluated. A one-way ANOVA test was performed at 95% probability level using SPSS Statistics 29.0 (IBM Co., New York, USA). In the case of significant differences between subgroups, the post hoc Tukey test was used as a statistical test ($P < 0.05$).

2.10. Microstructure Analysis. A scanning electron microscope was employed to analyse the morphology of dried turkey berries (FEI Quanta 200 F SEM, Netherlands). To get SEM micrographs, miniscule pieces of fruit skin were collected and coated with a thin layer of nano-gold under a vacuum environment to provide an illumination surface for the electron gun. Gold coat was done with an argon gas, at a pressure smaller than the ambient pressure on a sputter coater (HV-DSR1 Sputter Coater).

3. Results and Discussion

3.1. Drying Curves. As shown in Figure 3, the rate of dehydration of fruits with respect to time was reduced steadily during the dehydration of the samples. According to the investigational findings, the declining rate of drying was discovered throughout for all circumstances, as well as the fact that the water transport from the inner core of the sample to the outermost peel is predominantly regulated by the diffusivity phenomenon. Also, a large amount of evaporation of moisture was recorded in the early stages of drying of berries, but the final stage had a lower rate. The highest and lowest drying rates are 9.4 gram of water at 70°C and 8.6 gram of water at 50°C, respectively, with fluidized bed velocity of 3.4 m/s, during the initial stage (1 hour), whereas at fixed bed conditions (0.8 m/s), these values were detected as 6.4 gram of water at 70°C and 5.4 gram of water at 50°C.

According to Figure 3, a substantial drying rate was recorded at higher inlet air temperatures with fluidized bed velocity. At the same time, the maximum drying rate was detected at 70°C irrespective of all inlet air velocities [4]. During the dehydration at high temperatures, the vapor pressure vigorously developed on the cell walls of the inside fruit structures, so a considerable amount of the turgor pressure of the fruit structure was reduced.

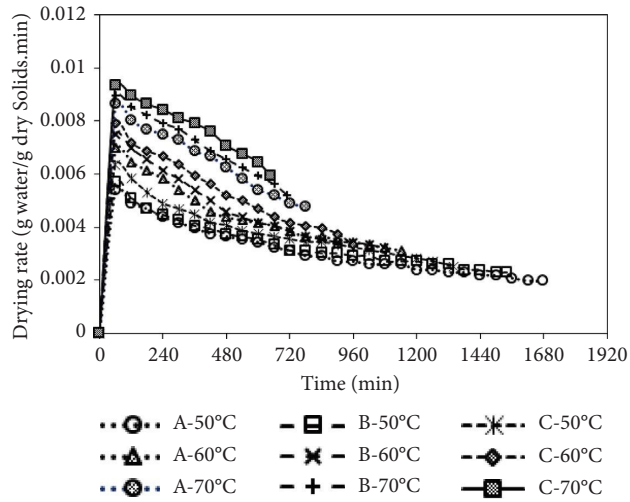

Figure 3: Drying rate with respect to time under various drying input parameters.

As a result of the preceding, the porous structure of the sample increases dramatically and has the proclivity to generate additional micropores and facilitate water movement from the center to the surface of the fruit [5]. At 70°C, cracks and micropores can appear, as can be seen in Figure 4(h). While there is no substantial effect on cell structure at a low temperature of 50°C, pore formation is inhibited, as seen in Figure 4(e). This is owing to the fruits' low water permeability, as shown in Figure 3.

Furthermore, at elevated temperatures and velocity, the phenomenon of heat and mass transfer processes is faster, contributing to rapid drying, thereby reducing the dehydration duration [8, 30, 31]. As a result of the experiment, at 70°C and fluidized bed condition, the rate of convective heat and mass transfer was superior to other conditions, resulting in a rapid drying rate and a shorter dehydration period. Figure 5 depicts the variation of the moisture level of the sample at various input parameters, and every line represents the amount of duration required to reduce the water potential from a beginning moisture content of 5.22 (d.b) to a final value of 0.14 (d.b).

It is demonstrated that the water level of the fruits progressively diminished with regard to time in all experiments, and that the dehydration period is significantly shorter in a fluidized velocity condition, irrespective of inlet air temperature, as shown in Figure 5. The dehydration duration of samples at temperatures of 50, 60, and 70°C was recorded as 1340, 960, and 645 min, respectively, at a superficial velocity of 3.4 m/s, as displayed in Figure 5. The drying period is shortened in terms of 2-fold times, once the temperature of incoming air rises from 50°C to 70°C; conversely, only around 20% was reduced when the inlet air velocities rise from 0.8 to 3.4 m/s. The drying of turkey berries was influenced more by the temperature of the incoming hot air than by its velocity [4, 11].

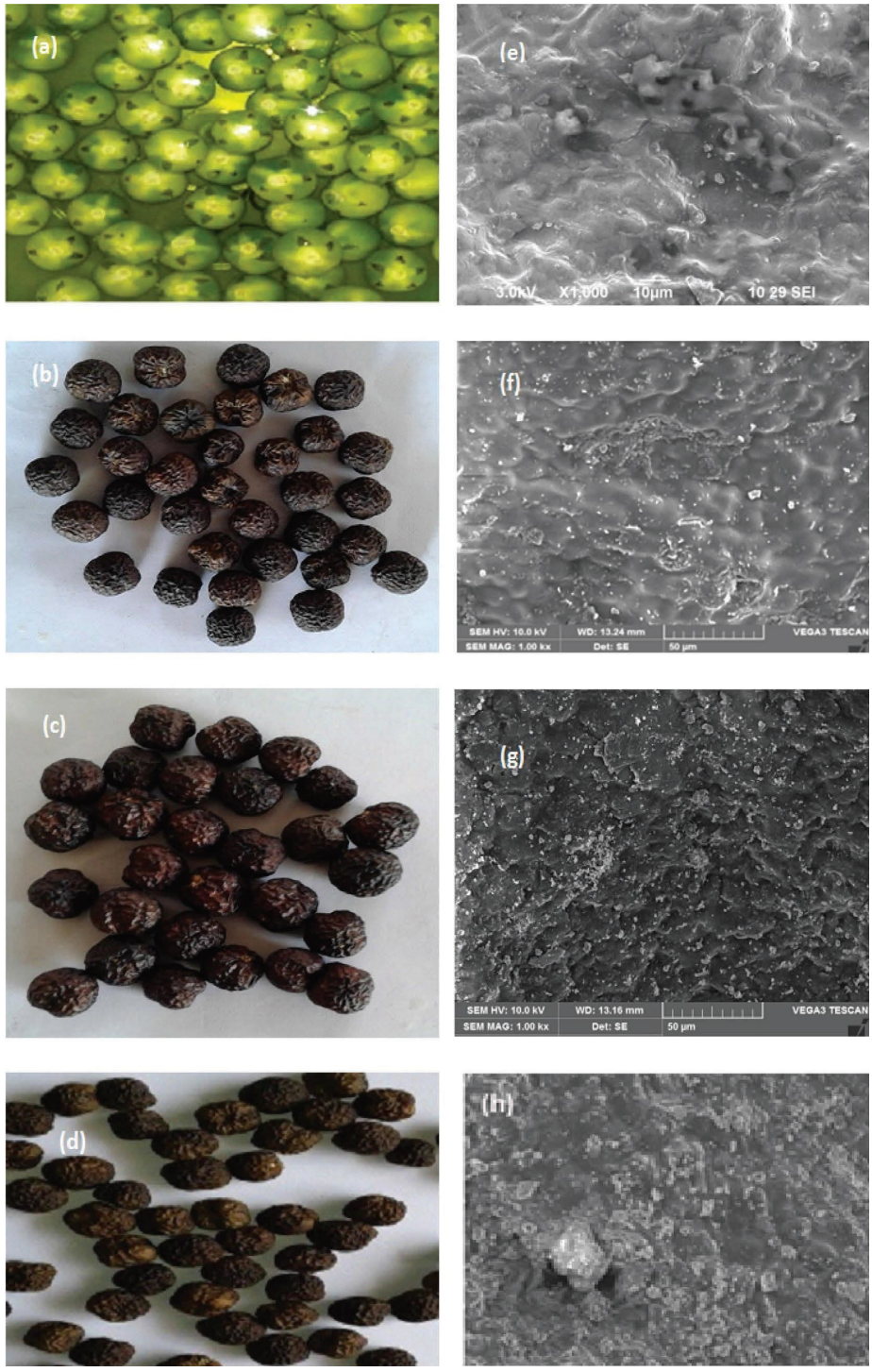

Figure 4: Photo view (a–d) and SEM picture (e–h) of fresh and dried samples at fluidized velocity.

3.2. Estimation of the Mathematical Models. In order to recognize an appropriate model that forecasts the drying kinetics of the fruits with the assistance of existing drying models, described in Table 1, the statistical information, including the estimations of R^2, RMSE, and SSE of various models utilized, is presented in Table 2.

The most appropriate drying model to address the dehydration behavior of the turkey berry was detected as the Midilli et al. [29] model, on the basis of the criteria of highest value of R^2 and lowest values of RMSE and SSE. As the estimated values of R^2 vary from 0.9992 to 0.9997, the RMSE values vary from 0.00006 to 0.00025, and the SSE values

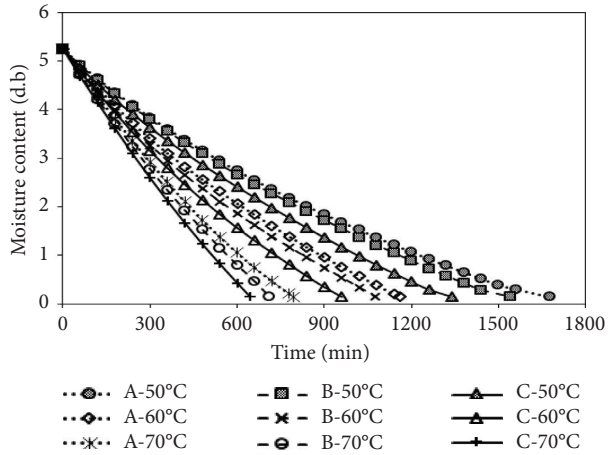

Figure 5: Moisture content of the sample with respect to time under various drying input parameters.

Table 2: Numerical values of various drying models at different input parameters.

Model name	T (°C)	R^2			SSE			RMSE		
		0.8 m/s	2.1 m/s	3.4 m/s	0.8 m/s	2.1 m/s	3.4 m/s	0.8 m/s	2.1 m/s	3.4 m/s
Newton	50	0.9642	0.9646	0.9598	0.0539	0.0580	0.0608	0.0572	0.0566	0.0596
	60	0.9614	0.9662	0.9714	0.0515	0.0436	0.0316	0.0585	0.0528	0.0512
	70	0.9538	0.9569	0.9482	0.0493	0.0429	0.0486	0.0669	0.0655	0.0734
Page	50	0.9938	0.9926	0.9865	0.0133	0.0119	0.0205	0.0244	0.0265	0.0204
	60	0.9881	0.9907	0.9886	0.0162	0.0122	0.0125	0.0336	0.0304	0.0125
	70	0.9878	0.9885	0.9879	0.0164	0.0115	0.0195	0.0364	0.0357	0.0194
Henderson and Pabis	50	0.9732	0.9729	0.9659	0.0415	0.0452	0.0519	0.0515	0.0518	0.0571
	60	0.9681	0.9724	0.9755	0.0433	0.0356	0.0274	0.0557	0.0524	0.0498
	70	0.9619	0.9644	0.9568	0.0645	0.0362	0.0413	0.0645	0.0635	0.0719
Logarithmic	50	0.9991	0.9993	0.9987	0.0004	0.0003	0.0016	0.0053	0.0039	0.0102
	60	0.9992	0.9994	0.9985	0.0004	0.0003	0.0017	0.0056	0.0048	0.0122
	70	0.9994	0.9993	0.9992	0.0002	0.0002	0.0009	0.0037	0.0046	0.0034
Midilli et al.	50	0.9994	0.9992	0.9992	0.00008	0.00018	0.00014	0.0034	0.0035	0.0096
	60	0.9995	0.9994	0.9994	0.00006	0.00013	0.00025	0.0022	0.0035	0.0092
	70	0.9996	0.9995	0.9997	0.00006	0.00006	0.00006	0.0012	0.0029	0.0033
Logistic	50	0.9967	0.9959	0.9923	0.0094	0.0067	0.0117	0.0181	0.0203	0.0275
	60	0.9924	0.9938	0.9914	0.0103	0.0081	0.0096	0.0282	0.0257	0.0308
	70	0.9905	0.9922	0.9921	0.0082	0.0079	0.0076	0.0305	0.0313	0.0327

range from 0.0012 to 0.0096, as presented in Table 2, and the evaluated values of the coefficients of the Midilli et al. model are shown in Table 3.

3.3. Effective Moisture Diffusivity. Figure 6 depicts the variation of Ln (MR) with function of drying time at various input parameters. The fruit's D_{eff} values were calculated using equation (7), and its R squared (R^2) was estimated using the linear equation, as listed in Table 4. The D_{eff} values exhibited a range between 8.792×10^{-11} and $2.898 \times 10^{-10}\ \text{m}^2\text{s}^{-1}$ across various drying conditions. It is noteworthy that the D_{eff} values for turkey berries falls within the established range of 10^{-8}–$10^{-11}\ \text{m}^2/\text{s}$, consistent with the D_{eff} values reported for a majority of food commodities, as documented by Xiao et al. [5]. In the course of dehydration, the D_{eff} values were increased due to better convective heat and mass transfer phenomena occurring at 70°C and superficial velocity (3.4 m/s) circumstances. Table 4 demonstrates that the D_{eff} values varied from 8.792×10^{-11} to $1.305 \times 10^{-10}\ \text{m}^2/\text{s}$ at 50°C, 1.535×10^{-10} to $1.918 \times 10^{-10}\ \text{m}^2/\text{s}$ at 60°C, and 2.382×10^{-10} to $2.898 \times 10^{-10}\ \text{m}^2/\text{s}$ at 70°C during the dehydration when the inlet air velocities varied from 0.8 to 3.4 m/s. The preceding data suggest that both input air velocity and temperature influenced moisture diffusivity favorably; moreover, the D_{eff} values were influenced greatly by the temperature rather than air velocity [7–14, 30, 31].

Elevating the processing air temperature serves to increase the vapor pressure within the cellular structure of the fruit, primarily the cell wall. Consequently, this leads to a significant alteration in the turgidity pressure of the cell wall and subsequently enhances the porosity of the sample tissues. These adjustments collectively contribute to a notable improvement in the permeability of the material, as observed in the previous research [14].

Table 3: Midilli et al. model values under various input conditions.

Inlet velocity (m/s)	Model coefficients	Drying temperature (°C)		
		@ 50	@ 60	@ 70
0.8	a_1	0.9949	1.0018	0.9998
	b_1	−0.0001	−0.0003	−0.00068
	k1	0.0006	0.0018	0.00172
	m	1.1221	0.8729	0.9119
2.1	a_1	0.9970	1.0011	1.0013
	b_1	−0.0002	−0.00012	−0.00068
	k1	0.00068	0.0015	0.0018
	m	1.0728	0.9599	0.9341
3.4	a_1	0.9979	1.0053	0.9989
	b_1	−0.00038	−0.00038	−0.00092
	k1	0.0021	0.0029	0.0017
	m	0.8831	0.8615	0.9662

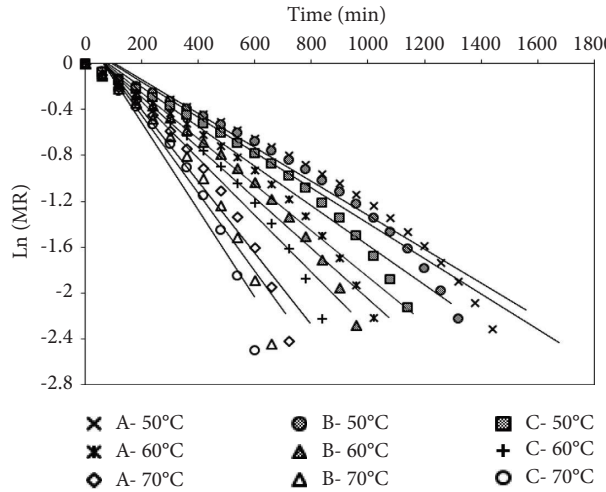

Figure 6: Ln (MR) with respect to time under various drying input parameters.

Table 4: Effective moisture diffusivity and activation energy values under various drying conditions.

Drying conditions	Input parameters					
	T_{in} (°C)	D_{eff}		Arrhenius equation		
		(m^2/s)	R^2	D_0 (m^2/s)	E_a (kJ/mol)	R^2
0.8 m/s	50	8.792×10^{-11}	0.9658	2.144×10^{-3}	45.63	0.9988
	60	1.535×10^{-10}	0.9666			
	70	2.382×10^{-10}	0.9465			
2.1 m/s	50	1.153×10^{-10}	0.9646	1.441×10^{-4}	37.73	0.9962
	60	1.689×10^{-10}	0.9665			
	70	2.612×10^{-10}	0.9359			
3.4 m/s	50	1.305×10^{-10}	0.9648	1.384×10^{-4}	36.82	0.9987
	60	1.918×10^{-10}	0.9639			
	70	2.898×10^{-10}	0.9249			

Based on the inference, the water migration from inner portion of fruit to outer surface remarkably increases and rapid convective mass transfer occurs rapidly using high air velocity flow over the samples.

3.4. Activation Energy (E_{act}). The energy needed to migrate the water molecules from the inner core of the foodstuff to outer peel and evaporate it is referred to as activation energy. Figure 7 depicts the Ln (D_{eff}) associated with the reciprocal of inlet air temperature ($1/T_{in}$) under various bed arrangements. E_{act} was evaluated through equation (9), and the coefficients of determination (R^2) for various inlet factors are shown in Table 4.

Average E_a values for various inlet parameters were discovered to be 36.82 to 45.63 kJ/mol in the experimental investigation of turkey berries dried in FBD. The value of E_{act} varies from 12.7 to 140 kJ/mol for various agro-foodstuffs

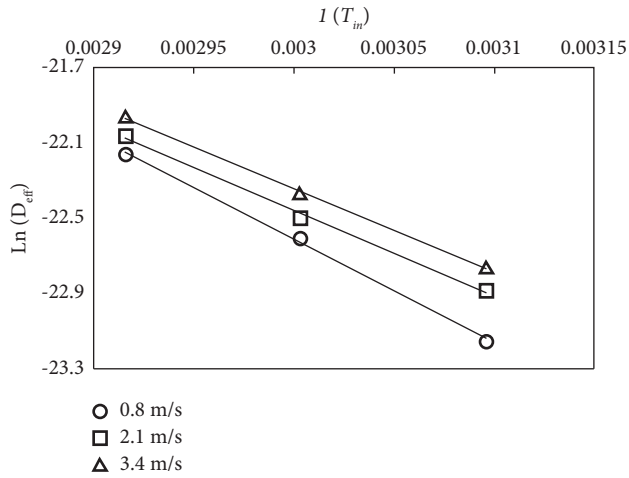

Figure 7: Ln (D_{eff}) vs. ($1/T_{\text{in}}$) under various drying conditions.

[16], which is consistent with the findings. Once the fruit was dried at fluidized bed condition, the E_{act} values decreased. As a result of the promising effect of heat and mass transfer by convection, the energy required to activate water molecules was reduced. Higher heat and mass transfer activity increases the dehydration rate as well as the diffusivity (D_{eff}) of the water molecules from inner core of the berry to the outermost peel layer of the sample. Table 4 shows that the minimum and maximum values of E_{act} are 3.4 m/s and 0.8 m/s, and Khanali et al. [13] and Taheri-Garavand and Meda [28] also showed the same tendency.

3.5. Quality Analysis

3.5.1. Volumetric Shrinkage. Table 5 shows the percentage of volumetric shrinkage at various bed conditions in FBD, and the change in dimensions of the berries was calculated by equation (13). The experimental results undoubtedly show that temperature and velocity have a substantial effect on the sample shrinking. Moreover, Table 5 shows that at fluidized bed conditions (70°C and 3.4 m/s), the volumetric shrinkage was $49.1 \pm 1.1\%$, while at fixed bed condition (50°C and 0.8 m/s), it was $71.1 \pm 0.9\%$.

ANOVA carried out for the volumetric shrinkage of turkey berries showed significant differences ($P < 0.05$) between the shrinkage percentages of various bed conditions of the dried samples, as presented in Table 5. The significant averages of samples dried at various temperatures (50 to 70°C) were also determined using a multiple comparison test, and it was shown that there were significant changes ($P < 0.05$) when the bed conditions changed from fixed to fluidized (0.8–3.5 m/s).

According to Figures 4(b)–4(d), the berries dehydrated at 50°C had a significantly greater effect on its original shape (greater shrinkage) than the products dehydrated at 60°C and 70°C. So, the water gradient between both the inside and external surfaces of the berry is minimal, and the removal of moisture evaporation was reduced during the low temperature involved in the drying, resulting in less internal stress developing on the cell wall. Furthermore, at relatively low temperatures, dried fruit was subjected to warm heat for a long duration, causing the cell walls of the tissues to be distorted. The largest dimension variations were noticed once the samples were dried at a low flow rate of air entering and a low inlet air temperature due to minimal permeability, smaller moisture differences on the inner and outer surfaces, and minimal vapor tension development on the cell structure [14, 32]. As a result, it is possible to deduce that the processing temperature has a substantial impact on the shape/volume of the fruits. According to Hatamipour and Mowla [32], reduction in volume/shape of the product is negatively related to the evaporation rate of moisture.

3.5.2. Total Color Difference (TCD). In the food sector, color is one of the most important quality indicators of food attributes, and color degradation is undesirable. Temperature and velocity had more influence on the change of color of the product, as seen in Table 5, and equation (14) was used to compute the total color change of the products. The brightness (L_i) of 71.2, greenness (a_i) of −7.83, and yellowish color (b_i) of 25.96 were used to calculate the fresh fruit color values in this investigation. The total color difference (TCD or ΔE) between dehydrated samples was determined to be substantively different as indicated in Table 5. At different bed conditions, the estimated TCD scores for dehydrated samples ranged from 11.08 to 21.12. ANOVA carried out for the volumetric shrinkage of turkey berries showed significant differences ($P < 0.05$) between the TCD values of various bed conditions of the dried samples, as presented in Table 5. The significant averages of samples dried at various temperatures (50 to 70°C) were also determined using a multiple comparison test, and it was shown that there were significant changes ($P < 0.05$) when the bed conditions changed from fixed to fluidized (0.8–3.5 m/s).

Table 5 shows that both parameters like brightness and yellowish color were dramatically lowered, resulting in a greater change in darkness as well as decreased greenness. Figures 4(a)–4(d) depict the influence of changing the surface color of the products as they dehydrate in FBD. When low inlet air velocity and low temperature were

Table 5: Variation of shrinkage and total color change of the turkey berry under various drying input parameters.

V (m/s)	T_{in} (°C)	Shrinkage (%)	Total color variations (ΔE)			
			L_{fi}	a_{fi}	b_{fi}	ΔE
0.8	50	71.2 ± 0.9^{a}	53.42 ± 0.8^{c}	-2.98 ± 0.12^{a}	15.34 ± 0.12^{c}	21.12 ± 0.14^{a}
	60	65.9 ± 1.2^{bc}	58.86 ± 0.6^{b}	-3.73 ± 0.07^{b}	15.31 ± 0.17^{c}	16.76 ± 0.22^{c}
	70	59.6 ± 1.4^{e}	64.12 ± 1.2^{a}	-5.22 ± 0.08^{c}	17.16 ± 0.14^{a}	11.65 ± 0.15^{e}
2.1	50	68.3 ± 1.6^{b}	53.5 ± 0.8^{c}	-3.12 ± 0.06^{a}	15.72 ± 0.28^{bc}	20.81 ± 0.11^{ab}
	60	60.7 ± 1.3^{de}	59.08 ± 0.6^{b}	-3.94 ± 0.04^{b}	15.93 ± 0.17^{b}	16.14 ± 0.16^{d}
	70	54.6 ± 1.8^{f}	64.28 ± 0.4^{a}	-5.28 ± 0.10^{c}	17.54 ± 0.16^{a}	11.25 ± 0.15^{fe}
3.4	50	63.9 ± 1.3^{cd}	53.82 ± 1.0^{c}	-3.26 ± 0.12^{a}	15.98 ± 0.12^{b}	20.39 ± 0.11^{b}
	60	55.8 ± 1.4^{f}	59.16 ± 0.6^{b}	-3.98 ± 0.08^{b}	16.11 ± 0.19^{b}	15.96 ± 0.14^{d}
	70	49.1 ± 1.1^{g}	64.37 ± 0.2^{a}	-5.31 ± 0.05^{c}	17.61 ± 0.15^{a}	11.08 ± 0.12^{f}

Different letters in same column indicate a significant statistical difference ($P < 0.05$).

Table 6: Variation of vitamin C content, antioxidant capacity, and total phenolic content of the turkey berries under various drying input parameters.

V (m/s)	T_{in} (°C)	Vitamin C content (mg/100 g d.m)	β-Carotene content (μg/100 g d.m)	Total phenolic content (mg GAE/100 g)	Total antioxidant capacity (mg AAE/100 g d.m)
Fresh	—	3.81 ± 0.44^{a}	400 ± 4.56^{a}	676.18 ± 8.38^{a}	53.42 ± 0.21^{a}
0.8	50	0.80 ± 0.01^{h}	100 ± 1.24^{i}	422.61 ± 9.12^{h}	11.75 ± 0.35^{h}
	60	1.07 ± 0.02^{g}	124 ± 1.56^{g}	453.04 ± 8.12^{efg}	14.96 ± 0.16^{f}
	70	1.37 ± 0.04^{e}	168 ± 1.56^{d}	486.85 ± 5.28^{cd}	18.68 ± 0.12^{d}
2.1	50	1.22 ± 0.05^{f}	108 ± 1.72^{h}	436.14 ± 7.24^{gh}	13.33 ± 0.21^{g}
	60	1.45 ± 0.02^{de}	132 ± 1.78^{f}	466.56 ± 8.15^{ef}	16.53 ± 0.17^{e}
	70	1.75 ± 0.04^{c}	176 ± 1.56^{c}	500.37 ± 5.17^{bc}	19.77 ± 0.33^{c}
3.4	50	1.49 ± 0.03^{d}	120 ± 2.15^{g}	446.28 ± 6.56^{fg}	14.93 ± 0.31^{f}
	60	1.68 ± 0.04^{c}	144 ± 1.98^{e}	473.33 ± 4.36^{de}	18.17 ± 0.23^{d}
	70	1.91 ± 0.01^{b}	184 ± 1.56^{b}	513.90 ± 8.38^{b}	21.34 ± 0.16^{b}

Different letters in same column indicate a significant statistical difference ($P < 0.05$).

involved in the dehydration of the sample by this means, it took drying for longer periods of time; consequently, it was strongly affected by both caramelization and enzymatic browning reactions [23]. Commonly, when the foodstuffs are subjected to high-temperature settings, total phenolic acids are oxidised, and carbohydrates or amino acids undergo chemical reactions. The amount of color deviation was affected by drying air temperature and processing duration, as well as the amount of oxygen present in flow of inlet air [13, 23, 24].

3.5.3. Retention of Vitamin C and β-Carotene. The vitamin C content of the dried turkey berries is shown in Table 6. Fresh fruit has 3.81 ± 0.44 mg/100 g d.m. This is consistent with past studies demonstrating that turkey berries contain 2.86 mg/100 g d.m [1] and 4 mg/100 g d.m [2], respectively. The analysis of variance revealed significant differences ($P < 0.05$) in the mean values of the vitamin C content of dried berries under various bed conditions, which are displayed in Table 6. In all nine studies, vitamin C retention was best when the sample was dried at an air temperature of 70°C and an air velocity of 3.4 m/s. The dried samples demonstrated a considerable loss of 79% in vitamin C at low intake air temperature and low inlet air velocity (0.8 m/s and 50°C), while at 70°C in fluidized bed conditions, only about 50% is lost. According to the findings of the experiments, 36–42% of the vitamin C content was maintained at an input temperature of 60°C that was constant and bed conditions that ranged from fixed to fluidized (0.8–3.5 m/s). According to López et al. [26], drying time, pretreatment choice, and processing temperature all affect how much vitamin C is retained. But in order to keep the vitamin C content unaltered, processing temperature is crucial.

β-Carotene is a carotenoid and a fat-soluble pigment. From the results, it was found that the percentage loss of β-carotene was slightly lower when the inlet temperature increased at the same bed conditions. During dehydration of turkey berries, degradation of β-carotene was more noticeable at 50°C with about 40–46% loss with respect to its original value when bed conditions varied from fixed to fluidized (0.8–3.5 m/s). At 60°C, losses of 31–36% were observed, as listed in Table 6, from fixed to fluidized bed conditions, respectively, while during drying at 70°C, losses in the range of 25%–30% occurred. Similar reports from other authors indicate that long drying times influence the loss of this compound [26, 27]. ANOVA carried out for the β-carotene of turkey berries showed significant differences ($P < 0.05$) between the β-carotene retention values of various bed conditions of the dried samples, as presented in Table 6. The significant averages of samples dried at various temperatures (50 to 70°C) were also determined using a multiple

comparison test, and it was shown that there were significant changes ($P < 0.05$) when the bed conditions changed from fixed to fluidized (0.8–3.5 m/s).

3.5.4. Retention of Total Phenolic Content (TPC) and Antioxidant Capacity (AOC). From basic phenolic molecules to highly polymerized compounds, phenolic substances all have an aromatic ring with one or more hydroxyl substitutions as part of their structural makeup. The analysis of variance revealed significant differences ($P < 0.05$) in the mean values of the TPC of dried berries under various bed conditions, which are displayed in Table 6. In all nine studies, the TPC retention was best when the sample was dried at an air temperature of 70°C and an air velocity of 3.4 m/s. The dried samples demonstrated a considerable loss of 37.5% in the TPC at 0.8 m/s and 50°C inlet conditions, while at 70°C in fluidized bed conditions, only about 24% is lost, as presented in Table 6. According to the findings of the experiments, 30–33% of the TPC values were maintained at an input temperature of 60°C that was constant and bed conditions that ranged from fixed to fluidized (0.8–3.4 m/s). According to Alkaltham et al. [18], the reduction of TPC during dehydration may be related to polyphenols binding with other substances, such as proteins, or changes in the chemical composition of polyphenols that are not accessible for extraction or analysis. The availability of phenolic molecule precursors resulting from nonenzymatic interconversion between the phenolic molecules may be the cause of the production of phenolic compounds at high temperatures [16–20].

Based on the experimental findings, it was discovered that decreasing the input temperature of the air while maintaining the same bed conditions (0.8 or 3.4 m/s) resulted in a somewhat higher percentage loss of the TAC. As the turkey berry dried, the TAC degraded more noticeably at 50°C, losing 72 to 78% of its original value when the bed condition changed from a fixed to fluidized bed state (0.8–3.5 m/s). From fixed to fluidized bed conditions, losses of 66 to 72% were seen at 60°C, whereas losses in the range of 65 to 60% occurred during drying at 70°C, as presented in Table 6.

The decrease of this antioxidant activity is influenced by long drying times, according to observations from other authors [16–20]. In order to establish the statistically significant difference among the nine samples dried at various temperatures (50 to 70°C), a multiple comparison test was also carried out. The results showed that fewer differences ($P > 0.05$) were seen when the bed conditions varied from fixed to fluidized (0.8–3.5 m/s). The major antioxidants in turkey berries, phenolic compounds and β-carotene, respond to drying temperature, oxygen content, and other processing variables in various ways. The experimental findings indicate a strong link between TPC, vitamin C, and β-carotene and the antioxidant activity of the berries [16–20].

3.6. Microstructural Analysis (SEM). Figure 4 shows the picture and SEM images of the sample skin prior to and after dehydration in FBD. The fresh sample picture and SEM images are depicted in Figures 4(a) and 4(e). The SEM picture of a fresh berry in Figure 4(e) shows a comprehensible vision of the waxy covering on its surface. Whenever the berries are dehydrated at hot air inlet temperatures (above 60°C), the waxy-covered surface begins to disintegrate or break, allowing pores to develop. Figure 4(f) shows a tiny waxy cover and some fragmented wax particles after drying at 50°C. The SEM images of berry peels dried at 60 and 70°C are shown in Figures 4(g) and 4(h). Both Figures 4(g) and 4(h) reveal a decomposed waxy surface layer, as well as micropores and tiny tears upon the peel of the berrydepicted in Figure 4(h).

It is reasonable to conclude that the superior drying rate and numerous micropores are created by high processing temperatures. The surface of the berry exhibits higher porous structures that are formed as a result of the drying of the berries at an incoming air temperature that was high, as observed from the SEM images. High temperature air supplied over the sample, consequently, increases the heat in cells, increasing the internal stress on the cell wall, which may enhance the vapor pressure and result in greater water permeability from the interior of the sample.

As a result of the high-temperature air passing over the sample, the heat in the cells rises, increasing the internal stress on the cell wall. This may increase the vapor pressure, resulting in greater water permeability in the sample's interior. Conversely, at a low processing temperature, insufficient vapor pressure developed, resulting in limited permeability and poor cell structures [14, 33]. Figures 4(a)–4(d) depict photos of fresh fruits and dried samples at 50, 60, and 70°C, and it can be seen that volumetric shrinkage was greater at 50°C (Figure 4(b)) than at 60°C and 70°C (Figures 4(c) and 4(d)).

4. Conclusions

The following results were obtained as a result of the extensive study of turkey berries dried in FBD. The mean value of the initial water content of the turkey berry was computed to be about $5.22 \pm 0.03\%$ (d.b), and the minimum fluidization velocity of the berries in FBD was observed to be 2.1 m/s. The processing temperature plays a predominant role in the course of turkey berry drying compared to the inlet air velocity. High temperature (70°C) and fluidized velocity (3.4 m/s) greatly influence the drying kinetics of turkey berries and improve their physical and chemical properties, such as color and shrinkage, vitamin C, β-carotene, antioxidant capacity, and total phenolic content. The maximum retention rates of vitamin C, β-carotene, antioxidant capacity, and total phenolic content were 1.91 1.91 mg/100 g.d.m, 184 μg/100 g d.m, 21.34 mg AAE/100 g d.m, and 513 mg GAE/100 g, respectively. The maximum effective

moisture diffusivity (D_{eff}) and minimum energy required to activate water molecules (E_a) were detected at high temperatures (70°C) and fluidized velocity conditions (3.4 m/s). The drying performance of the sample is far more precisely described by the Midilli et al. model compared to other mathematical models.

Nomenclature

a, b, k, and n:	Model coefficients
W_{st}:	Sample weight at a specific time (g)
W_{dry}:	Sample dry weight (g)
DR:	Drying rate (kg water/kg dry matter. min)
t, t_1, t_2:	Drying time (minutes)
R_p:	Radius of the product (meter)
S_p:	Shrinkage of the product (%)
T_{in}:	Inlet temperature of air (°C)
E_{act}:	Activation energy (m^2/s)
D_0:	Preexponential factor of the Arrhenius equation (m^2/s)
R_{Ug}:	Universal gas constant (kJ/kg-mol/K)
M_{eq}:	Equilibrium moisture content of the sample (kg water/kg dry matter)
M_{st}:	Moisture content at any time (kg water/kg dry matter)
M_{in}:	Initial moisture content of the sample (kg water/kg dry matter)
V_{in}:	Initial volume of the product (m^3)
V_{in}:	Final volume of the product (m^3).

Data Availability

The data supporting the findings of this study are included within the article.

Conflicts of Interest

The authors declare that they have no conflicts of interest.

References

[1] T. K. Lim, *Solanum Torvum. Edible Medicinal And Non-medicinal Plants*, Springer, Dordrecht, Netherlands, 2013.

[2] P. N. Y. Otu, F. Sarpong, J. E. Gidah, A. M. Labanan, and D. Anim, "Characterization of Turkey berry (Solanum torvum)-fresh, dry & powder," *African Journal of Food and Integrated Agriculture*, vol. 1, pp. 9–14, 2017.

[3] D. S. Sivakumar, S. Subramani, N. V. Thirumalai, M. K. Marimuthu, and G. A. Arockiaraj, "Mathematical modeling of thin layer drying characteristics and proximate analysis of Turkey berry (Solanum torvum)," *Thermal Science*, vol. 26, no. 00, 2021.

[4] N. Parlak, "Fluidized bed drying characteristics and modeling of ginger (zingiber officinale) slices," *Heat and Mass Transfer*, vol. 51, no. 8, pp. 1085–1095, 2015.

[5] H. W. Xiao, C. L. Pang, L. H. Wang, J. W. Bai, W. X. Yang, and Z. J. Gao, "Drying kinetics and quality of Monukka seedless grapes dried in an air-impingement jet dryer," *Biosystems Engineering*, vol. 105, no. 2, pp. 233–240, 2010.

[6] S. Erenturk, M. S. Gulaboglu, and S. Gultekin, "The thin-layer drying characteristics of rosehip," *Biosystems Engineering*, vol. 89, no. 2, pp. 159–166, 2004.

[7] C. Srinivasakannan and N. Balasubramanian, "Estimation of diffusion parameters in fluidized bed drying," *Advanced Powder Technology*, vol. 20, no. 4, pp. 390–394, 2009.

[8] R. AmiriChayjan and M. Kaveh, "Physical parameters and kinetic modeling of fix and fluid bed drying of terebinth seeds," *Journal of Food Processing and Preservation*, vol. 38, no. 3, pp. 1307–1320, 2014.

[9] R. Barathiraja, P. Thirumal, G. Saraswathy, and I. Rahamathullah, "Effects of pretreatments on drying of Turkey berry (Solanum torvum) in fluidized bed dryer," *Chemical Industry and Chemical Engineering Quarterly*, vol. 28, no. 3, pp. 169–178, 2022.

[10] R. Barathiraja, P. Thirumal, G. Saraswathy, and I. Rahamathullah, "Drying of Turkey berry in a fluidized bed dryer with mild steel, copper and aluminum inert materials: kinetics and quality determination," *Journal of Mechanical Science and Technology*, vol. 35, no. 6, pp. 2707–2717, 2021.

[11] R. Barathiraja, P. Thirumal, D. Thirumalaikumarasamy, A. Kajavali, M. Ashokkumar, and J. Thiyagaraj, "Investigation of drying kinetics and qualities of Turkey berry in fluidized bed dryer," *Materials Today: Proceedings*, vol. 46, pp. 7711–7718, 2021.

[12] W. Senadeera, B. R. Bhandari, G. Young, and B. Wijesinghe, "Influence of shapes of selected vegetable materials on drying kinetics during fluidized bed drying," *Journal of Food Engineering*, vol. 58, no. 3, pp. 277–283, 2003.

[13] M. Khanali, A. Banisharif, and S. Rafiee, "Modeling of moisture diffusivity, activation energy and energy consumption in fluidized bed drying of rough rice," *Heat and Mass Transfer*, vol. 52, no. 11, pp. 2541–2549, 2016.

[14] S. Aral and A. V. Beşe, "Convective drying of hawthorn fruit (Crataegus spp.): effect of experimental parameters on drying kinetics, color, shrinkage, and rehydration capacity," *Food Chemistry*, vol. 210, pp. 577–584, 2016.

[15] H. Darvishi, "Quality, performance analysis, mass transfer parameters and modeling of drying kinetics of soybean," *Brazilian Journal of Chemical Engineering*, vol. 34, no. 1, pp. 143–158, 2017.

[16] M. Aghbashlo, M. H. Kianmehr, and H. Samimi-Akhijahani, "Influence of drying conditions on the effective moisture diffusivity, energy of activation and energy consumption during the thin-layer drying of berberis fruit (Berberidaceae)," *Energy Conversion and Management*, vol. 49, no. 10, pp. 2865–2871, 2008.

[17] M. P. Zia and I. Alibas, "Influence of the drying methods on color, vitamin C, anthocyanin, phenolic compounds, antioxidant activity, and in vitro bio accessibility of blueberry fruits," *Food Bioscience*, vol. 42, Article ID 101179, 2021.

[18] M. S. Alkaltham, A. M. Salamatullah, M. M. Özcan, N. Uslu, K. Hayat, and I. A. Mohamed Ahmed, "Influence of different drying methods on antioxidant activity, total phenol, and phenolic compounds of myrtle (Myrtus communis L.) fruits," *Journal of Food Processing and Preservation*, vol. 45, no. 4, Article ID e15308, 2021.

[19] Y. Li, P. Li, K. Yang et al., "Impact of drying methods on phenolic components and antioxidant activity of sea Buckthorn (Hippophae rhamnoides L.) berries from different varieties in China," *Molecules*, vol. 26, no. 23, p. 7189, 2021.

[20] I. Taneva and Z. Zlatev, "Total phenolic content and antioxidant activity of yoghurt with goji berries (Lycium barbarum)," *Scientific Study & Research. Chemistry & Chemical*

Engineering, Biotechnology, Food Industry, vol. 21, no. 1, pp. 125–131, 2020.

[21] Aoac, *Official Methods of Analysis*, Assoc Anal Chem, Washington, DC, USA, 1990.

[22] D. Kunii and O. Levenspiel, *Fluidization Engineering*, Butterworth-Heinemann, London, UK, second edition, 1991.

[23] D. V. N. Lakshmi, P. Muthukumar, A. Layek, and P. K. Nayak, "Drying kinetics and quality analysis of black turmeric (Curcuma caesia) drying in a mixed mode forced convection solar dryer integrated with thermal energy storage," *Renewable Energy*, vol. 120, pp. 23–34, 2018.

[24] J. E. Vásquez-Parra, C. I. Ochoa-Martínez, and M. Bustos-Parra, "Effect of chemical and physical pretreatments on the convective drying of Cape gooseberry fruits (Physalisperuviana)," *Journal of Food Engineering*, vol. 119, no. 3, pp. 648–654, 2013.

[25] Aoac, "Official method of analysis," *No.21 Ascorbic Acid in Vitamin Preparation and Juices)*, Association of Official Analytical Chemists, Aithersburg, MD, USA, 17th edition, 2000.

[26] J. López, E. Uribe, A. Vega-Gálvez et al., "Effect of air temperature on drying kinetics, vitamin C, antioxidant activity, total phenolic content, non-enzymatic browning and firmness of blueberries variety O Neil," *Food and Bioprocess Technology*, vol. 3, no. 5, pp. 772–777, 2010.

[27] X. N. Chen, J. F. Fan, X. Yue, X. R. Wu, and L. T. Li, "Radical scavenging activity and phenolic compounds in persimmon (Diospyros kaki L. cv. Mopan)," *Journal of Food Science*, vol. 73, no. 1, pp. C24–C28, 2007.

[28] P. Prieto, M. Pineda, and M. Aguilar, "Spectrophotometric quantitation of antioxidant capacity through the formation of a phosphomolybdenum complex: specific application to the determination of vitamin E," *Analytical Biochemistry*, vol. 269, no. 2, pp. 337–341, 1999.

[29] A. Midilli, H. Kucuk, and Z. Yapar, "A new model for single-layer drying," *Drying Technology*, vol. 20, no. 7, pp. 1503–1513, 2002.

[30] K. Luthra and S. S. Sadaka, "Challenges and opportunities associated with drying rough rice in fluidized bed dryers: a review," *Transactions of the ASABE*, vol. 63, no. 3, pp. 583–595, 2020.

[31] M. Yahya, A. Fudholi, and K. Sopian, "Energy and exergy analyses of solar-assisted fluidized bed drying integrated with biomass furnace," *Renewable Energy*, vol. 105, pp. 22–29, 2017.

[32] M. S. Hatamipour and D. Mowla, "Shrinkage of carrots during drying in an inert medium fluidized bed," *Journal of Food Engineering*, vol. 55, no. 3, pp. 247–252, 2002.

[33] H. C. P. Karunasena, "Scanning electron microscopic study of microstructure of gala apples during hot air drying," *Drying Technology*, vol. 32, no. 4, pp. 455–468, 2014.

Hindawi
Journal of Food Quality
Volume 2023, Article ID 6259211, 13 pages
https://doi.org/10.1155/2023/6259211

Research Article

Impact of Different Drying Techniques on Neem Seeds Drying Kinetics and Oil Quality

S. Ganga Kishore,[1,2] **P. Rajkumar**,[2] **P. Sudha**,[2] **J. Deepa**,[2,3] **P. Subramanian**,[4] **J. Gitanjali**,[4] **and R. Pandiselvam**[5]

[1]*Department of Agricultural Engineering, Saveetha Engineering College, Chennai 602105, India*
[2]*Department of Food Process Engineering, Tamil Nadu Agricultural University, Coimbatore 641003, India*
[3]*Department of Food Technology, Hindustan College of Engineering and Technology, Coimbatore 641032, India*
[4]*Department of Renewable Energy Engineering, Tamil Nadu Agricultural University, Coimbatore 641003, India*
[5]*Physiology, Biochemistry and Post-Harvest Technology Division, ICAR-Central Plantation Crops Research Institute, Kasaragod 671124, Kerala, India*

Correspondence should be addressed to R. Pandiselvam; r.pandiselvam@icar.gov.in

Received 16 September 2022; Revised 18 April 2023; Accepted 22 May 2023; Published 30 May 2023

Academic Editor: Gianfranco Picone

Neem oil is a promising alternative for synthetic chemicals in food preservation and an active functional agent in food packaging. Drying studies were conducted on neem seeds using different drying methods, and the oil yield profile and nutritional content such as azadirachtin content, functional groups, and elemental composition were analysed. Tray drying at 60°C showed a faster drying rate with a minimum quality of the oil. The process parameters were statistically optimized by analysing the effect of drying methods and thickness (15 and 30 mm) on azadirachtin content and oil yield. Maximum oil yield and azadirachtin content of 42.1 and 0.053% were obtained in solar drying with 15 mm bed thickness. Fourier-transform infrared spectroscopy analysis showed that there is no change in the functional group when the neem seeds were dried, and the peak absorption wavenumber confirmed the presence of O-H stretching, C-H stretching, C-O stretching, C-H bending, O-H bending, C=O stretching, and N-H stretching. Sun- and solar-dried neem seeds showed maximum retention in elemental composition when compared to the tray-drying method.

1. Introduction

Neem (*Azadirachta indica*) which is known as "Geed Hindi" in Somalia which means that "the Indian tree" belongs to the mahogany family "Meliaceae." There are about 14 million neem trees in India which can grow well up to 40 to 60 feet high in all types of soil [1]. Neem oil has excellent antibacterial, antifungal, antioxidant, and plasticizer properties and finds its applications in food preservation, packaging, and storage due to the presence of bioactive phytochemicals such as azadirachtin, salannin, nimbidin, gedunin, nimbin, isomargolonone, margolone, nimbolide, and margolone. Neem oil is an attractive choice for active food packaging applications due to its antibacterial and antioxidant characteristics with maximum tensile strength, elongation, and transparency [2]. Neem fruit pulp represents, about half the weight of neem fruits which serves as a carbohydrate, a rich substrate for industrial fermentations [3].

Neem tree seeks attention worldwide due to its medicinal properties in the field of ayurveda and due to the presence of azadirachtin ($C_{35}H_{44}O_{16}$), a tetranortriterpenoid. Apart from azadirachtin, it also contains other bioactive components such as nimbin, nimbinin, nimbidin, oleic stearic and palmitic acids, quercetin, and other limonoids. Neem seed area, oil content, and azadirachtin content vary among individual tree and agroclimatic zones of India [4].

The neem tree starts fruiting after 3 to 5 years of planting and yields upto 50 kg of neem fruits annually from the 10th

year onwards. Neem fruit is usually oval or nearly round in shape which has a thin exocarp, yellowish white mesocarp (bittersweet pulp) of thickness in the range of 3–5 mm, and the endocarp has a white hard inner shell containing brown kernel which contains 25–45% oil [5].

Neem oil is a vegetable oil which contains high fatty acids and low terpene content which adds an advantage over tea tree oil. It is also used in medicines, soap industries, and cosmetics and can also be used as a mosquito repellent [4]. Every year neem tree yields 3.5 million tonnes of kernels which can produce 7 lakh tonnes of neem oil. Due to a lack of processing equipment, India produces only 2.5 lakh tonnes of the total oil which is just 30% of the total potential [6].

Neem fruit contains 40 to 60% of water which makes it a highly perishable product and the depulping followed by drying has to be performed within 3 to 4 days to maintain its oil quality [7]. It is reported that 50% of the neem seeds collected have been wasted as there is no attention among researchers and there is a lack of depulping facilities. The manual processing of neem fruits is laborious and time-consuming and the quality of the oil is greatly affected [1]. Timely depulping and drying are required to get a good quality oil.

Previous works are available on the aspects of different methods for extracting oil from neem seeds and analysing the azadirachtin content. However, to the best of our knowledge there is no study regarding the effect of different drying methods on azadirachtin content, oil yield, and quality parameters of neem oil and seed cake. To address this limitation and to reduce the wastage of neem seeds, this study has been attempted to dry the neem seeds using different drying methods with the following objectives:

(1) To study the drying characteristics of neem seeds under different drying methods

(2) To analyse and compare the effect of drying methods on the quality of neem seeds

2. Material and Methods

2.1. Collection of Neem Fruits. Fresh neem fruits were collected from Forestry College and Research Institute, Mettupalayam, India, and were used for the oil production. The pulp of the fresh neem fruits (38% w.b.) was removed using the single drum neem fruit depulper (capacity: 125 kg/h and depulping efficiency: 94.29%) developed by the Department of Food Process Engineering, Tamil Nadu Agricultural University (TNAU), India.

2.2. Drying Studies. During March 2022, 50 kg of depulped neem seeds having a moisture content of 30% (w.b.) were sun-dried (2 days) at an average temperature of 35 ± 5°C and 45 ± 5% RH. Similarly, 100 kg of seeds were dried in a compound parabolic collector (CPC) solar dryer at 45 ± 5°C and a tray dryer at 40 ± 2, 50 ± 2 and 60 ± 2°C until they reached a final moisture content of 8% (w.b.). The weight of the neem seeds was measured using an electronic weighing balance (Ohaus Corporation, NJ, USA) with an accuracy of ±0.01 g at every one-hour interval. The drying characteristics of the neem seeds and the quality of the oil obtained from the neem seeds were evaluated.

2.2.1. Open Sun Drying. Neem seeds were dried under the open sun from 9.00 a.m. to 5.00 p.m. Since black painted trays (41 × 81 × 4 cm) absorb more heat, they were used instead of regular trays. Ten kilograms of fresh neem seeds with an initial moisture content of 30% (w.b.) were kept in black-painted trays in the open sun until they reached a moisture content of 8% (w.b.).

2.2.2. Solar Drying. Solar drying of neem seeds was carried out in a CPC type of solar dryer (1.98 m dia. × 2.30 m height with a capacity of 100 kg) provided with temperature and humidity controllers available in the Department of Renewable Energy Engineering, TNAU, India. The experiment was carried out between 9.00 am and 5.00 pm.

2.2.3. Tray Drying. Depulped neem seeds with a moisture content of 30% (w.b.) were dried in a tray dryer (M/s. Teqto Scientific, Coimbatore) available at the Department of Food Process Engineering, AEC & RI, TNAU, India. The constant set temperature of 40 ± 2°C, 50 ± 2°C, and 60 ± 2°C were used in the tray dryer for drying 50 kg of neem seeds until it reached 8% (w.b.) moisture content.

2.3. Estimation of Azadirachtin Content. The azadirachtin content in fresh and dried neem seeds was estimated using the high-performance liquid chromatography method described by Kaushik [8]. Hexane was used as a solvent to extract oil from the seed kernel powder and ethanol was used to extract azadirachtin. Azadirachtin was separated using acetonitrile-water (40 : 60) at a rate of 1 mL·min^{-1} with a monitoring peak of 214 nm. 10 μL of the sample was injected into the HPLC using an autoinjector, and helium was used as a degassing agent.

2.4. Oil Yield. To extract oil from the dried neem seeds, a standardised oil extraction method using a Soxhlet apparatus (NF ISO 734-1) was used. The oil yield percentage was calculated using the following equation as mentioned by Tesfaye and Tefera [9]:

$$\mathrm{OY}\,(\%) = \frac{W_{\mathrm{IN}} - W_{\mathrm{FI}}}{W_{\mathrm{IN}}} \times 100, \tag{1}$$

where OY represents the oil yield, %. W_{IN} and W_{FI} represent the initial weight of the sample placed in the thimble and the final sample weight of the dried sample in the oven, g.

2.5. Physiochemical Properties of Oil. The specific gravity was determined using the AOAC method (1984). Standardized methods were used to determine the density (AFNOR T60−214), viscosity (ASTM D−445), iodine value (AFNOR T60−203), and peroxide value (AFNOR T60−220). The acid and saponification values were determined using the AOAC recommended methods (1990). The color value (lightness (L^*),

Table 1: Experimental design for the optimization of azadirachtin content and oil yield.

Variable	Independent variable		Dependent variable
Number	Temperature, °C	Bed thickness, mm	(1) Azadirachtin content, % (2) Oil yield, %
Levels	Sun drying (35 ± 5) Solar drying (45 ± 5)Tray drying (40 ± 2, 50 ± 2 and 60 ± 2)	15 ± 1 and 30 ± 1	

redness to greenness (a^*), yellowness to blueness (b^*), and ΔE) of the extracted neem oil was determined using a Lovibond Tintometer (Lovibond, LC 100, The Tintometer Ltd., UK).

2.6. Particle Size Analysis. Fresh and dried neem seeds were powdered using a ball mill (Yatherm Scientific, India). The particle size analyser (Horiba Scientific, SZ-100) was used to measure the particle size of the powdered samples (fresh and dried neem seeds).

2.7. FTIR Analysis. FTIR (fourier-transmission infrared) spectrometer (model number: FT/IR-6800, incident angle: 45°, detector: TGS, accumulation: 64, resolution: 4 cm^{-1}, zero filling: on, apodization: cosine, gain: auto (8), aperture: auto (7.1 mm), scanning speed: auto (2 mm/sec), and filter: auto (10000 hz)) was used to analyse the functional groups present in the samples. It consisted of a source, interferometer, beam splitter, fixed mirror, movable mirror, sample holder, and a detector. FTIR sampling procedure was used to analyse the functional groups in powdered fresh and dried neem seeds as mentioned by Elzey et al. [10].

2.8. Elemental Analysis. Inductively coupled plasma mass spectrometer (model: Thermo Scientific™ ICAP™ RQ, type: single quadrupole ICP-MS, hertz: 2 MHz, nebulizer: borosilicate glass, and spray chamber: quartz, cyclonic) was used to analyse the elements present in the samples. The elemental composition of 7 Li (lithium), 24 Mg (magnesium), 39 K (potassium), 48 Ti (titanium), 51 V (vanadium), 52 Cr (chromium), 55 Mn (manganese), 57 Fe (iron), 59 Co (cobalt), 60 Ni (nickel), 75 As (arsenic), 133 Cs (cesium), 63 Cu (copper), 23 Na (sodium), 44 Ca (calcium), 11 B (boron), 121 Sb (antimony), 31 P (phosphorus), 66 Zn (zinc), 95 Mo (molybdenum), 111 Cd (cadmium), 118 Sn (tin), and 208 Pb (lead) in fresh and dried neem seeds were evaluated using the standard ICPMS procedure as mentioned by Novotnik et al. [11].

2.9. Statistical Optimization. The experimental data were statistically analysed using the central composite design (CCD) technique from Design Expert Software (Version 13.0) and SPSS 2020 software (IBM Corporation, New York, USA). The regression coefficients were calculated using the quadratic model. The analysis of variance (ANOVA) was used to identify the model's significant terms. Drying methods and bed thickness were investigated for their effects on azadirachtin content and oil yield. Table 1 shows the dependent and independent variables used in the experimental design.

3. Results and Discussion

3.1. Drying Studies. The drying characteristics curve (moisture content and drying time) of neem seeds dried in a tray dryer, solar dryer, and sun drying is shown in Figures 1(a)–1(c)–3. The moisture content of neem seeds decreased from 30% to 8% (w.b.) in 300 and 240 minutes of tray drying, respectively, a with bed thickness of 30 and 15 mm at a constant temperature of 60 ± 2°C. It was also noted that there was an increase in the drying time of 480 and 420 minutes at 30 and 15 mm bed thicknesses when the temperature was reduced to 50 ± 2°C. Furthermore, a decrease in temperature to 40 ± 2°C resulted in an increased drying time of 660 and 590 minutes, at 30 and 15 mm bed thicknesses for drying neem seeds from 30% to 8% (w.b.) moisture content.

In solar drying, the time required to dry neem seeds with a bed thickness of 30 and 15 mm from an initial value of 30% (w.b.) to a final value of 8% (w.b.) was recorded at 540 and 420 minutes, respectively, with the maximum recorded temperature of 50 ± 5°C. Corresponding to sun drying with the same two-bed thicknesses, resulted in a maximum drying time of 780 and 630 minutes to dry neem seeds to 8% (w.b.) moisture content with the maximum recorded temperature of 35 ± 5°C.

It is clear that a higher temperature of 60 ± 2°C reduced the drying time to 300 minutes, whereas sun drying at a low temperature of 35 ± 5°C resulted in the longest drying time of 780 minutes. This is because of higher heat transfer at higher temperatures [12, 13]. Higher vaporisation of water also resulted in faster drying of neem seeds [14].

Figures 4(a)–4(c) to 6 show the drying rate curve of neem seeds dried in a tray dryer, solar dryer, and sun drying. Initially, tray-dried neem seeds at 40, 50, and 60°C showed a drying rate of 0.02 ± 0.01–0.049 ± 0.01 (g/g. min) for different bed thicknesses (15 and 30 mm) until critical moisture content was reached, and then it showed a drying rate from 0.002 ± 0.001 to 0.007 ± 0.001 (g/g. min), respectively. The constant high temperature in tray drying caused faster drying. The drying rate increased as the drying temperature and time increased.

Similarly, an initial drying rate of 0.036 ± 0.01–0.041 ± 0.01 (g/g. min) was observed for solar-dried neem seeds under 15 and 30 mm bed thicknesses, respectively, until a critical moisture content was reached. It showed a falling drying rate of 0.0027 ± 0.0001 (g/g. min) in solar drying after 6 hours. Likewise, the sun-dried neem seeds showed an initial drying rate of 0.022 ± 0.01–0.028 ± 0.01 (g/g. min) followed by a falling drying rate of 0.0006 ± 0.0001 (g/g. min) after 6 hours. This decrease in drying rate was due to the subsurface removal of water from the neem seeds at a lower rate.

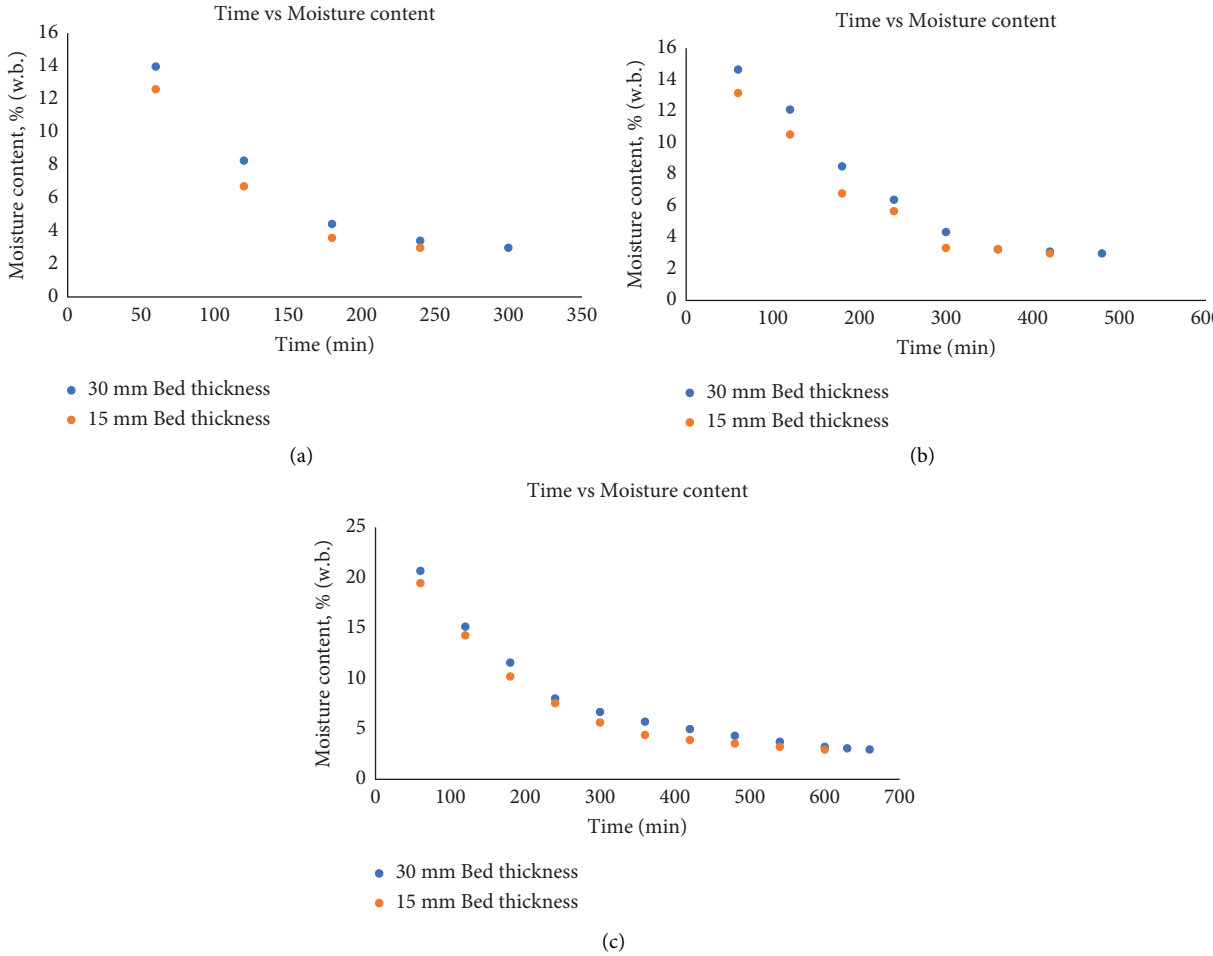

Figure 1: (a) Moisture content of neem seeds under tray drying at 60°C. (b) Moisture content of neem seeds under tray drying at 50°C. (c) Moisture content of neem seeds under tray drying at 40°C.

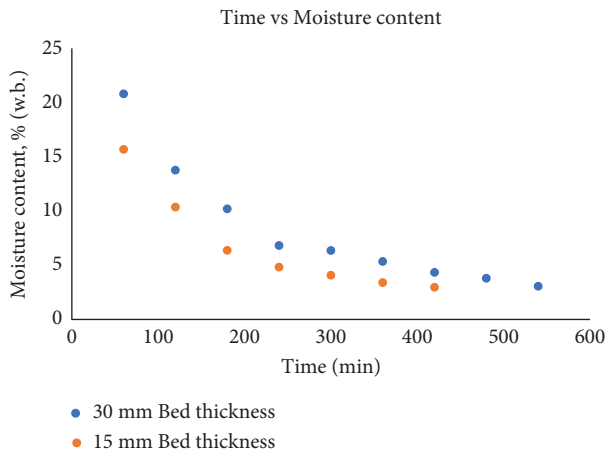

Figure 2: Moisture content of neem seeds under solar drying.

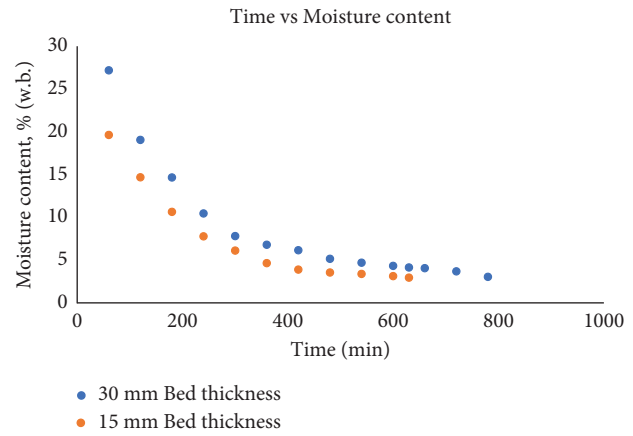

Figure 3: Moisture content of neem seeds under sun drying.

Similar results were obtained by Bhaskara Rao and Murugan [15] for neem leaves drying, Firdissa et al. [16] for Arabica coffee variety drying, Curtis et al. [17] for galip nuts drying, and Olalusi et al. [18] for drying of locust beans Figure 5.

3.2. Effect of the Drying Method and Bed Thickness on Azadirachtin Content. Figures 7(a) and 7(b) show the effect of drying methods and bed thickness on the azadirachtin content of neem seeds. Azadirachtin content of fresh neem seeds was found to be 0.057%. It was observed that the azadirachtin content ranged between 0.040 and 0.054% at

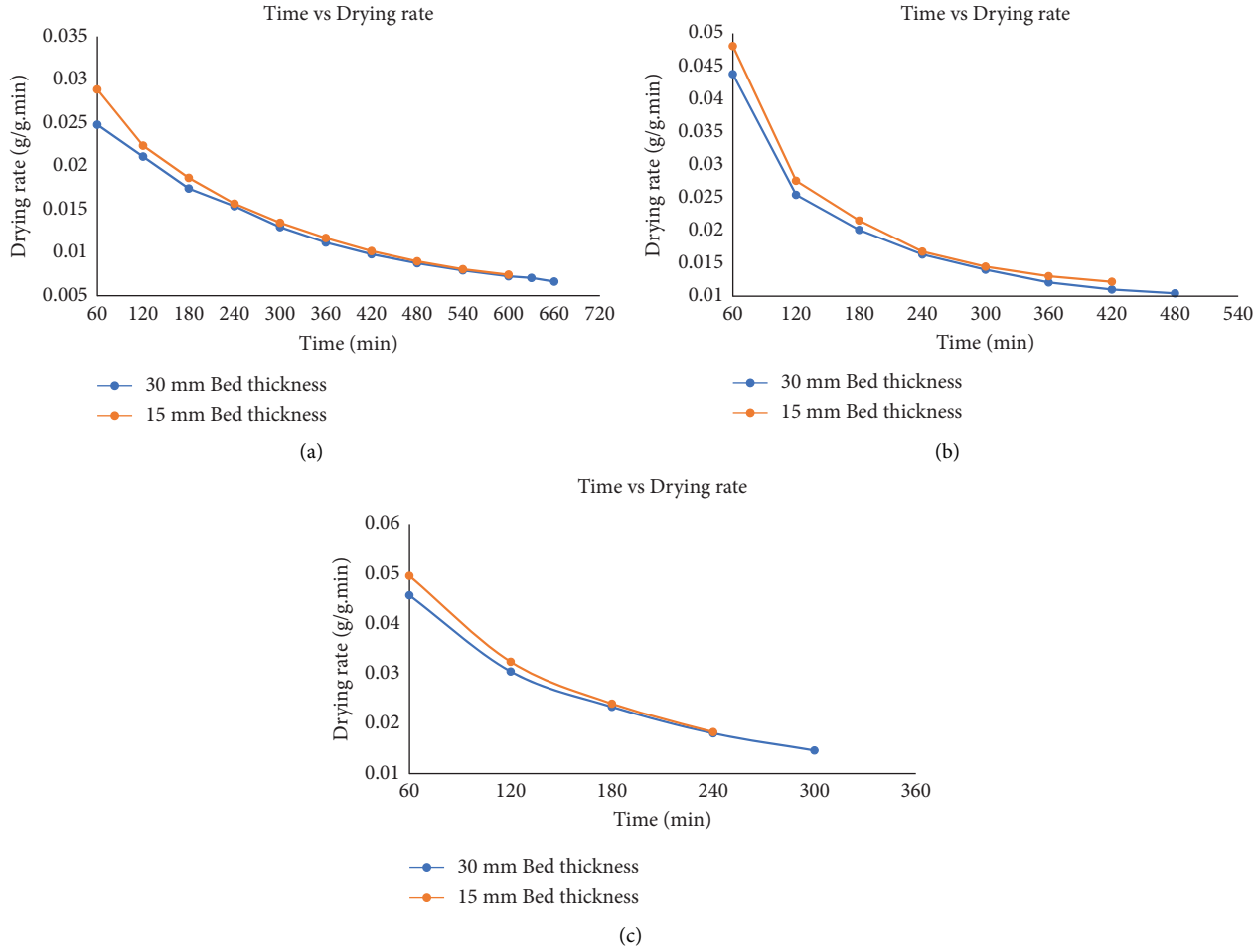

Figure 4: (a) Drying rate of neem seeds under tray drying at 40°C. (b) Drying rate of neem seeds under tray drying at 50°C. (c) Drying rate of neem seeds under tray drying at 60°C.

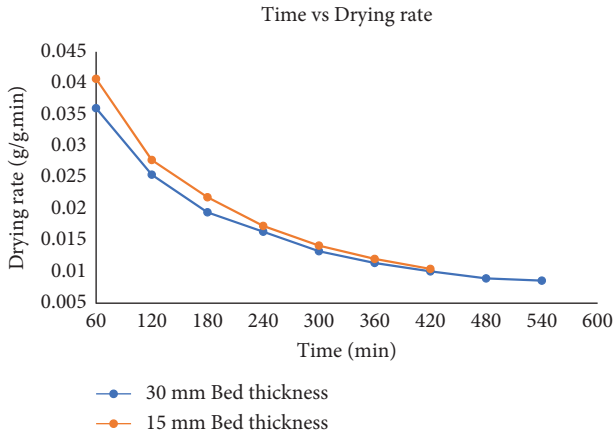

Figure 5: Drying rate of neem seeds under solar drying.

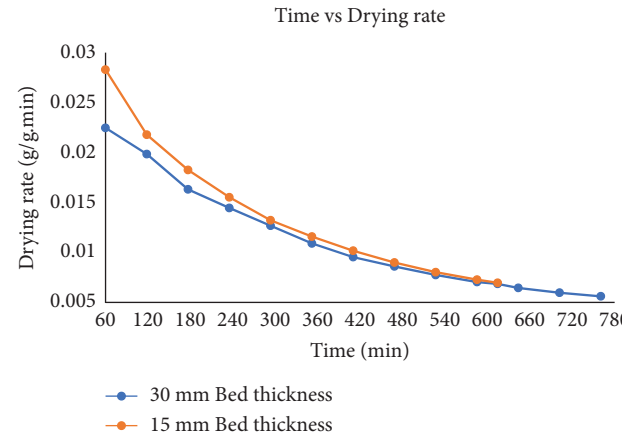

Figure 6: Drying rate of neem seeds under sun drying.

different combinations of drying methods and bed thicknesses. Minimum azadirachtin content in the range of 0.040–0.046% was obtained in the tray drying method at temperature of 60 ± 2°C and a bed thickness of 15 mm. It was noted that with an increase in temperature above 50 ± 2°C in tray drying, a decrease in azadirachtin content was observed. This might be due to the exposure of neem seeds to more heat which resulted in the reduction of the azadirachtin content.

Similar results were reported by Bhaskara Rao and Murugan [15] for neem leaves drying and Firdissa et al. [16] for Arabica coffee variety drying. Maximum temperature of up to 50 ± 2°C in tray drying resulted in azadirachtin content

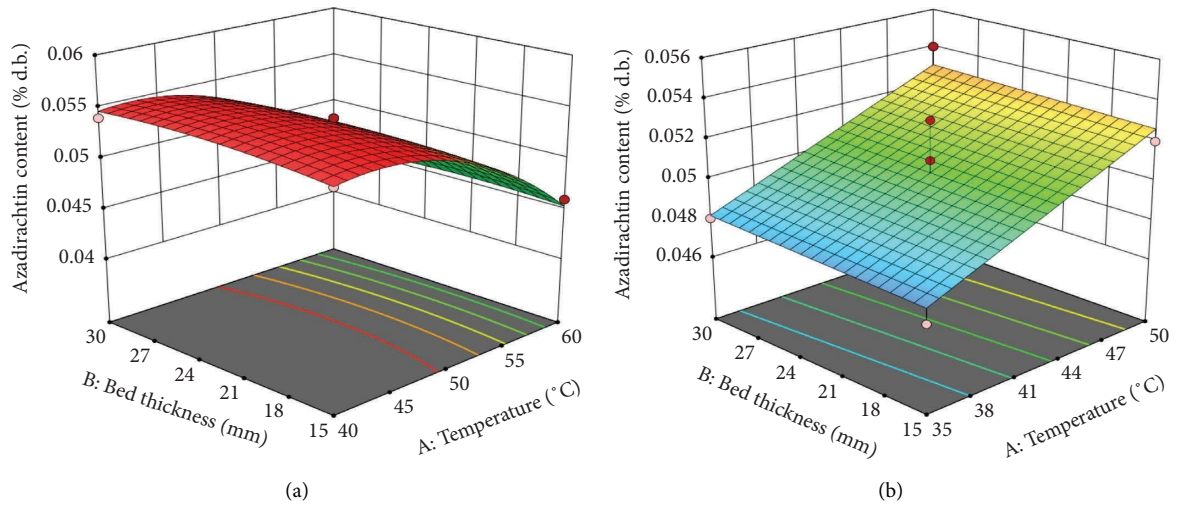

Figure 7: (a) Effect of tray drying and bed thickness on azadirachtin content. (b) Effect of drying methods (sun and solar drying) and bed thickness on azadirachtin content.

in the range of 0.049–0.054%. Decreasing the bed thickness to 15 mm, resulted in the azadirachtin content of 0.046–0.051% for different combinations of tray drying with the temperature of 40 ± 2 and 50 ± 2°C. Azadirachtin content of 0.040–0.049% and 0.048–0.054% was obtained in sun and solar drying at the temperatures of 35 ± 5 and 45 ± 5°C with 15 and 30 mm bed thicknesses, respectively.

Tables 2 and 3 show the F value of the statistically analysed azadirachtin content of neem seeds dried under different drying methods (sun, solar, and tray drying) and bed thicknesses. The R^2 value was found to be 0.988 for the different combinations of tray drying (40, 50, and 60°C) and bed thickness (15 and 30 mm). Whereas, sun and solar drying with 15 and 30 mm bed thickness had an R^2 value of 0.712. The suggested quadratic model revealed that different drying methods and bed thickness had a significant effect on azadirachtin content ($p \leq 0.05$). The azadirachtin content was statistically analysed and mentioned in the following equations:

$$\begin{aligned}\text{Azadirachtin content } (\%) = {} & +0.0536 - 0.0046A + 0.0001B \\ & - 0.0002AB - 0.0033A^2 \\ & - 0.0006B^2,\end{aligned} \tag{2}$$

$$\text{Azadirachtin content } (\%) = +0.050 + 0.0024A + 0.0001B. \tag{3}$$

3.3. Effect of the Drying Method and Bed Thickness on Oil Yield. The effect of drying methods and bed thickness on oil yield is shown in Figures 8(a) and 8(b). It was observed that a minimum oil yield of 33–37% was obtained at a minimum temperature of 35 ± 5 and 40 ± 2°C in sun and tray drying with a maximum bed thickness of 30 mm, respectively. This decrease in oil yield might be due to less exposure of heat to the neem seeds. Increasing the temperature and decreasing the bed thickness to 50 ± 2°C and 15 mm in tray drying resulted in an increase in oil yield from 40.3 to 42.5%. The solar (45 ± 5°C) and tray drying (50 ± 2 and 60 ± 2°C) with bed thickness of 15 mm resulted in a maximum oil yield of 42.5–45.6%, respectively.

Similar work of oil extraction from neem seeds by Tesfaye and Tefera [9] and Djibril et al. [19] showed an oil yield of 43.71% and 48.98 ± 0.34%, respectively. A little lower oil yield of 32.5% was obtained in neem seed kernels using 50% of ethanol as solvent by Saha et al. [20]. Also, a maximum oil yield of 53.5% was obtained by Subramanian et al. [21] at an optimum condition of extraction time (6 h) using a solvent mixture of 50 : 50 (n-hexane : ethanol).

The combination of drying methods and bed thickness showed a significant effect at ($p \leq 0.05$) on oil yield with an R^2 value of 0.981 and 0.966 using the suggested quadratic model as shown in Tables 2 and 3. The obtained data were statistically analysed and are represented by the following equations:

$$\begin{aligned}\text{Oil yield } (\%) = {} & +40.92 + 4.34A - 2.19B + 0.7750\text{AB} \\ & - 0.6350A^2 - 0.9100B^2,\end{aligned} \tag{4}$$

$$\begin{aligned}\text{Oil yield } (\%) = {} & +41.52 + 5.50A - 1.81B + 0.025\text{AB} \\ & - 1.81A^2 - 1.33B^2.\end{aligned} \tag{5}$$

3.4. Optimization of Process Parameters. The experimental results showed a maximum azadirachtin content of 0.050–0.054% at different combinations of drying methods and bed thicknesses (solar and tray drying with 15 and 30 mm). The central composite design was used to find the optimum combination of temperature and bed thickness, which resulted in maximum azadirachtin content and oil yield. The RSM showed that the maximum azadirachtin content and oil yield of 0.052 and 0.054%, 42.1, and 45.6%, respectively was obtained under solar (45 ± 5°C) and tray drying (50 ± 2°C) at a bed thickness of 15 mm with

Table 2: Analysis of variance of effects of different combinations of tray drying and bed thickness on azadirachtin content and oil yield.

Source	Degrees of freedom	Azadirachtin content (%) F value*	Oil yield (%) F value
Model	5	118.15	72.36
Temperature (°C) (A)	1	407.48	273.89
Bed thickness (mm) (B)	1	0.0516	69.64
AB	1	0.6018	4.37
A^2	1	182.37	5.10
B^2	1	5.07	10.47

* Fvalue-ANOVA coefficient (it is the ratio between the mean sum of squares between the groups to the mean sum of squares within the groups).

Table 3: Analysis of variance of effects of different combinations of drying methods (sun and solar drying) and bed thickness on azadirachtin content and oil yield.

Source	Degrees of freedom	Azadirachtin content (%) F value*	Oil yield (%) F value
Model	5	12.37	37.97
Temperature (°C) (A)	1	24.59	153.26
Bed thickness (mm) (B)	1	0.1628	16.69
AB	1	—	0.0016
A^2	1	—	14.46
B^2	1	—	7.87

* Fvalue-ANOVA coefficient (it is the ratio between the mean sum of squares between the groups to the mean sum of squares within the groups).

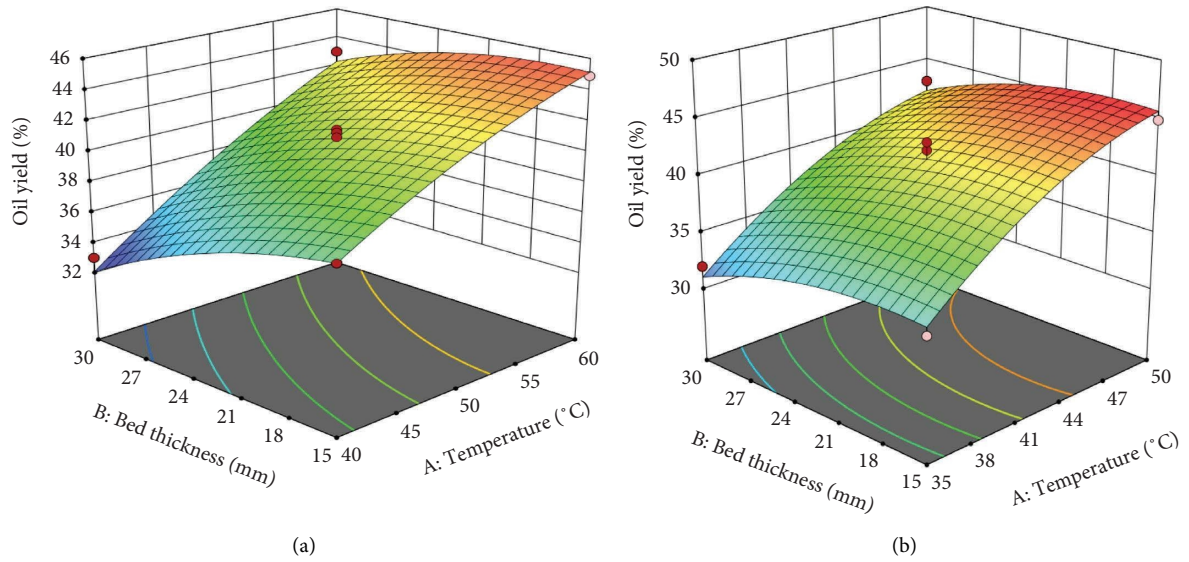

Figure 8: (a) Effect of tray drying and bed thickness on oil content. (b) Effect of drying methods (sun and solar drying) and bed thickness on oil yield.

a desirability value of 0.88 and 0.93 and was found to be statistically significant at $p \leq 0.05$. The optimum combination of azadirachtin content and oil yield is shown in Figure 9.

3.5. Quality Analysis. Quality analyses were carried out for the dried neem seeds and oil obtained from different drying methods i.e., sun drying (35 ± 5°C), solar drying (45 ± 5°C), and tray drying (50 ± 2°C). Since the optimized drying combination of tray drying (50 ± 2°C with 15 mm bed thickness) showed maximum azadirachtin content and oil yield, this combination was used for quality analysis.

3.6. Physiochemical Properties of Oil. Figures 10(a)–10(e) show the physicochemical properties of oil obtained from the sun-dried, solar-dried, and tray-dried neem seeds. The oil obtained from the tray-dried neem seeds had a higher specific gravity (0.93 ± 0.008), acid value (8.3 ± 0.18 mg/g), saponification value (189.4 ± 2.90 KOH/g), viscosity (45.21 ± 1.25 mm^2/s), and peroxide value (1.45 ± 0.023 meq of O_2/kg), respectively. When compared to the solar- and sun-dried neem seed oil, the higher temperature in the tray dryer caused lipid hydrolysis, which resulted in oil degradation and indirectly increased acid and peroxide value [9]. The constant set temperature in the tray dryer resulted in

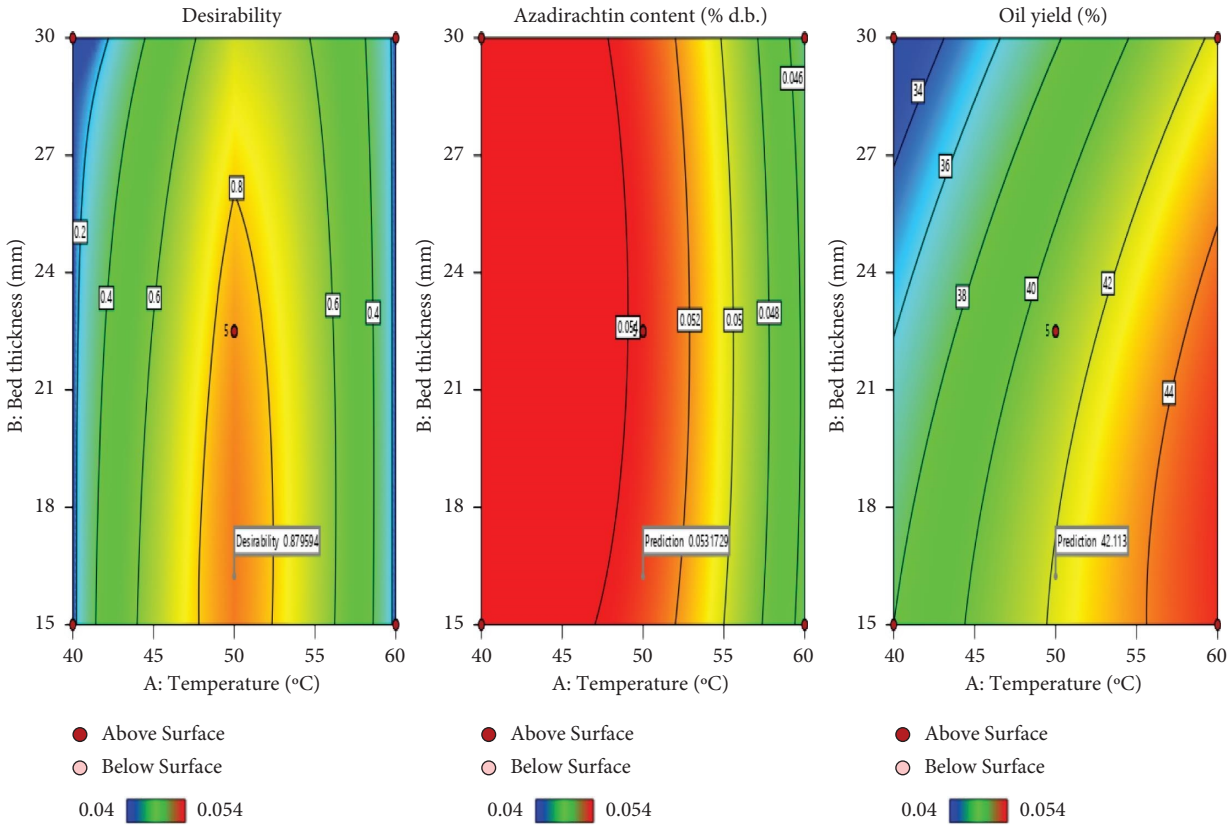

Figure 9: Optimum combination of azadirachtin content and oil yield.

lipid breakdown and a reduction in the molecular weight of the triglycerides present in the oil, resulting in an increased saponification value [9]. The oil of the tray-dried neem seeds was found to be darker than that of the solar- and sun-dried neem seeds.

Similar studies were carried out by Tesfaye and Tefera [9], and they obtained the minimum acid value (14.46 mg KOH/g), saponification value (194.48 mg KOH/g), specific gravity (0.90), and pH (4.86). Also, Djibril et al. [19] found that neem oil had an acid value of 10.2 $mg \cdot g^{-1}$, a saponification value of 200 $mg \cdot g^{-1}$, and an iodine value of 72.8 g. 100 g^{-1} for neem seed. The variations in the quality and quantity of neem oil obtained might be due to the varietal differences and extraction methods.

The color values in terms of L^*, a^*, and b^* were found to be 53.9 ± 0.127, 12.8 ± 0.24, and 35.9 ± 0.42 for sun-dried neem seeds, 36.7 ± 1.173, 10.54 ± 0.344, and 20.21 ± 0.3163 for solar-dried neem seeds, and 26.5 ± 0.143, 7.4 ± 0.153, and 6.3 ± 1.104 for tray-dried neem seeds, respectively. The effect of drying methods on the color value of neem seed oil was statistically significant at $p \leq 0.01$. Due to the increased heat exposure, the L^* value of neem oil decreased as the drying temperature increased [22].

3.7. Particle Size Analysis. Table 4 shows the particle size analysis of fresh and dried powdered neem seed kernels under different drying methods. The particle size of the powdered fresh, sun-, solar-, and tray-dried neem seeds was recorded as 711.5 ± 92.2, 265.3 ± 26.1, 662.0 ± 81.1, and 1335.5 ± 273.3 nm, respectively. The particle size of the tray-dried neem seed powder was found to be higher than the solar- and sun-dried seed powders. This is because of the uniform drying of neem seeds in the tray drying method. Similar to the present work, Shewale and Rathod [23] analysed the different particle sizes of neem leaf powder (0.1–0.2, 0.2–0.3, and 0.3–0.4 mm) to study the effect of drying methods on the phenolic contents of neem. Also, Tesfaye and Tefera [9] analysed the powder size of neem seed (355 μm) for extracting neem oil using the Soxhlet extraction methods. The particle size is also equally important for the effective oil extraction.

3.8. FTIR Analysis. Figure 11 shows the results of the FTIR analysis of powdered fresh and dried neem seeds. It showed the presence of different functional groups in different absorption wave numbers and it was found to be varied among samples based on the drying method opted. The total number of functional groups found in the seeds is 6. Fresh neem seeds showed peaks at a wavenumber of 2970.44, 1737.73, 1375.12, 1220.27, 904.42, and 518.05 cm^{-1}, respectively. Similarly, sun-dried neem seeds showed peaks in the wavelength of 2928.27, 1732.36, 1375.12, 1214.13, 1005.62, and 535.68 cm^{-1}. The solar-dried neem seeds exhibited the peaks at the wavenumber of 2916.78, 1743.86, 1375.12, 1214.13, 1029.38, and 518.05 which was followed by the tray-dried neem seeds at 2910.64, 1732.36, 1380.49,

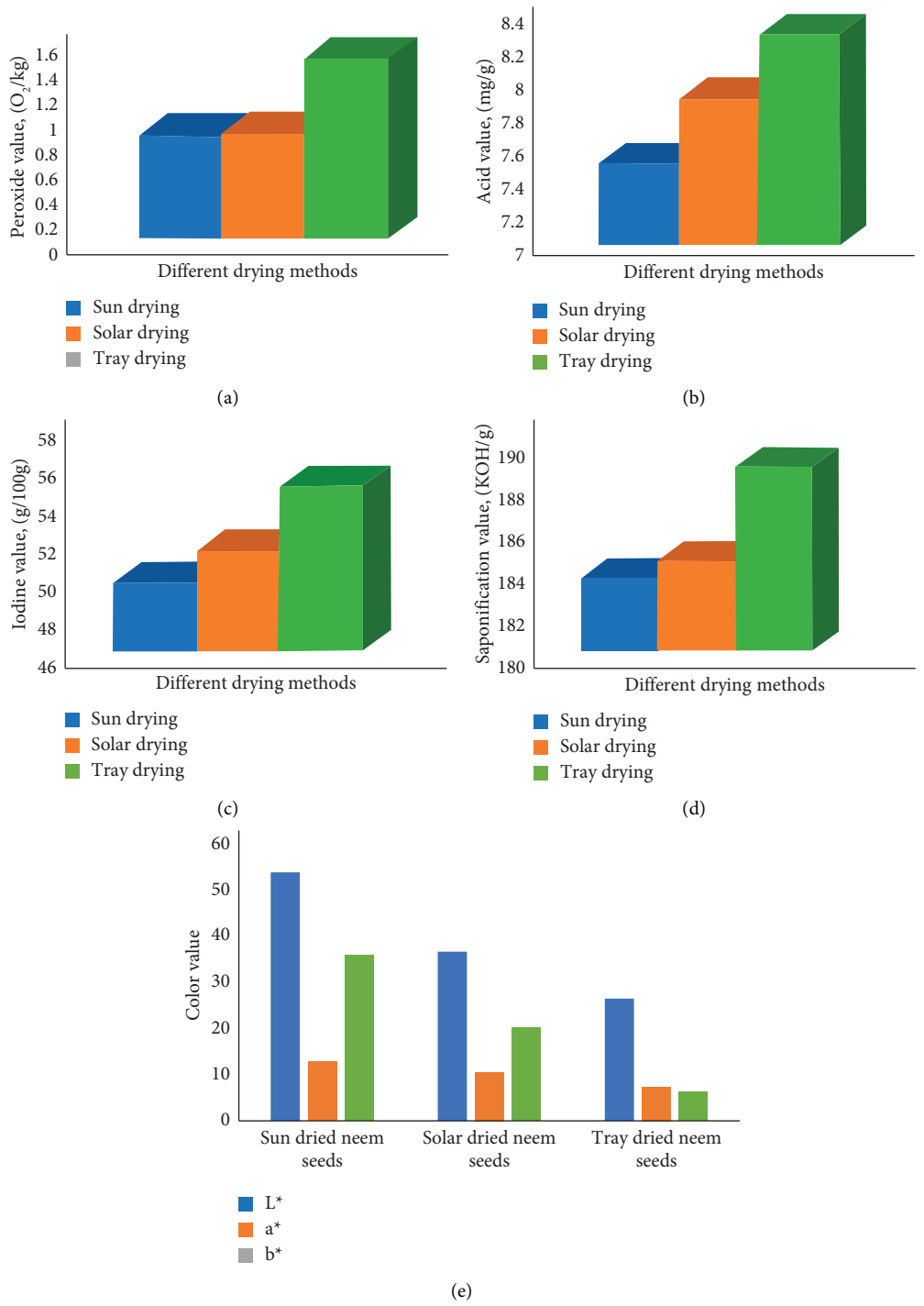

Figure 10: (a) Peroxide value of neem oil under sun, solar, and tray drying. (b) Acid value of neem oil under sun, solar, and tray drying. (c) Iodine value of neem oil under sun, solar, and tray drying. (d) Saponification value of neem oil under sun, solar, and tray drying. (e) Color value of neem oil under sun, solar, and tray drying.

1214.13, and 541.82 cm^{-1}. The spectra of FTIR verified the occurrence of amines, aromatic compounds, carboxylic acid, amino acids, alkyl halide, alkanes, and phenols in the seeds.

The peak absorption wavelength of 2910.64, 2916.78, 2928.27, and 2970.44 represents the C-H stretching vibration modes in the hydrocarbon chain which was observed in fresh, sun-dried, solar-dried, and tray-dried neem seeds. Whereas, the peak values at 1737.73 cm^{-1} matching with the stretching vibrations of the C=O in carboxylic acids, aldehydes, and ketones were found in tray-dried neem seeds and at 1732.36 cm^{-1} in solar-dried neem seeds, and at 1743.86 cm^{-1} in sun-dried neem seeds compared to the fresh neem seeds with a peak value of 1732.36, respectively [24].

Table 4: Particle size analysis of powdered neem seed kernels under different drying methods.

S. No	Method of drying	Particle size of neem seed powder (nm)
1	Fresh neem seeds	711.5 ± 92.2
2	Sun-dried	265.3 ± 26.1
3	Solar-dried	662.0 ± 81.1
4	Tray-dried (50 ± 2°C with 15 mm bed thickness)	1335.5 ± 273.3

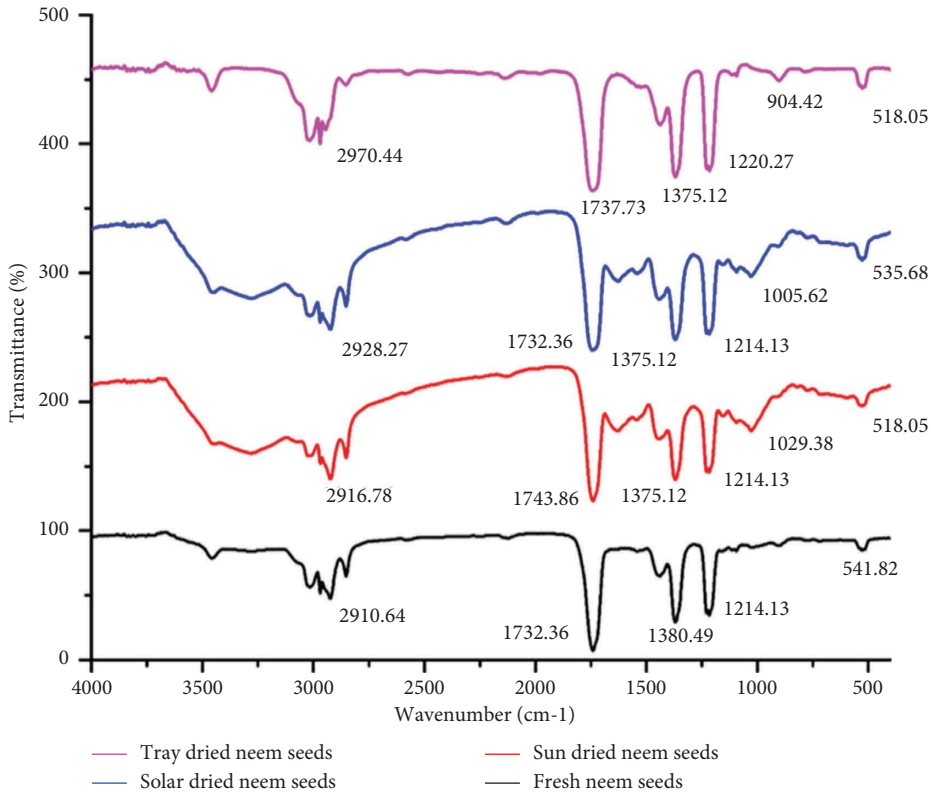

Figure 11: FTIR analysis of powdered neem seeds.

The absorption bands of dried neem seeds in the range of 1375 cm^{-1} were designated to the frequency stretching that comes from the C-O bonds of acetyl esters, C=O, CH_2 wagging, and C-H stretching compared to the peak value of fresh neem seeds at 1380.49 cm^{-1}. It was reported that the aliphatic C-C position occurred in the range of 1214.13–1220.27 cm^{-1} and frequency values of around 1005.62 cm^{-1} in neem seeds was the stretching vibration C-O. The FTIR spectra verified the occurrence of halides, aliphatic amines, aromatic, carboxylic groups, amides, alkanes, and alkenes. Similar to the present study, the presence of the terpenoid group was confirmed with the same level of peak by Senthilkumar and Sivakumar [25].

Similar studies of FTIR spectroscopy on the determination of the composition of adulterated neem and flaxseed oil, performed by Elzey et al. [10] showed that 2900, 1700, and 1100 cm^{-1} confirmed the presence of C-H stretching, C=O stretching, and C-O stretching. Correspondingly, Iqbal et al. [26] studied FTIR analysis for highly stabilized neem oil and mixture (neem and grass oil) emulsion and found that the wavenumber of 1642 and 2928 cm^{-1} was not changed when neem oil was added with grass oil which confirmed that there is no interaction between these oils and other ingredients.

3.9. Elemental Analysis. Elemental compositions such as Li, Mg, K, Ti, V, Cr, Mn, Fe, Co, Ni, As, Ce, Cu, Na, Ca, B, Sb, P, Zn, Mo, Cd, Sn, and Pb are shown in Figure 12.

Increases in the percentage of 117.51, 19.791, 20.662, 20, 15.404, 25.011, 16, 166.667, 192.727, and 10.417 ppm were observed in the elemental composition of Na, Ca, B, Sb, P, Zn, Mo, Cd, Sn, and Pb. The elemental composition was found to be 92.113 ± 0.87, 1359.02 ± 24.04, 4.922 ± 0.137, 0.005 ± 0.0001, 927.7 ± 20.19, 18.636 ± 0.35, 0.075 ± 0.0007, 0.009 ± 0.0002, 0.055 ± 3.742, and 0.432 ± 0.0061 ppm for fresh neem seeds, respectively. The minimum elemental composition of 78.773 ± 0.64, 1442.79 ± 14.72, 5.939 ± 0.044, 0.006 ± 0.34,

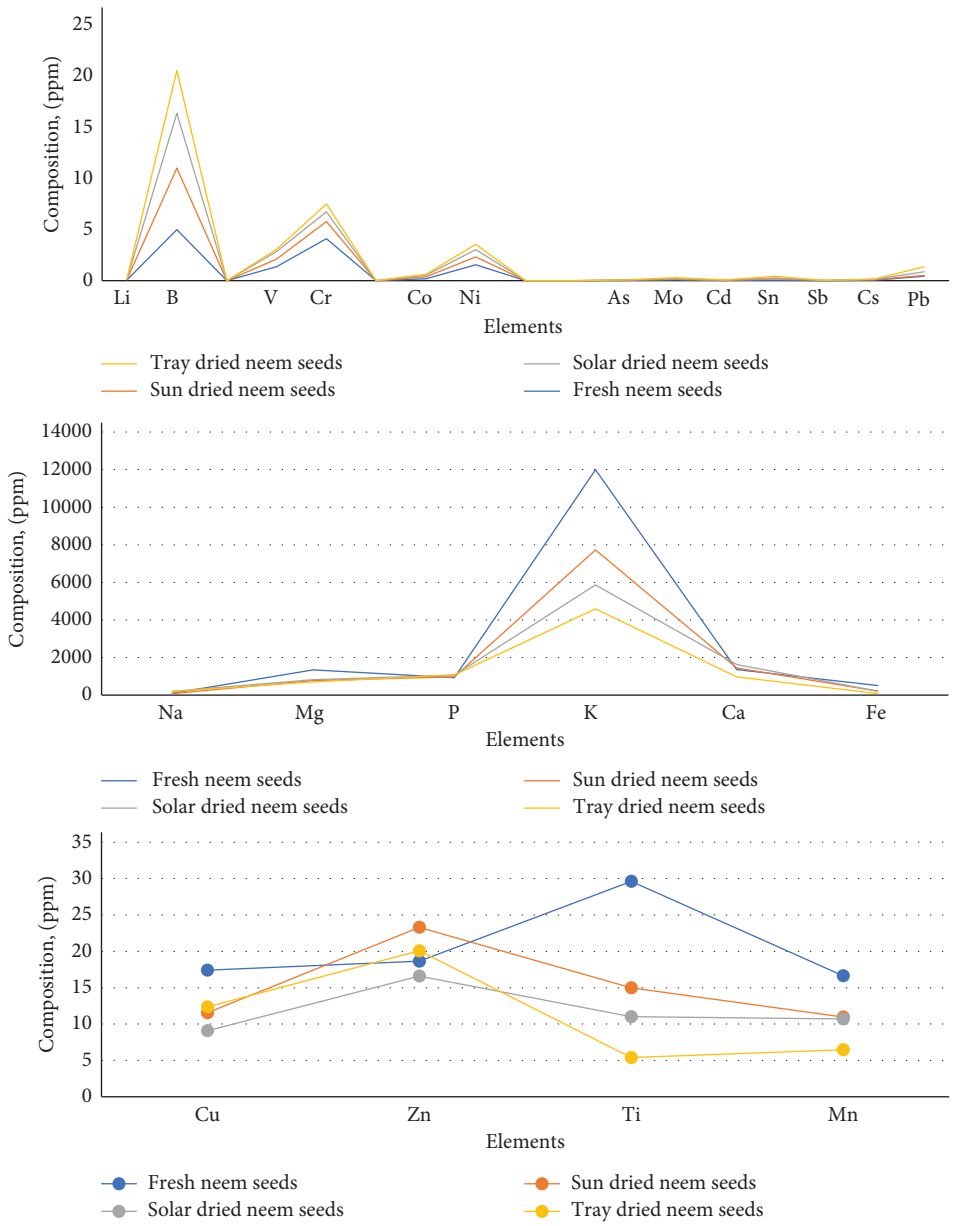

Figure 12: Elemental composition of fresh and dried neem seeds.

964.602 ± 14.43, 23.297 ± 0.634, 0.063 ± 0.0003, 0.023 ± 0.0006, 0.136 ± 0.003, and 0.0675 ± 0.002 ppm were obtained for sun-dried neem seeds. Solar-dried neem seeds showed maximum retention in the elemental composition of 200.356 ± 2.95, 1627.99 ± 34.33, and 5.289 ± 0.028 for Na, Ca, and B. The elemental composition of Sb, P, Zn, Mo, Cd, Sn, and Pb was found to be maximum for tray-dried neem seeds with 0.004 ± 6.25, 1070.6 ± 5.82, 20.076 ± 0.150, 0.087 ± 0.0002, 0.024 ± 0.001, 0.161 ± 0.0004, and 0.477 ± 0.0021 ppm, respectively. This increase in composition was observed since the seeds were concentrated during drying by the removal of water.

Similar studies by Novotnik et al. [11] on neem powder showed that trace elements, namely, Al, Fe, Co, Cu, Ni, Cd, V, Zn, As, Se, M, Pb, and Cr were present in the composition of 3100 ± 10, 1510 ± 40, 1.56 ± 0.02, 19.9 ± 0.2, 17.8 ± 0.8, 0.034 ± 0.001, 9.3 ± 0.4 29, 16.2 ± 0.7, 0.63 ± 0.02, 0.54 ± 0.01, 1.57 ± 0.06, 4.6 ± 0.1, and 197 ± 5 $mg \cdot kg^{-1}$, respectively. Correspondingly, Zhang et al. [27] mentioned that 17 trace elements, namely, B, Na, Ca, Cr, Cd, Cu, Fe, Se, Pb, Al, Mn, Ni, As, Mg, P, K, and Zn was recorded with the composition of 18.86 ± 0.08, 10215 ± 248, 6967 ± 338, 1.75 ± 0.4, 0.024 ± 0.001, 2.7 ± 0.1, 107 ± 20, 0.21 ± 0.00007, 0.257 ± 0.100, 101 ± 4.00, 17.40 ± 0.11, 0.92 ± 0.17, 0.066 ± 0.001, 2487 ± 67, 4873 ± 185, 15860 ± 947, and 26.4 ± 3.7 $\mu g \cdot g^{-1}$ in freeze-dried blueberry and the strawberry. The quality of neem oil depends on the elemental composition and the difference in content might be due to the variety, varying climatic conditions, and extraction techniques [28].

4. Conclusion

In this study, three different drying methods (sun drying, solar drying, and hot air at 40, 50, and 60°C) were applied to

neem seeds and the effects of these drying methods on the azadirachtin content, functional groups, and elemental composition were studied. The drying methods significantly affected the oil yield and azadirachtin content of the neem samples. The optimum conditions for obtaining maximum azadirachtin and oil yield were found in solar drying at a bed thickness of 15 mm. Based on the study, there was a change in the quality of the oil for different drying methods and this might be because of an increase in temperature and drying time. Regarding the functional groups, FTIR results showed that there is no change in functional groups when the neem seeds are dried under different drying methods without allowing the functional compounds to degrade in the specified temperature ranges. Among the drying methods, sun-dried samples showed the least values of elemental composition while solar-dried and hot air-dried samples contributed to the maximum retention of elements. This study will be highly useful for food sectors that use neem oil in preservation, packaging, and storage.

5. Disclosure

The first author and third author presented the same work "Impact of different drying techniques on neem seeds drying kinetics and oil quality" in International Symposium "Agricultural Engineering Innovation for Global Food Security and India @2047: Agricultural Engineering Perspective" organized by Indian Society of Agricultural Engineers, New Delhi, and Agricultural Engineering College and Research Institute, Tamil Nadu Agricultural University, Coimbatore, India.

Data Availability

The data that support the findings of this study are available from the corresponding author upon reasonable request.

Conflicts of Interest

The authors declare that they have no conflicts of interest.

Acknowledgments

The authors (P. Rajkumar and P. Sudha) gratefully acknowledge the funding of the Coromandel International Limited (Bioproduct division), Chennai, for this research work.

References

[1] M. A. Adedeji and O. K. Owolarafe, "Some physical properties of neem seeds & kernels (*Azadirachta indica*) as a function of moisture content," *Carbon*, vol. 86, pp. 78–92, 2015.

[2] S. Sanuja, A. Agalya, and M. J. Umapathy, "Synthesis and characterization of zinc oxide – neem oil – chitosan bio nanocomposite for food packaging application," *International Journal of Biological Macromolecules*, vol. 74, pp. 76–84, 2015.

[3] P. Kumar, N. Singh, L. S. Devi et al., "Neem oil and its nanoemulsion in sustainable food preservation and packaging: Neem oil and its nanoemulsion in sustainable food preservation and packaging: Current status and future prospectsurrent status and future prospects," *Journal of Agriculture and Food Research*, vol. 7, Article ID 100254, 2022.

[4] S. Dubhashi, V. Pranay, M. Singaiah, J. Satwik, V. V. L. N. Prasad, and P. V. Diwan, "Studies on extraction and HPLC analysis of azadirachtin from kernels of neem seeds," *Journal of Advanced Pharmacy Education & Research*, vol. 3, no. 1, pp. 27–30, 2013.

[5] S. H. Heroor and S. R. Bharadwaj, "Production of bio-fuel from crude neem oil and its performance," *International Journal of Environmental Engineering and Management*, vol. 4, no. 5, pp. 425–432, 2013.

[6] R. C. Solanki, S. N. Naik, S. Santosh, and A. P. Srivastava, "Design, development and evaluation of neem depulper," *Agricultural Mechanization in Asia Africa and Latin America*, vol. 48, no. 4, p. 46, 2017.

[7] N. D. Bup, E. N. Aweh, and I. N. Mbangsi, "Physical properties of neem (*Azadirachta indicaa. juss*) fruits, nuts and kernels," *Sky Journal of Food Science*, vol. 2, no. 8, pp. 14–23, 2013.

[8] N. Kaushik, "Determination of azadirachtin and fatty acid methyl esters of Azadirachta indica seeds by HPLC and GLC," *Analytical and Bioanalytical Chemistry*, vol. 374, no. 7-8, pp. 1199–1204, 2002.

[9] B. Tesfaye and T. Tefera, "Extraction of essential oil from neem seed by using soxhlet extraction methods," *International Journal of Advanced Engineering, Management and Science*, vol. 3, no. 6, pp. 646–650, 2017.

[10] B. Elzey, D. Pollard, and S. O. O. Fakayode, "Determination of adulterated neem and flaxseed oil compositions by FTIR spectroscopy and multivariate regression analysis," *Food Control*, vol. 68, pp. 303–309, 2016.

[11] B. Novotnik, T. Zuliani, J. Ščančar, and R. Milačič, "Content of trace elements and chromium speciation in Neem powder and tea infusions," *Journal of Trace Elements in Medicine and Biology*, vol. 31, pp. 98–106, 2015.

[12] G. Jeevarathinam, R. Pandiselvam, T. Pandiarajan et al., "Infrared assisted hot air dryer for turmeric slices: Infrared assisted hot air dryer for turmeric slices:Effect on drying rate and quality parametersffect on drying rate and quality parameters," vol. 144, Article ID 111258, 2021.

[13] D. S. A. Delfiya, K. Prashob, S. Murali et al., "Drying kinetics of food materials in infrared radiation drying: Drying kinetics of food materials in infrared radiation drying: A review review," *Journal of Food Process Engineering*, vol. 45, no. 6, Article ID e13810, 2022.

[14] R. Richa, N. C. Shahi, U. C. Lohani et al., "Design and development of resistance heating apparatus-cum-solar drying system for enhancing fish drying rate," *Journal of Food Process Engineering*, vol. 45, no. 6, Article ID e13839, 2022.

[15] T. S. Bhaskara Rao and S. Murugan, "Experimental investigation of drying neem (*Azadirachta indica*) in an evacuated tube solar dryer: performance, drying kinetics and characterization," *Solar Energy*, vol. 253, pp. 270–284, 2023.

[16] E. Firdissa, A. Mohammed, G. Berecha, and W. Garedew, "Coffee Coffee Drying and Processing Method Influence Quality of Arabica Coffee Varieties (Coffee arabica L.) at Gomma I and Limmu Kossa, Southwest Ethiopiarying and processing method influence quality of Arabica coffee varieties (*Coffee arabica L.*) at gomma I and limmu kossa, southwest Ethiopia," *Journal of Food Quality*, vol. 2022, Article ID 9184374, 8 pages, 2022.

[17] T. Curtis, R. Corkish, R. J. Fuller, and A. B. Sproul, *A mixed mode low profile solar tunnel dryer for canarium indicum nuts*, Deakin University, Geelong, Australia, 2015.

[18] A. P. Olalusi, M. O. Omosebi, and O. Y. Agbola, "Influence of drying methods on the drying characteristics and nutritional quality of fermented Locust beans," *International Journal of Environment, Agriculture and Biotechnology*, vol. 4, no. 6, pp. 1695–1703, 2019.

[19] D. Djibril, F. Mamadou, V. Gérard, M. D. C. Geuye, S. Oumar, and R. Luc, "Physical characteristics, chemical composition and distribution of constituents of the neem seeds (*Azadirachta indica A. Juss*) collected in Senegal," *Research Journal of Chemical Sciences*, vol. 3, no. 2, pp. 606–612, 2015.

[20] S. Saha, D. Singh, S. Rangari et al., "Extraction optimization of neem bioactives from neem seed kernel by ultrasonic assisted extraction and profiling by UPLC-QTOF-ESI-MS," *Sustainable Chemistry and Pharmacy*, vol. 29, Article ID 100747, 2022.

[21] S. Subramanian, R. T. Bachmann, and M. S. Hossain, "Simultaneous extraction and separation of oil and azadirachtin from seeds and leaves of Azadirachta indica using binary solvent extraction," *Natural Product Sciences*, vol. 25, no. 2, pp. 150–156, 2019.

[22] S. Turan, S. Keskin, and R. Solak, "Determination of the changes in sunflower oil during frying of leavened doughs using response surface methodology," *Journal of Food Science and Technology*, vol. 59, no. 1, pp. 65–74, 2022.

[23] S. Shewale and V. K. K. Rathod, "Extraction of total phenolic content from *Azadirachta indica* or (neem) leaves: kinetics study," *Preparative Biochemistry & Biotechnology*, vol. 48, no. 4, pp. 312–320, 2018.

[24] A. A. Oyekanmi, U. S. U. Kumar, N. G. Olaiya et al., "Functional Functional Properties of Antimicrobial Neem Leaves Extract Based Macroalgae Biofilms for Potential Use as Active Dry Packaging Applicationsroperties of antimicrobial neem leaves extract based macroalgae biofilms for potential use as active dry packaging applications," *Polymers*, vol. 13, no. 10, p. 1664, 2021.

[25] S. R. Senthilkumar and T. Sivakumar, "Green tea (Camellia sinensis) mediated synthesis of zinc oxide (ZnO) nanoparticles and studies on their antimicrobial activities," *International Journal of Pharmacy and Pharmaceutical Sciences*, vol. 6, no. 6, pp. 461–465, 2014.

[26] N. Iqbal, N. Kumar, A. Agrawal, and J. Kumar, "Development of highly stabilized neem oil microemulsion system: a green approach," *World Journal of Pharmaceutical Research, Microemulsion Formulation of Botanical Oils as an Efficient Tool to Provide Sustainable*, vol. 8, no. 3, pp. 1507–1517, 2019.

[27] H. Zhang, Z. Y. Wang, X. Yang et al., "Determination of free amino acids and 18 elements in freeze-dried strawberry and blueberry fruit using an Amino Acid Analyzer and ICP-MS with micro-wave digestion," *Food Chemistry*, vol. 147, pp. 189–194, 2014.

[28] P. Sudha and S. Ganga Kishore, "Impact of Different Drying Techniques on Neem Seeds Drying Kinetics and Oil Quality," *International Symposium on Agricultural Engineering Innovation for Global Food Security and India @2047: Agricultural Engineering Perspective*, Indian Society of Agricultural Engineers, New Delhi and Agricultural Engineering College and Research Institute, Tamil Nadu Agricultural University, p. 359, Coimbatore, India, 2022.

Hindawi
Journal of Food Quality
Volume 2023, Article ID 4939468, 11 pages
https://doi.org/10.1155/2023/4939468

Research Article

Quality Improvement of Dried Anchovies at Three Solar Drying Methods

Aaisha Al-Saadi,[1] Pankaj B. Pathare,[1] Mohammed Al-Rizeiqi,[2] Ismail Al-Bulushi,[2] and Abdulrahim Al-Ismaili[1]

[1]*Department of Soils, Water and Agricultural Engineering, College of Agricultural & Marine Sciences, Sultan Qaboos University, Muscat, Oman*
[2]*Department of Food Sciences and Nutrition, College of Agricultural & Marine Sciences, Sultan Qaboos University, Muscat, Oman*

Correspondence should be addressed to Pankaj B. Pathare; pankaj@squ.edu.om

Received 30 November 2022; Revised 16 April 2023; Accepted 4 May 2023; Published 15 May 2023

Academic Editor: Kaavya Rathnakumar

Fish drying is one of the traditional methods where the fishermen land their catch on the beaches for drying traditionally under sun for several days. Dried fish provides valuable and economical sources of animal protein. The quality of dried fish is significantly influenced by the presence of microorganisms. Therefore, this study aims to determine the physical quality changes in anchovy under three different solar drying methods which are open sun drying (OSD), solar greenhouse tunnel dryer (GTD), and forced convective solar dryer (FCD) and to verify the chemical and microbial contamination in solar-dried anchovy. About (20 kg) of fresh anchovy were taken for experiments. Quality analyses were conducted in the samples before, during, and after drying. The parameters analyzed included three main analyses which are physical, chemical, and microbial analyses. The drying rate was higher in GTD compared to the two other methods. Moisture content, drying rate, and moisture ratio were significantly affected by drying methods. GTD required less time (6 hr) to dry anchovies compared to other drying methods (9 hr time). The highest reduction in lightness is in GTD dried anchovies followed by FCD and OSD. The drying methods and drying time statistically affect the lightness (L) of dried anchovies ($p \leq 0.05$). The water activity of solar-dried anchovies was 0.3. Experimentally dried anchovies were found to have lower microbial count compared to the dried fish quality standards. The total viable count (TVC) in fresh anchovy was 6.44 log CFU/g compared to the greenhouse tunnel dryer 2.90 log CFU/g, open sun dryer 4.16 log CFU/g, and forced convective dryer 4.19 log CFU/g anchovies. Water activity and moisture content did not affect total viable count (TVC) significantly, but it affects total fungal count (TFC) ($p \leq 0.05$). There was a significant difference on Krusal Wallis between the samples of three methods of drying and a fresh one on the water activity, ash content, and fat content ($p \leq 0.05$).

1. Introduction

The high protein and nutritious content of fish makes it the staple diet in many countries around the world. The coastline of Oman is very long comparing to other Gulf countries, and therefore, fishing is the most economic activity for many people in the coastal area. Oman is the biggest fish producer in the Gulf region [1]. Fish production in Oman is estimated at about 840,000 tons, with a total value of RO 364 million in 2020 [2].

Anchovy is a small coastal fish that can be found in many different environments in most seasons. It also used to produce different traditional products like dried, marinated, salted, smoked, and pickled anchovies. The anchovies are usually caught using a trawling net in the Arabian Gulf regions and that carried out in conditions with low hygienic, where it is dried traditionally in the open sun drying for three to five days, and then it is stored in conditions with ambient temperature [3]. Also, anchovies are considered as traditional products in Oman and other countries. Anchovies are a very healthy food

that are especially useful for supplying high-quality protein that is superior to that found in meat and eggs [4]. However, in areas with hot climates, fish perishes quickly and for that reason people normally try to extend their shelf life by employing various methods like smoking, salting, and drying [5]. Sun drying is a traditional method of preserving fish that is used all around the world [6]. Drying fish especially anchovies creates income for local communities in many countries. The process of drying fish is a physical process as the fish is exposed to hot air and the moisture evaporates from the surface area to the air. This process can extend the shelf life of the products and produce the desired texture and flavors and these practices are done in many communities and societies [7]. Anchovy fish contains high moisture content, which leads to faster deterioration. Moisture content is a key factor affecting the quality of anchovy fish during storage and handling [8].

The process of drying is not only used to increase the shelf life of any fresh product but also to reduce the weight, volume, package, storage, and cost of transportation and to increase the productivity of marine and agriculture [9]. Traditional fish drying methods have the drawback of losing 30–40% of the dried fish's quantity to dogs, birds, cats, and rodents [10]. In fact, this component lowers the earnings from dried fish. In addition, sun-dried fish could develop health risks and unhygienic when insects and larva attack the dried fish. Microorganisms have an impact on dried fish's quality. Nowadays, health concerns of consumers make the determination of microbiological quality and safety of dried fish very important. The quality of products is also considered to be the main influential parameter in the open solar drying technique as it was affected by unexpected rain and foreign bodies left by the animals and birds. As fish products are very perishable, because of their important microbial load, satisfactory solar drying may preserve their physicochemical quality which allows their storage over an extended period. No specific study was conducted to assess the impact of drying methods on microflora and fatty acids content of anchovies in the Oman seas. Therefore, the objective of this study is to improve the quality of locally produced dried fish using solar driers. It determines the physical quality changes in anchovy under solar drying methods. This study also verifies the chemical and microbial contamination in solar-dried anchovy.

2. Materials and Methods

About 20 kg of fresh anchovies were purchased from Oman local market and stored in a cool box with ice to being transported from a Barka's beach, Oman to be finally shifted to the Laboratory in College of Agricultural and Marine Sciences. Before drying, there were three different analyses carried out which are physical, chemical, and microbial analyses, and each analysis has different tests as shown in Figure 1. During drying, there were three different methods of drying which are open sun drying (OSD), greenhouse tunnel drier (GTD), and forced convective solar drier (FCD). Water activity, color, and weight were measured each hour during drying. Weather data like temperature, relative humidity, and solar radiation were recorded each hour during July 2021 from 7 AM to 4 PM at SQU Experimental Station. Physical, microbial, and chemical analysis were conducted before and after drying experiment.

2.1. Fish Drying Experiments

2.1.1. Open Sun Drying (OSD) Method. A quantity of fresh anchovy was purchased from the local market and placed on perforated trays. The anchovy samples were placed at a 1-meter height from ground to obtain an appropriate amount of solar radiation.

2.1.2. Forced Convective Solar Dryer (FCD). A preliminary model design of a forced convective solar dryer was installed at Sultan Qaboos University Experimental Station, Muscat, as shown in Figure 2. It consisted of two main parts: (1) upper inclined solar collector and (2) lower flat drying chamber. The solar collector is composed of a single glass cover tilted by an angle of 23.6° to the south and black granite was used on the bottom to absorb the highest amount of solar radiation [11]. The surrounding air was drawn through the forced convective solar dryer by centrifugal fans with an air velocity of 0.36 m/s that were placed in the lower chamber. The fish samples, placed inside the drying chamber, are dried by the conventional hot air flush that is coming from the main solar collector.

2.1.3. Greenhouse Tunnel Dryer (GTD). Greenhouse tunnel dryers consist of two parts which are a solar heat collection section and a drying chamber and it is 15 m length with 2 m width as shown in Figure 3. The structure of GTD was covered by a polyethylene sheet and the air inlet (1.8×0.2 m) was protected by a fine nylon mesh to prevent the intrusion of small particles such as dust and insects. Two fans were fixed opposite to the air inlet side to withdraw the heated drying air through the cavity of the GTD, and they were operated at an air velocity of constant flow at 0.36 m/s [11].

2.2. Physical Quality Analysis

2.2.1. Moisture Content. In order to calculate the moisture content of fresh fish, whole sample of anchovy was weighed before and after oven drying at 105°C for 24 hours with five replicates. The percentage of moisture content in wet-basis (X_m, %) was calculated as follows:

$$\text{moisture content \%} = \frac{\text{fish samples wet weight (g)} - \text{fish samples dr ied weight (g)}}{\text{fish samples wet weight (g)}} \times 100. \quad (1)$$

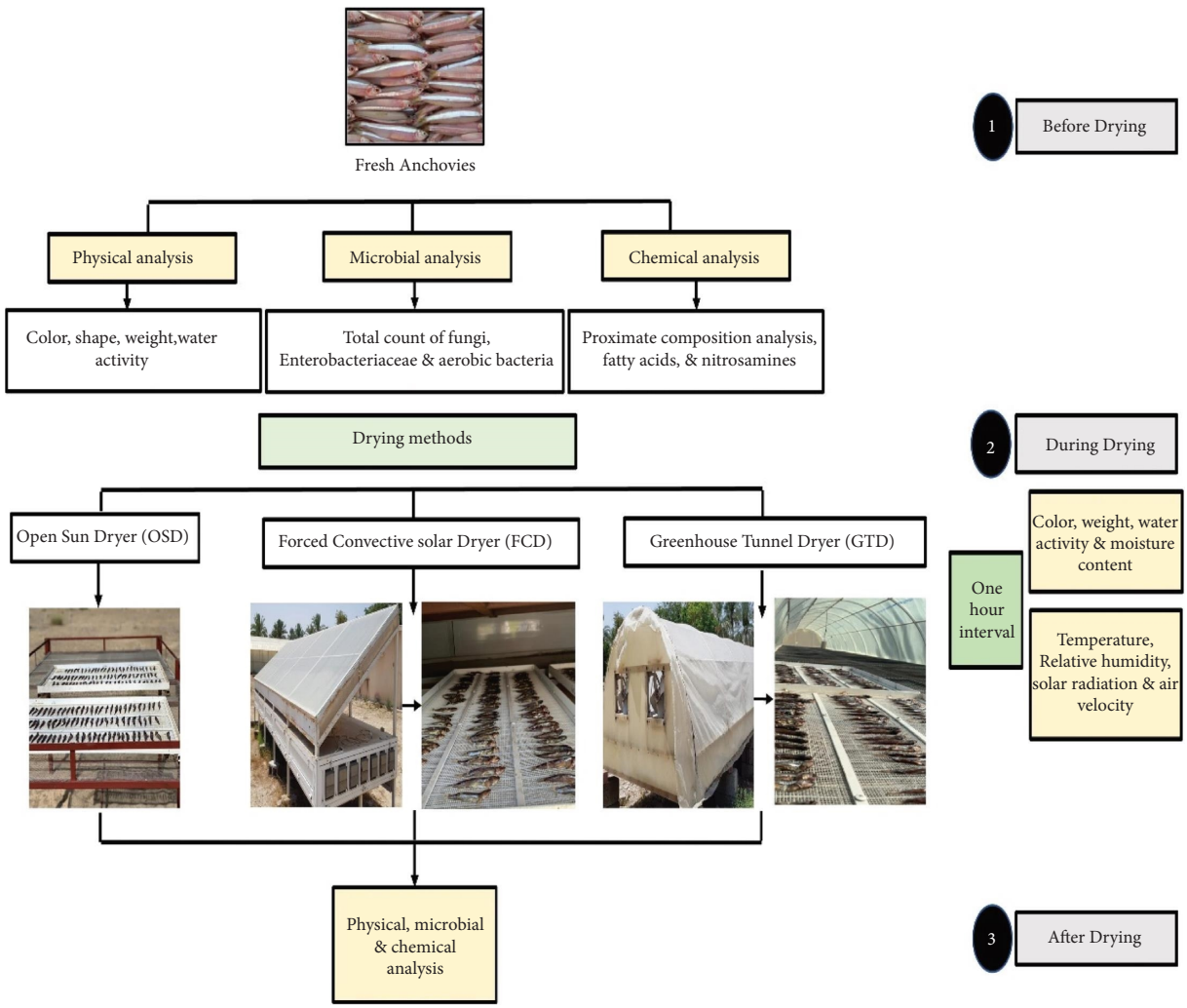

Figure 1: Overall experimental design.

Figure 2: Installed forced convective solar dryer (FCD) at agricultural experimental station, SQU.

Figure 3: Greenhouse tunnel dryers (GTDs), agricultural experimental station, SQU.

2.2.2. Color Measurements. In the color measurement of the study, the values of color for fresh samples and dried treated anchovies were taken using a colorimeter (NR110, Shenzhen ThreeNH Tech, China). For each method of drying, three samples were taken and five replicated were taken for each measurement (N). The color was measured in the central part of anchovy body. The color coordinates of L^*, a^*, and b^* were taken by the colorimeter device. Furthermore, the Chroma for the color intensity and hue for the color purity angle were detected in the study [12].

2.2.3. Water Activity Measurement (a_w). Water activity measurement (a_w) for the anchovy's samples were determined using a lab-based water activity meter (M.10′972, HygroLab C1, Rotronic, USA). For each method of drying, whole sample was taken and three samples were measured, and the measurements of each sample were recorded in every hour of drying starting from the start of the fish drying process.

2.3. Chemical Quality Analysis

2.3.1. Fatty Acids. The fish sample (0.2 grams) was weighted in a 10.0 ml Sovirell pyrex tube and then grounded to small pieces. Then, a 4.0 ml of chloroform : methanol mixture of 2 : 1 (v/v) was mixed in the tube. 1.0 ml of the internal standard was then added and clearly mixed for around 30 seconds using a lab vortex mixer. The mixture was left in a freezer at −20°C for overnight. Next, the frozen sample was clearly filtered and then dried using a rotary evaporator. The remained residue was dissolved in a 6.0 ml of diethyl ether. Then, it was easily transferred to a test tube and let dried in a stream of treated nitrogen. Next, a 1.0 ml portion of Caustic Soda (NaOH) was added to a 0.5 M methanol. The sample was then mixed using a lab vortex mixer. It was heated for around 15 minutes at a boiling temperature of 100°C. Next, the mixture was cooled in liquid water for rapid heat loss. Nearly 2.0 ml of BX_3/CH_3OH (X F or Cl) mix was then added and mixed using a vortex mixer [13]. The mixture was heated for nearly 5 min at a boiling temperature of 100°C. The mixture was then cooled. A subsequent portion of 1.0 ml of hexane and 2.0 ml of water (H_2O) were added to the mix. It was mixed for nearly 15 seconds using a lab vortex mixer. The mixture was placed in a lab centrifuge at 3000 rpm. Nearly 1.0 ml of hexane was added to the available mixture using a lab vortex mix. The sample was centrifuged for the collection of the hexane phase of 1.0 ml. The total 2.0 ml hexane phase was collected. The collection was concentrated or diluted based on the final fat content. Finally, a gas chromatographic analysis was conducted using a GC (M. GC-2010 Plus, brand Shimadzu, United States) for the fatty acid analysis.

2.3.2. Ash. The weight of porcelain crucible was recorded. 2.0 grams sample was placed on the crucible. The weight (g) of the crucible with the sample was taken. The crucibles were placed in muffle furnace (Model: RWF 12/5, CARBOLITE) and heated at 600°C ± 2°C for 5 hours. Then, the crucibles were allowed to cool into a lab desiccator. Finally, the weight of the crucibles (g) after ashing was recorded. Three replicates were taken for each ashing method. The ash content (%) is calculated as follows:

$$\text{ash \%} = \frac{\text{crucible weight after ashing} - \text{crucible and sample weight before ashing}}{\text{weight of sample}} \times 100. \quad (2)$$

2.3.3. Fats. A number of flasks were oven dried, cooled, and weight recorded prior to soxhlet extraction. 1–5 g of fish samples were placed into numbered extraction thimbles. 100 ml of petroleum spirit was added into the soxhlet distillation flask. The extractor was fixed to each of the individual flask and placed on the heater part. The extraction solvent was then heated at 50°C. The extraction was performed for 8 hours. Thimbles were removed from the Soxhlet apparatus. The distilled solvent was collected and stored in a separate bottle. The collected fat was removed in the flask. Then, it was dried in a conventional air-drying oven at 80°C for 1 hour to remove remained solvent in the flask. Weight of the flasks (g) in replicates (N) including the collected fat was taken. The percentage of fat (%) is calculated by using the following equation:

$$\text{fat \%} = \frac{\text{removed flask with fat weight (g)} - \text{empty flask weight (g)}}{\text{sample}^{'}\text{s weight (g)}} \times 100. \quad (3)$$

2.4. Microbial Assessment

2.4.1. Preparation of Media. Several selective and nonselective media were prepared according to Al Bulushi [14] as in Table.1. 19.5 g of Sigma powder of Potato Dextrose Agar (PDA) was mixed with a 500 ml of distilled water.

11.75 g of Sigma powder of standard plate count (SPC) was mixed with a 500 ml of distilled water in a media bottle. 9.5 grams of the Sigma powder of maximum recovery diluent (MRD) was mixed with 1000 ml of distilled water. Following the same sterilization process, 225 ml of the diluent was placed for each experiment. 9.0 ml test tubes were used for each diluent. 18.3 g of Sigma powder of tryptone bile X-glucuronide agar (TBXA) was mixed with 500 ml of the distilled water. 15.0 ml of the agar media was poured in Petri dishes and cooled at room temperature °C. 33.16 g of Sigma powder of baird parker agar (BPA) was thoroughly mixed with 500 ml of distilled water on a boiling plate using a lab vortex mixer. 25 ml of concentrated egg yolk emulsion was then added to the agar. 15 ml of the agar was poured on a petri dish plate for the *S. aureus* microbial count. Violet-red bile agar was used for the enumeration of coliforms species and *Enterobacteriacea* count. 20.76 g of Sigma-powder of violet-red bile agar (VRBA) was mixed with 500 ml of distilled water on a boiling plate using a vortex mixer. All prepared medium were then sterilized at 121°C for 2.5 hours in an autoclave (Tomy SX-500 Lab Autoclave, TOMY, USA). 15.0 ml of individual agar media was placed and cooled to room temperature in a separate Petri dish.

2.4.2. Total Fungal Count (TFC). The total fungal count was conducted for the fish sample. 25.0 g of the fish sample was placed into a sterile stomacher bag (Seward, UK). Nearly, 225 ml of the maximum recovery diluent was added to the collected mass in the stomacher bag to achieve the initial 10^{-1} dilution. The mixture was then homogenized using a lab-based stomacher (Seward, UK) for 1 minute. Solutions were serially up to 10^{-3} dilutions.

0.1 ml or 100 μl from each test tube of the three dilutions of 10^{-1}, 10^{-2}, and 10^{-3} dilution was aseptically transferred into duplicate plates of the Potato Dextrose Agar (PDA) plate. The mixture was then spread on a flame starting from the highest dilution of 10^{-3} to the lowest dilution 10^{-1}. All the petri dish plates were incubated aerobically at an ambient temperature of nearly 25°C for 3–5 days in a lab incubator. The colony forming units counts were counted using a colony counter equation:

$$\text{cfu} = \sum_{n=1} \text{number of colonies on the plate} \times \frac{1}{\text{di lution factor X volume taken}}. \quad (4)$$

2.4.3. Total Aerobic Bacterial Count (TABC). 25.0 grams of the fish sample was placed into a sterile stomacher bag. Nearly 225 ml of the maximum recovery diluent was added making a 10^{-1} dilution. This mixture was homogenized in a stomacher bag for 1 minute. Dilutions of 10^{-2} and 10^{-3} were prepared using 1.0 ml into 9.0 dilutions.

0.1 ml or 100 μl from the three dilutions were transferred aseptically in duplicate plates of Standard Plate Count Agar (SPCA) plate. The mixture was then spread on the petri dishes on alcohol flamed spreading from the highest dilution of 10^{-3} to the lowest dilution of 10^{-1}. All petri dish plates were incubated aerobically at 35°C for 48 hours. Colony counts were taken after the 48 hours using the colony counters. Equation (4) was used to calculate the colony forming units per gram of the fish sample.

2.4.4. Enterobacteriaceae Count. For *Enterobacteriaceae* count, 12.0 ml of molten VRB Agar at 44–47°C was added using a pouring plate technique. All petri dish plates were incubated for 24 hours at 35°C in a lab microbial incubator. Colony counters were used to count the pink colonies on the plates. Colony forming units per gram of the fish sample was calculated using equation (4).

Table 1: Types of media used in the microbial assessment.

Tests	Media	Manufacturer
Total fungal count (TFC)	Potato dextrose agar (PDA)	Sigma-Aldrich
Total viable count (TVC)	Standard plate count agar (SPCA)	Sigma-Aldrich
The diluent	Maximum recovery diluent	Sigma-Aldrich
Escherichia coli counts c.f.u/g	Tryptone bile X-glucuronide agar (TBXA)	Sigma-Aldrich
Staphylococcus aureus counts c.f.u/g	Baird–Parker media agar (simply BPA)	Sigma-Aldrich
Coliforms total counts and *Enterobacteriacea* count c.f.u/g	Violet-red bile agar (simply VRBA)	Sigma-Aldrich

2.4.5. Bacterial Test

(1) Enumeration of E. coli in Dried Fish. 50 grams of fish sample was placed in a beaker and mixed well. 25 grams of the mix was taken to the stomacher bag of 225 ml of diluent to make a 10^{-1} dilution. 10^{-2} and 10^{-3} dilutions were made using a vortex mixer of mixing 1.0 ml into 9 ml of dilutions. 0.1 ml from each test tube of 10^{-1}, 10^{-2}, and 10^{-3} dilution was aseptically transferred in duplicate of Tryptone Bile X-Glucuronide Agar (TBXA) plate. Next, spreading of 0.1 ml from the dilution using alcohol flamed spreading was conducted starting from the highest dilution of 10^{-3} to the lowest dilution of 10^{-1}. Colony counters were used to count the blue or green colonies on the plates. Colony forming units per gram of the fish sample was calculated using equation (4).

(2) Enumeration of Staphylococcus aureus. The dilution mixes of 10^{-1}, 10^{-2}, and 10^{-3} were prepared using the same tools and techniques explained in the previous sections. Molten Baird–Parker Agar was used in the agar medium for the incubation of *S. aureus*. All petri dish plates were incubated for 24 hours at 35°C in a lab microbial incubator. Colony counters were used to count the black colonies on the plates. Colony forming units per gram of the fish sample was calculated using equation (4).

(3) Enumeration of Coliforms. The dilution mixes of 10^{-1}, 10^{-2}, and 10^{-3} were prepared using the same tools and techniques explained in the previous sections. 1.0 ml from each dilution in duplicate was aseptically transferred to sterile petri dishes. Around 12 ml of molten VRB Agar at 47°C was prepared on microbial petri dishes. All petri dish plates were incubated for 24 hours at 35°C in a lab microbial incubator. Colony counters were used to count the pink colonies on the plates. Colony forming units per gram of the fish sample was calculated using equation (4).

2.5. Data Analysis.

Three tests of repeated drying were conducted throughout the experiment. All data were tabulated in an excel sheet for data analysis. Summary statistics was carried out for the study analysis. Mean and standard deviation were reported. Analysis of Variance ANOVA with a $p \leq 0.05$ was considered for the significance difference analysis. Chi-square analysis along with Pearson's correlation methods was conducted. $p \leq 0.05$ was considered for significance level.

3. Results and Discussion

3.1. Solar Data.

The maximum temperature was 49.35°C and that was around 12 PM. The average temperature was around 43.99 ± 3.34°C and the minimum temperature was 39.04°C (Figure 4). Maximum relative humidity was 28.76% at around 8 AM and the average was around 19.17 ± 5.07%, and the minimum RH was11.99%. Average solar radiation was 565.50 ± 0.18 W/m^2.

3.2. Effect of Drying Methods on Physical Quality Characteristics of Anchovy

3.2.1. Moisture Content, Drying Rate, and Moisture Ratio.

Moisture content was significantly affected by drying time ($p = 0.04345$) and drying methods ($p \leq 0.00001$) (Figure 5(a)). The percentage of moisture content reduction for OSD was about 78.90% after 9 hours drying, for FCD was about 79.08% after 9 hours drying and for GTD was 80.27% after 6 hours of drying, and it is the highest reduction comparing to the other methods. The results showed that the GTD sample has the lowest moisture content compared to FCD and OSD and that could be related to high temperature inside the greenhouse tunnel dryer [11]. Similarly, the drying rate was highly influenced by drying methods ($P \leq 0.00001$) and the time of drying ($p = 0.03874$) (Figure 5(b)). The study confirmed that the drying rate was higher in GTD compared to the two other methods. Similar trend was observed in the moisture ratio of dried anchovy in all three methods, where drying time (($P \leq 0.00001$)) and drying methods ($p = 0.03511$) significantly influenced the moisture ratio of dried anchovy. This might be related to the lowest average RH and highest average temperature during daytime in GTD and for that the evaporation process of the drying air would be increased [11].

3.2.2. Color Change.

Color is a key factor in drying technique selection and optimization, as well as market value. The results showed that the lightness of anchovy was highly affected by drying methods ($P \leq 0.01$) and drying time ($P \leq 0.01$) (Figure 6). The L^* value of anchovies was changed during the drying process in all drying methods. The lightness was high in the fresh sample and decreased significantly at the end of drying. During drying, anchovies dried in GTD showed the highest decrease on L^* value from 51.19 ± 1.19 to 9.95 ± 0.82 from hour 0 to hour 6, respectively. This was followed by anchovies dried in FCD

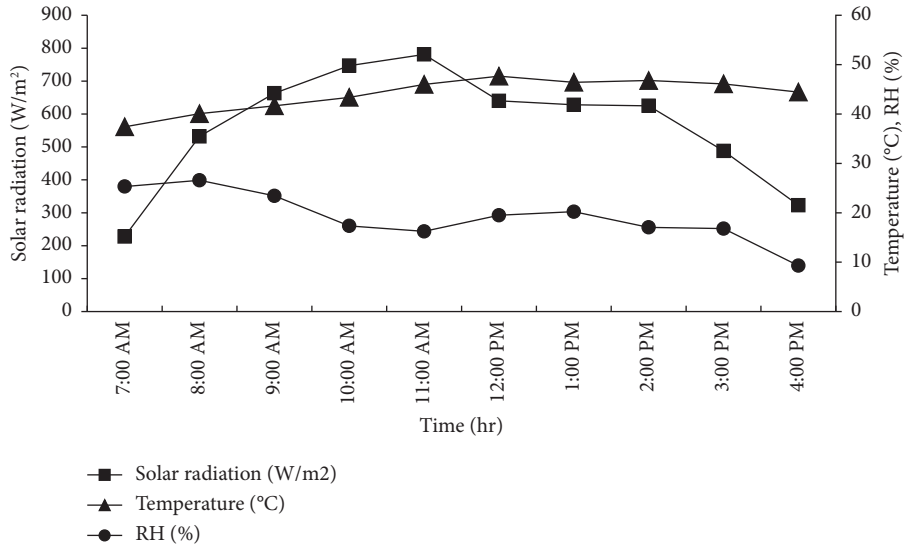

Figure 4: A typical day weather data during the experimental period.

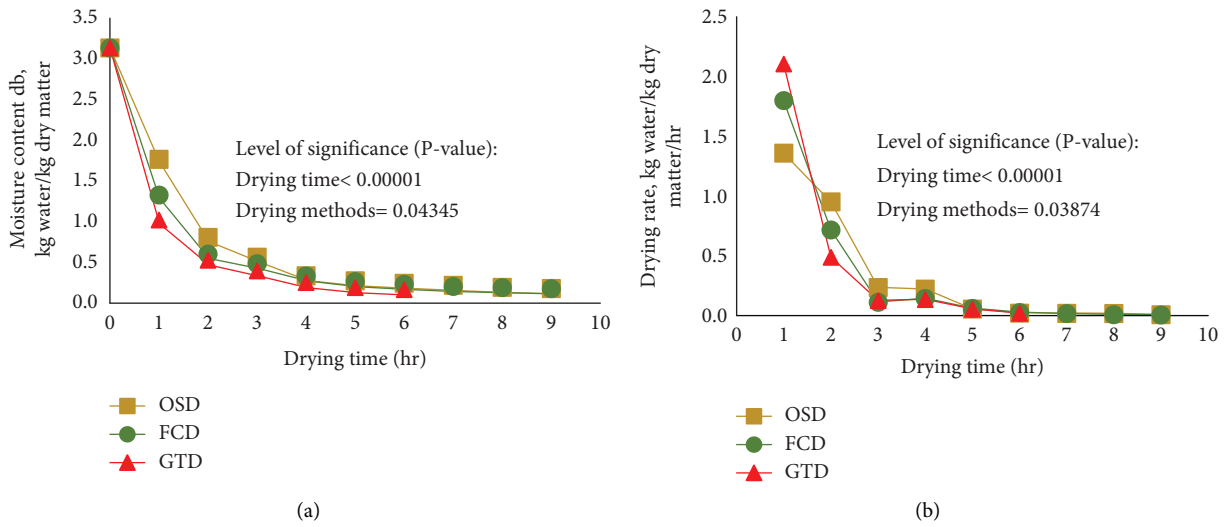

Figure 5: Changes in moisture content (a) and drying rate (b) of anchovy using GTD, OSD, and FCD.

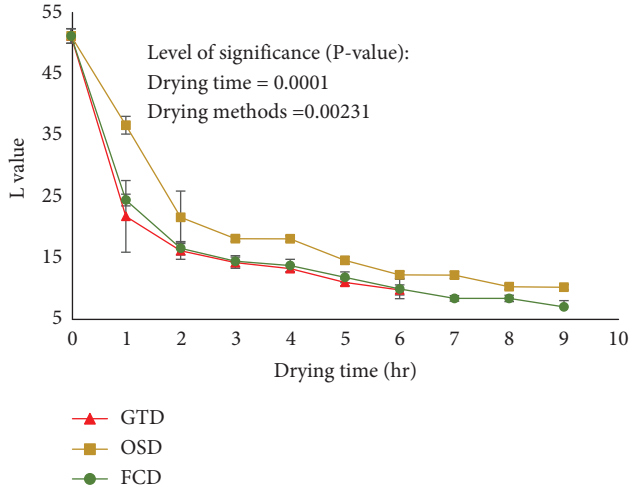

Figure 6: Lightness value of anchovy dried using GTD, OSD, and FCD.

lightness was decreased from 51.19 ± 1.19 to 7.20 ± 1.02 from hour 0 to hour 9, respectively (Figure 6). Same scenario was observed on anchovies dried in OSD, where the L^* value reported was decreased from 51.19 ± 1.19 to 10.39 ± 0.42 from hour 0 to hour 9, respectively. This could be due to the reaction of nonenzymatic and decomposition of pigments of color which produce darkness [11]. Nadia et al. [15] reported similar results for air dried sardine (*Sardina pilchardus*) muscles. With drying time, the color attribute of L^* is showed a decrease trend for all drying methods. The anchovy L^* values decreased due to the binding of the unsaturated fatty acids with oxygen, thereby accelerating anchovy oxidation and affecting the Maillard reaction [16]. In addition, the highest reduction in lightness is in GTD dried anchovies followed by FCD and OSD and this might be related to high temperature in GTD. It has been reported in different researches that the decrease in L^* value increases the darkness of some food materials and destruction of the pigments [11, 17].

3.2.3. Water Activity. The water activity is a very reliable indicator for food preservation and of microorganism growth and spoilage of dry fish products. Each type of food has exhibited a water activity limit below which microbial growth stops. Almost all bacteria grow at about $a_w = 0.85$, while fungi at $a_w < 0.7$ and mould and yeast at about $a_w = 0.61$ [18]. Figure 7 shows the water activity value of dried anchovy using GTD, OSD, and FCD. The water activity was statistically influenced by drying method ($p < 0.01$) and drying time ($p < 0.01$). The GTD showed the highest reduction in water activity during drying time. During drying process, the water activity of anchovies dried in GTD was decreased from 0.92 ± 0.02 to 0.30 ± 0.04, water activity of FCD anchovies was decreased from 0.92 ± 0.02 to 0.30 ± 0.01, and the water activity of anchovies dried in OSD was decreased from 0.92 ± 0.02 to 0.35 ± 0.04. After the drying process, it was found that the percentage of water activity reduction in GTD was 67.95% after 6 hours drying. However, it was 49.23% and 43.33% for FCD and OSD after 9 hours drying, respectively. In addition, the water activity level in GTD was decreased rapidly compared to other methods and that showing the anchovy fish are sufficiently dried and are able to prevent the growth of hazardous microorganisms. The reduction in the water activity prevents oxidation and enzymatic reaction [19]. Oparaku et al. [20] found that moulds keep their growth at water activity not less than 0.7, while bacteria likes to grow at water activity of 0.9 [21]. Therefore, keeping water activity at a level of about $a_w = 0.6$ ensures the absence of microbial growth of most microorganisms. The storage stability of the product is also affected by a_w, as dried products have a longer shelf life than moist products. Controlling water activity can help to prevent fish spoilage. For every microorganism, there are minimal, optimum, and maximum levels of water activity for growth. Reducing water activity (a_w) can thus decrease putrefaction and improve fish preservation [22].

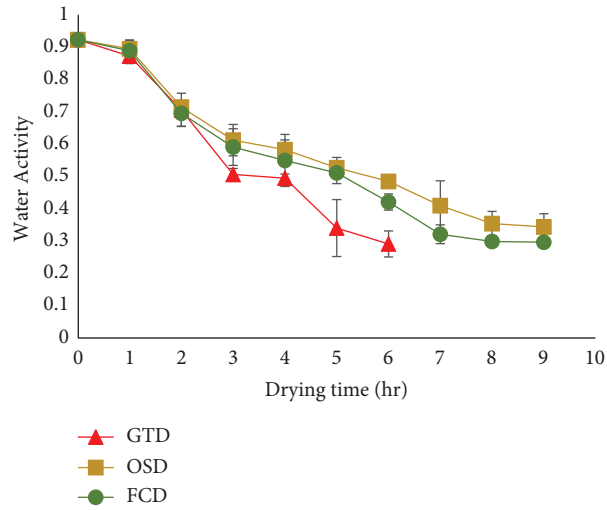

Figure 7: Water activity values of anchovy dried using GTD, OSD, and FCD.

3.3. Effect of Drying on Chemical Quality Characteristics of Anchovy

3.3.1. Fatty Acids. The study revealed a significant difference in fatty acids compositions among the three different drying methods as well as fresh samples with ($p \leq 0.05$). There is also a significant correlation between polyunsaturated fatty acids contents in mg/g and the amount of Omega-3 fatty acids compositions mg/g with ($p \leq 0.05$). As polyunsaturated fatty acids increase the Omega-3, fatty acids increase. This explains the presence of 5,8,11,14,17-Eicosapentaenoic acid, methyl ester, (all-Z)- and 4,7,10,13,16,19-Docosahexaenoic acid, methyl ester in the anchovies fish sample. Results showed a significance difference of fatty acid composition for tunnel dried sample (p value = 0.039), forced convective drying (p value = 0.0282), and open sun-dried sample (p value = 0.0300) from that of the fresh sample prior to drying. Table 2 shows fatty acids in fresh, GTD, OSD, and FCD anchovy's samples for the four main types of fatty acids which are Omega-3, saturated, mono-unsaturated, and poly-unsaturated. In the fresh sample, Omega-3 fatty acids were the highest (9.32 ± 0.22), followed by saturated fatty acids (4.81 ± 1.37), polyunsaturated fatty acids (2.95 ± 0.92), and monounsaturated fatty acids (1.68 ± 0.23). The omega-3 fatty acids are the highest in all different samples compared to the other fatty acids. For the comparison between samples of anchovies before and after drying, the results of this study show sample after drying has a high amount of fatty acids in all dried samples compared to fresh sample.

3.3.2. Fat Contents in Wet-Basis of Samples. Figure 8 shows the percentage of fat content in anchovy's samples before and after drying. Fat content was increased in dried samples after the drying process compared to fresh samples. It was highly increased in FCD anchovy samples followed by GTD and OSD and this due to the reduction that happens of moisture content after the drying process. This finding of an

Table 2: Fatty acids in fresh, GTD, OSD, and FCD anchovies samples.

	Fresh	OSD	FCD	GTD
Omega-3	9.32 ± 0.22	40.05 ± 6.47	42.44 ± 4.94	50.99 ± 4.69
Saturated	4.81 ± 1.37	22 ± 6.13	23.49 ± 6.54	21.80 ± 6.06
Monounsaturated	1.68 ± 0.23	7.47 ± 1.43	8.78 ± 1.19	7.31 ± 1.30
Polyunsaturated	2.95 ± 0.92	14.35 ± 4.97	15.41 ± 4.65	21.35 ± 7.82

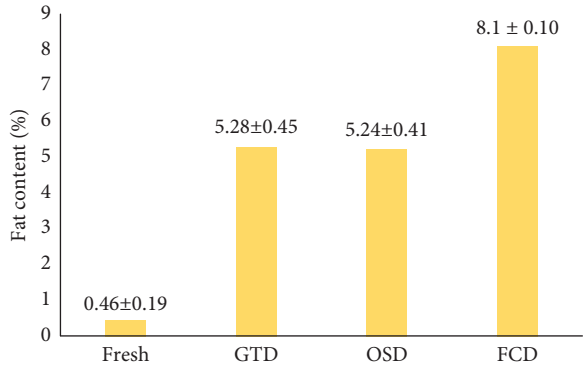

Figure 8: Fat content (%) value of anchovy before and after drying using GTD, OSD, and FCD.

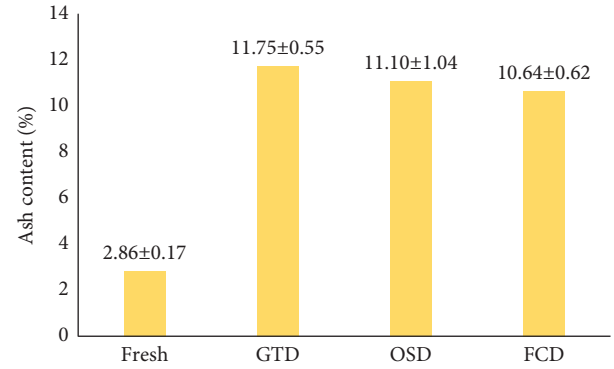

Figure 9: Ash content (%) value of anchovy before and after drying using GTD, OSD, and FCD.

increase in fat content after drying is similar to the study of Abraha et al. [23] who have carried out a comparative study on the quality of dried anchovy (*Stelophorus heterolobus*) using open sun rack and solar tent drying methods. The increase of fat content could be related to dehydration that was caused by increasing the temperature during drying process [24].

3.3.3. Total Ash Contents of Sample. Figure 9 shows the percentage of ash content in anchovy's samples before and after drying. Ash content was increased in samples after drying process. Increasing of ash content in anchovies after drying can be related to decreasing of moisture content in anchovies. This result is similar with those Tenyang et al. [24] who reported that the ash content of fish is increasing during drying process. Besides, there was a significant effect of water activity (a_w) and moisture content (MC) on ash content. As well, increasing ash content can be related to increasing the dry matter content per unit of weight for sample after dehydration [25].

3.4. Effect of Drying on Microbial Quality Characteristics of Anchovy

3.4.1. Total Fungal Count (TFC), Total Aerobic Bacterial Count (TABC), and Enterobacteriaceae Count. Table 3 shows the results of different microbial counts in Fresh, GTD, OSD, and FCD, and it is clear that the microbes were decreased in the samples after the drying process. Using statistical analysis found that water activity and moisture content do not affect TVC significantly with ($p = 0.072$, $p = 0.081$), respectively. However, they significantly affect TFC with $p \leq 0.05$. Experimentally dried anchovies found lower microbial content values compared to the dried fish

Table 3: Different microbial analysis tests in fresh, GTD, OSD, and FCD of anchovies samples.

Tests	Type of sample			
	Fresh	OSD	FCD	GTD
TVC (log CFU/g)	6.44	4.16	4.19	2.90
TFC (log CFU/g)	n.d	0.60	0.60	0.78
Enterobacteriaceae count (log CFU/g)	2.45	n.d	n.d	n.d
a_w	0.92	0.35	0.30	0.29
MC wb (%)	75.82	16.44	15.86	14.96

quality standards that reported by the studies of [26, 27]. Similarly, various research studies reported that the allowable level of TVC has to be less than 10^5 log cfu/g, TFC has to be less than 10^3 log CFU/g, and *Enterobacteriacea* has to be less than 10^2 log CFU/g [26, 27]. Microorganism growth is accelerated by long periods of open sun drying in high humidity environments [10]. Bacterial activity stops when the moisture content of the fish falls below 25%, while fungal activity stops when the moisture level falls below 15% [28]. The stability of microbiological growth in dried fish is determined by the amount of moisture present during the processing and storage period [29].

4. Conclusions

Anchovies are among the highest quantity fish in Oman. It has a lot of socioeconomic dimension to food and feed security in the country. The most common problem that influenced the safety and quality of dried anchovies is contamination caused by fungi and bacteria. The present study used three types of drying methods (open sun dryer, greenhouse tunnel dryer, and forced convective dryer) to

determine each drying method characteristics and to determine the physical, chemical, and microbial quality changes in anchovy under solar drying methods. Generally, temperature plays a vital role in the process of drying as it lay to increase the drying rate and leads to reduce the drying time. GTD required less time (6 hr) to dry anchovies compared to other drying methods (9 hr). The independence variable (drying methods and drying time) showed a significant effect ($p \leq 0.05$) on anchovy's lightness values. There was a significant difference between the fresh and dried samples on the water activity, ash content, and fat content ($p \leq 0.05$). Experimentally dried anchovies found lower microbial content values compared to the dried fish quality standards. Water activity does not affect TVC significantly, but it significantly affects TFC with $p \leq 0.05$. Solar dryers protect the dried fish from atmospheric and insect contaminations as well as microbial contaminations as they dry fish in a significantly shorter time and shelter the dried fish from rain, dust, insects, rodents, animals, and humid environments.

Data Availability

The data used to support the study are available upon request.

Conflicts of Interest

The authors declare that they have no conflicts of interest.

Acknowledgments

This work is based on the research supported in part by Sultan Qaboos University under the Project code IG/AGR/SWAE/23/02. The authors would like to acknowledge Ms. Mai Al-Dairi and Er. Mohammad Al-Balushi for their help in conducting the experiment.

References

[1] Fao, *Fishery and Aquaculture Country Profiles*, Food and Agriculture Organization, Rome, Italy, 2019.

[2] S. M. Al Jufaili, "Decadal status of sardine fishery in Oman: contribution of the omani-indian oil sardine sardinella longiceps valenciennes, 1847 (teleostei: clupeidae)," *Iranian Journal of Ichthyology*, vol. 8, no. 4, pp. 271–285, 2021.

[3] I. M. Al Bulushi, N. Guizani, M. Ayyash et al., "Bacterial diversity, biogenic amines and lipids oxidation in traditional dried anchovy (Encrasicholina punctifer) during ambient storage," *International Journal of Food Studies*, vol. 9, no. 1, 2020.

[4] C. Litaay, A. Indriati, N. Mayasti, I. Tribowo, R. Andriansyah, and A. Daryanto, "Characteristics of sago noodles high in protein and calcium," *IOP Conference Series: Earth and Environmental Science*, vol. 1033, Article ID 012061, 2022.

[5] N. Sultana, M. Hossain, M. Siddique, M. Uddin, M. Dina, and Z. Farhana, "Microbial quality of dried fish of different areas Chittagong and Mymensingh districts of Bangladesh," *International Journal of Bioresearch*, vol. 2, no. 8, pp. 1–5, 2010.

[6] R. O. Lamidi, L. Jiang, P. B. Pathare, Y. Wang, and A. Roskilly, "Recent advances in sustainable drying of agricultural produce: a review," *Applied Energy*, vol. 233-234, pp. 367–385, 2019.

[7] N. U. Karim, N. F. A. Sufi, M. Hasan, and S. M. Z. S. Hasan, "Quality analysis of anchovies, Stelophorus commersonii dried in drying racks," *Journal of Sustainability Science and Management*, vol. 3, pp. 111–118, 2017.

[8] S. Şevik, "Design, experimental investigation and analysis of a solar drying system," *Energy Conversion and Management*, vol. 68, pp. 227–234, 2013.

[9] A. W. Noori, M. J. Royen, and J. Haydary, "Effect of ambient parameters change on mint leaves solar drying," *Acta Chimica Slovaca*, vol. 14, no. 1, pp. 14–24, 2021.

[10] S. Sablani, M. S. Rahman, O. Mahgoub, and A. Al-Marzouki, "Sun and solar drying of fish sardines," in *Proceedings of the International Drying Symposium*, pp. 1662–1666, Beijing, China, January 2002.

[11] T. Seerangurayar, A. M. Al-Ismaili, L. Janitha Jeewantha, and N. A. Al-Habsi, "Effect of solar drying methods on color kinetics and texture of dates," *Food and Bioproducts Processing*, vol. 116, pp. 227–239, 2019.

[12] P. B. Pathare, U. L. Opara, and F. A.-J. Al-Said, "Colour measurement and analysis in fresh and processed foods: a review," *Food and Bioprocess Technology*, vol. 6, no. 1, pp. 36–60, 2013.

[13] Aoac, "Association of official analytical chemists," in *Official Methods of Analysis of AOAC International,*Association of Official Analytical Chemists, Rockville, Maryland, 2000.

[14] I. M. Al Bulushi, *The Handbook of Food Microbiological Analytical Methods*, Nova Science Publishers, Hauppauge, NY, USA, 2017.

[15] D. Nadia, B. Catherine, K. Nabil, and M. Nourhène, "Effect of air drying on color, texture and shrinkage of sardine (Sardina pilchardus) muscles," *Journal of Nutrition & Food Sciences*, vol. 1, p. 113, 2011.

[16] E.-S. Lee, H.-J. Lee, J.-S. Bae, Y.-K. Kim, J.-H. Lee, and S.-T. Hong, "Effects of packaging materials on the physicochemical characteristics of seasoned anchovies during storage," *Journal of the East Asian Society of Dietary Life*, vol. 23, no. 4, pp. 461–469, 2013.

[17] C. H. Chong, C. L. Law, M. Cloke, L. C. Abdullah, and W. R. W. Daud, "Drying kinetics, texture, color, and determination of effective diffusivities during sun drying of Chempedak," *Drying Technology*, vol. 26, no. 10, pp. 1286–1293, 2008.

[18] V. Belessiotis and E. Delyannis, "Solar drying," *Solar Energy*, vol. 85, no. 8, pp. 1665–1691, 2011.

[19] K. Jayaraman, D. Gupta, and A. Mujumdar, *Handbook of Industrial Drying*, Marcel Decker Inc, New York, NY, USA, 1995.

[20] N. F. Oparaku, B. Mgibenka, and J. E. Eyo, "Proximate and organoleptic characteristics of sun and solar dried fish," *Animal Research International*, vol. 7, no. 2, pp. 1169–1175, 2010.

[21] I. M. Al Bulushi, N. Guizani, and G. A. Dykes, "Effect of ambient storage on the microbial characteristics of traditional dried anchovies (Encrasicholina punctifer)," *African Journal of Microbiology Research*, vol. 7, no. 28, pp. 3575–3581, 2013.

[22] K. Abbas, A. Saleh, A. Mohamed, and O. Lasekan, "The relationship between water activity and fish spoilage during cold storage: a review," *Journal of Food Agriculture and Environment*, vol. 7, no. 3/4, pp. 86–90, 2009.

[23] B. Abraha, M. Samuel, A. Mohammud, H.-M. Habte-Tsion, H. Admassu, and N. Q. M. Al-Hajj, "A comparative study on quality of dried anchovy (Stelophorus heterolobus) using

open sun rack and solar tent drying methods," *Turkish Journal of Fisheries and Aquatic Sciences*, vol. 17, no. 6, pp. 1107–1115, 2017.

[24] N. Tenyang, R. Ponka, B. Tiencheu, F. T. Djikeng, and H. M. Womeni, "Effect of traditional drying methods on proximate composition, fatty acid profile, and oil oxidation of fish species consumed in the far-north of Cameroon," *Global Challenges*, vol. 4, no. 8, Article ID 2000007, 2020.

[25] S. Adeyeye, O. Oyewole, A. Obadina et al., "Quality and safety assessment of traditional smoked fish from Lagos State, Nigeria," *International Journal of Aquaculture*, vol. 5, 2015.

[26] A. Aliya, P. Sudheesh, A. Nasser et al., "Microbiological, chemical and nutritional quality and safety of salted cured fishery products from traditional dry fish p," *Food Research*, vol. 2, no. 3, pp. 279–286, 2018.

[27] G. Praveen Kumar, K. Martin Xavier, B. B. Nayak, H. S. Kumar, G. Venkateshwarlu, and A. K Balange, "Effect of different drying methods on the quality characteristics of Pangasius hypophthalmus," *International Journal of Current Microbiology and Applied Sciences*, vol. 6, no. 10, pp. 184–195, 2017.

[28] D. Sen, B. Anandaswamy, N. Iyengar, and N. Lahiry, "Studies on the storage characteristics and packaging of sun-dried salted mackerel (Rastrelliger kanagurta Cuv)," *Food Science*, vol. 10, pp. 148–156, 1961.

[29] A. Logesh, M. Pravinkuma, S. Raffi, and M. Kalaiselva, "An investigation on microbial screening on salt dried marine fishes," *Journal of Food Resource Science*, vol. 1, no. 1, pp. 15–21, 2011.

Hindawi
Journal of Food Quality
Volume 2023, Article ID 7426793, 12 pages
https://doi.org/10.1155/2023/7426793

Research Article

The Effect of Drying Temperature and Thickness on the Drying Kinetic, Antioxidant Activity, Phenolic Compounds, and Color Values of Apple Slices

Engin Demiray,[1] **Julide Gamze Yazar**,[1] **Özgür Aktok**,[1] **Burçin Çulluk**,[1] **Gülşah Çalışkan Koç**,[2] **and Ravi Pandiselvam**[3]

[1]*Department of Food Engineering, Faculty of Engineering, Pamukkale University, Kinikli, Denizli 20160, Turkey*
[2]*Uşak University, Eşme Vocational High School, Food Processing Department, Food Technology Program, Eşme, Uşak, 64600, Turkey*
[3]*Physiology, Biochemistry and Post-Harvest Technology Division, ICAR-Central Plantation Crops Research Institute, Kasaragod 671124, Kerala, India*

Correspondence should be addressed to Ravi Pandiselvam; r.pandiselvam@icar.gov.in

Received 18 July 2022; Revised 14 February 2023; Accepted 5 April 2023; Published 26 April 2023

Academic Editor: Ayon Tarafdar

Dried fruit slices are important, healthy, and popular snacks and gain importance day by day due to their high nutritional content. In this context, this study mainly focused on the production of healthy apple chips snacks and the determination of degradation kinetics of antioxidant activity, total phenolic compounds, and color values of apple chip snacks during convective hot air drying at three different temperatures (45, 55, and 65°C) and sample thicknesses (1.5 and 5 ± 0.5 mm). The drying kinetics, desorption isotherms, activation energy, and half-life of the apple chip snack were also calculated. The Page and GAB models are the best models for the determination of the drying (>0.992) and desorption (>0.9979) behavior of apple snacks with the highest R^2 values. The drying of all samples took place in the falling rate period. The D_{eff} values increased depending on the increasing air temperature and slice thickness. The antioxidant activity, total phenolic compounds, and total color change of the 5 mm thick samples were degraded following the first-order reaction kinetics. The higher antioxidant activity, phenolic compounds, L^* values, and lower half-life values were observed in conditions where the thickness (1.5 mm) and temperature (45°C) are low. The activation energy values calculated for the total phenolic compounds are higher than those calculated for the antioxidant activity. As a result, it can be concluded that apple chip snacks with high nutritional value can be produced by choosing low temperatures and slice thickness.

1. Introduction

Apple is a very popular fruit consumed both in season and out of season. The high nutritional value (ascorbic acid and polyphenol contents, and antioxidant activity), health-promoting effects (cardioprotective effects, and so on), and the desired taste are among the reasons for the preference for this fruit [1–3]. Apple chip snack, as a novel food product, has desired crispy taste and high nutritional value, and flavor. Apple chip snacks can be obtained by hot air drying, freeze-drying, puffing drying, or combined drying techniques such as hot air drying + puffing drying [4]. Zhu et al. [4] reported that the hot air + CO_2 puffing dried apple chip snacks have a higher rehydration rate, and sensorial and textural properties compared to other drying techniques. In addition, several studies related to the development of functional apple snacks using emerging technologies such as vacuum impregnation [5–7], ohmic heating [7], and novel integrated freeze-drying process [8], are in the literature.

Hot air drying is a suitable technique for the production of apple chip snacks because of providing uniform hot air and temperature distribution over the product, the simplicity of the process, ease of the production, low energy consumption and drying time, and is cheap [9]. The air

temperature, airflow rate, relative humidity, and product thickness are important factors in terms of both determinations of drying behavior and the quality (color, total phenolic content, and antioxidant activity) of the product [9–11]. For this reason, the effect of process parameters has to be investigated and optimum conditions have to be determined. When the studies were examined, although there were studies in which different methods were used to obtain apple chips, there was no study examining the change in the phenolic content and antioxidant activity of apples during the drying process. The aim of this study is to determine the effect of different drying temperatures (45, 55, and 65°C) and thicknesses (1.5 and 5 ± 0.5 mm) on the drying kinetics, drying rate, effective moisture diffusivity, color, antioxidant activity, and total phenolic compounds of apple chip snacks. In addition, desorption isotherms and color, antioxidant activity, and total phenolic degradations during drying were also investigated. The activation energy and half-life of the apple slices were also calculated.

2. Material and Methods

2.1. Material. Granny Smith variety of apples (12 ± 1 cm) that were at the same maturity level were supplied from Pamukkale/Denizli. The apples were taken from equal sizes as much as possible and stored in the refrigerator (4°C) until drying. The apples were washed, dried, peeled, and inedible parts were removed. The thickness of the apple slices was determined using a caliper, and the apples were sliced with a knife (1.5 and 5 ± 0.5 mm).

2.2. Methods

2.2.1. Drying Apple Slices with Hot Air. The apple slices were dried at three different drying temperatures (45, 55, and 65°C) and constant air velocity (0.2 m/s) in a drying cabinet (Yücebaş Makine Tic. Ltd. Şti., İzmir, Turkey). From the beginning, the tray used for weighing was removed from the dryer every 30 min and weighed, and the data were recorded. After drying, the product was first kept at room temperature for 30 minutes in the desiccator, then at 4°C for 1 hour, and then cooled and frozen at −20°C. During the drying process (every 30 min), the total antioxidant and total phenolic compounds, and color values were determined.

Drying kinetics were determined and effective moisture diffusivity (D_{eff}) and activation energy (E_a) values were calculated.

Moisture content (equation (1)) and drying rate (equation (2)) were calculated according to the given equations:

$$M_t = \frac{m - \text{DM}}{\text{DM}}, \tag{1}$$

$$\text{Drying Rate (DR)} = \frac{M_{t+\text{d}t} - M_t}{\text{d}t}, \tag{2}$$

where M_t is the moisture content at any time t (kg water/kg dry matter (DM)), m is the weight of the sample (g), DM is the amount of DM contained in the sample (g), $M_{t+\text{d}t}$ is the moisture content at time $t + \text{d}t$ (kg water/kg DM), and dt is the drying time (min).

D_{eff} was calculated according to Fick's second law (equation (3)); the series was simplified and the first term was used [12].

$$\begin{aligned}\text{MR} &= \frac{M - M_e}{M_0 - M_e} \\ &= \frac{8}{\pi^2} \sum_{n=0}^{\infty} \frac{1}{(2n+1)^2} \exp\left[-(2n+1)^2 \frac{\pi^2}{4} \frac{D_{\text{eff}} t}{L^2}\right],\end{aligned} \tag{3}$$

where t is the time (s), D_{eff} is the effective moisture diffusivity (m^2/s), L is the thickness (m). For long drying times (MR < 0.6), a limiting case of equation (3) was assumed and expressed in the logarithmic form as in the following equation:

$$\ln\text{MR} = \ln\left(\frac{8}{\pi^2}\right) - \left(\frac{\pi^2 D_{\text{eff}}}{4L^2}\right)t, \tag{4}$$

where D_{eff} is typically calculated by plotting the experimental moisture ratio in the logarithmic form versus drying time. From equation (4), a plot of lnMR versus drying time gives a straight line with a slope of the following equation:

$$\text{Slope} = \frac{\pi^2 D_{\text{eff}}}{4\text{L}^2}. \tag{5}$$

The relationship between the D_{eff} and the air temperature was assumed to be the Arrhenius function and E_a was calculated using the following equation:

$$D_{\text{eff}} = D_0 \exp\left(-\frac{E_a}{\text{RT}}\right), \tag{6}$$

where D_0 is the preexponential factor (m^2/s), E_a is the activation energy (kJ/mol), T is the absolute temperature (K), and R is the gas constant ($R = 8.31451$ J/molK).

2.2.2. Modeling Studies of the Drying Kinetics. The selected thin-layer drying models are shown in Table 1. The fit of the models was determined by the regression coefficient (R^2), the error of the root mean square (RMSE), and the chi-square (χ^2) values [12].

2.2.3. Modeling of the Desorption Isotherms. The models used to determine the moisture sorption isotherms of foods are given in Table 1. The parameters (k, C, and M_0) of the sorption models were determined from the experimental data by nonlinear regression analysis using the Microsoft Excel program (MS Office Excel 2016). The fit of the models was determined by the regression coefficient (R^2), the error of the root mean square (RMSE), and the chi-square (χ^2) values.

Table 1: Thin layer drying and desorption models.

Models		Equation	Reference
Thin layer drying models	Page	$MR = \exp(-kt^n)$	[13]
	Henderson and Pabis	$MR = a \exp(-kt)$	[14]
	Lewis	$MR = \exp(-kt)$	[15]
	Logarithmic	$MR = a \exp(-kt) + b$	[16]
Desorption models	Guggenheim, Anderson and de Boer (GAB)	$M = (M_0 Cka_w/[(1-ka_w)(1-ka_w+Cka_w)])$	[17]
	Braunauer, Emmett and Teller (BET)	$M = (M_0 Cka_w/[(1-a_w)(1+(C-1)a_w)])$	[18]
	Oswin	$M = k(a_w/1-a_w)^n$	[19]
	Henderson	$M = k(-\ln(1-a_w)/C)^{(1/n)}$	[20]
	Halsey	$M = (-C/\ln a_w)^{(1/n)}$	[21]

2.2.4. Analysis

(1) Water Activity Measurement. The water activity values of fresh and dried apple slices were determined using a water activity measuring device (GBX, Fast-Lab, France) with an accuracy of ±0.001.

(2) Preparation of Extracts. In order to obtain the extract, approximately 2 g of apples were taken during the drying process and crushed with a mortar. The crushed samples were taken into flasks and 10 mL of 70% ethanol was added. It was exposed to ultrasonication in an ultrasonic water bath (Wise Clean Wisd WUC-D06H, Daihan, South Korea) for 10 min, then agitated for 15 min in an orbital shaker (SHO-1D, Daihan, South Korea) at 200 rpm and centrifuged for 10 minutes at 10°C at 7450 rpm (NF 800R, Nüve, Turkey). The upper phase was taken into a 25 mL flask, the remaining residue was passed through the same processes again and the obtained upper combined with the previous one, and the extract was completed with 70% ethanol to 25 mL volume. The prepared extracts were stored at −20°C.

(3) Determination of Antioxidant Activity by DPPH Method. DPPH stock solution was prepared in methanol with a final concentration of 24 mg/100 mL. The solution was diluted with methanol by diluting the stock solution so that the final absorbance was 1.20 ± 0.02. The calibration curve was obtained with Trolox®. Trolox® solution was prepared with a concentration of 12.5 mg/25 mL and a final concentration of less than 50 μM in the spectrophotometer cuvette for the Trolox® calibration curve. In the experiments, 150 μL of the sample or standard 2850 μL of DPPH working solution was mixed in test tube and the reaction was continued for 60 minutes in a dark environment. At the end of the time, the absorbance was read in a spectrophotometer (EMC-11, Duisburg, Germany) at a wavelength of 515 nm. Samples that did not fall within the calibration curve range at the end of the reading were diluted until they entered this range [22].

(4) Determination of Total Phenolic Compounds. The Folin–Ciocalteu (FC) method has used the determination of the total phenolic compounds of samples. The Folin–Ciocalteu agent was diluted 1 : 10 by volume using distilled water. To prepare the sodium carbonate solution (20%), sodium carbonate was weighed to 75 g/L and the measuring flask was filled to the volume line with distilled water. In order to prepare the gallic acid calibration curve, 500 mg/L stock solution was prepared and dilution was made so that the final concentration was 5–100 mg/L in the linear region. 2 mL of sample or standard was taken and 10 mL of diluted FC agent was added. 8 mL of 20% sodium carbonate was added between 1–8 minutes after the reaction started and the mixture was left in a dark environment for 2 hours. At the end of the period, absorbances were read at 760 nm wavelength. If the results read did not fall within the calibration curve, necessary dilutions were made [23].

(5) Color Measurement. The color values of the samples were measured with a colorimeter (Hunter Associates Laboratory, Model: MiniScan XE, USA). In addition, Hue Angle, Chroma, and total color change (ΔE) values were calculated [24].

2.2.5. Modeling Studies for Investigation of Bioactive Components and Color Changes

(1) Kinetic Models. The zero-order, first-order, and second-order kinetic models were presented in equations (7–9), respectively.

$$C = C_0 \pm k_0 * t, \tag{7}$$

$$C = C_0 * \exp(\pm k_1 * t), \tag{8}$$

$$\frac{1}{C} = \frac{1}{C_0} \pm k_2 * t. \tag{9}$$

where C is the value of bioactive component or color parameter at any time t, C_0 is the bioactive component or color parameter value at time $t = 0$, k_0, k_1, and k_2 are the kinetic constants (1/min), and t is the drying time (min).

The degree of dependence of the reaction on temperature was determined by calculating both Q_{10} and activation energy values. The relationship between reaction rate and temperature was defined by Arrhenius in 1889, and this expression, which is still valid today, is given in equation (10). The activation energy was calculated using this equation. E_a was calculated by using the slope of the line obtained by drawing the $1/T$-ln$k$ graph:

$$k = k_0 * \exp\left(\frac{-E_a}{\mathrm{RT}}\right), \quad (10)$$

where k is the kinetic constant (min^{-1}), k_o is the Arrhenius constant or frequency factor, R is the gas constant (8.314 J/mol·K), and T is the temperature (K).

2.2.6. Calculation of the Q_{10} Value and Half-Life Time. Q_{10} value, which is another kinetic coefficient showing the dependence of the reaction on temperature, is a criterion that shows the effect of increasing the temperature by 10°C on the reaction rate [23] and was calculated using the following equation:

$$Q_{10} = \left(\frac{k_2}{k_1}\right)^{\left(10/T_2 - T_1\right)}, \quad (11)$$

where k_1 is the kinetic constant at temperature T_1 (1/min), k_2 is the kinetic constant at temperature T_2 (1/min), T_1 and T_2 are the temperatures (K).

Half-life time is the time required for the loss of 50% of the bioactive components [23]; for the first-order reactions, it is presented in the following equation:

$$t_{(1/2)} = -\ln(0.5) * k^{-1}. \quad (12)$$

2.2.7. Statistical Analysis. The data obtained as a result of the experiments carried out in two parallels and three replications were analyzed by using the SPSS statistical package program 20.0 (SPSS Inc., USA). The level of difference between the means was determined using the Duncan multiple comparison test ($p \leq 0.05$).

3. Results and Discussion

3.1. Drying Kinetics of Apple Slices. The initial moisture content and water activity of the apple slices were found as 6.74 kg water/kg DM and 0.962, respectively. The water activity values of apple chip snacks were measured as 0.348 (45°C), 0.278 (55°C), and 0.299 (65°C) for 1.5 mm thick samples and 0.425 (45°C), 0.396 (55°C), and 0.353 (65°C) for 5 mm thick samples, respectively. The changes in the moisture content of samples versus drying time are given in Figure 1. As can be seen in Figure 1, the drying times decreased with the increase in the drying temperature and the decrease in the slice thickness. The drying time of 1.5 mm and 5 mm thick samples ranged between 120–180 min and 180–330 min, respectively. As a matter of fact, it took 120 min for the moisture content of 1.5 mm thick apple slices to decrease from 6.74 to 0.27 kg water/kg DM at a temperature of 65°C. During the process, the process was completed in 180 minutes for apple slices with a thickness of 5 mm at the same temperature. In this context, it can be said that both drying temperature and slice thickness have a significant effect on the drying time ($p < 0.05$). Similarly, Jeevarathinam et al. [25] reported that temperature has a significant effect on drying time, moisture removal, and drying rates. It is expected that the drying time will decrease as the product thickness decreases and the temperature rises. As the thickness decreases, the amount of water that will evaporate from the product will decrease as well as the distance related to the water reaching the surface will decrease, thus reducing the drying time [26, 27]. With the increase in temperature, the evaporation rate of water increases, which shortens the drying time. It is also known that the temperature gradient is inversely proportional to the drying time. As the temperature increases, the gradient increases, and the drying time becomes shorter. Similar findings were also obtained by several researchers [25, 27–30]. The hot air drying times of apple slices (4 mm thickness × 20 mm radius) were found as 195, 170, and 140 min for 50, 60, and 70°C temperatures and 1.5 m/s air velocity [28]. Hot air (60–65°C, 0.5 m/s), microwave-vacuum (2 W/g), freeze (plate temperature of 30°C at 0.2 kPa), microwave-vacuum (2 W/g) + freeze-drying time (plate temperature of 30°C at 0.2 kPa) of apple slices (20 × 20 × 8 mm) were found as 5.5 h, 0.6 h, 24 h, and 12.5, respectively [29]. The hot air drying times of organic apple slices were found as 400, 300, and 240 min (5 mm thick slices) and 640, 560, and 460 min (9 mm thick slices) for 40, 50, and 60°C drying temperatures, respectively [27]. Different drying techniques, product thicknesses, and drying conditions affect the drying time. A study has investigated the effect of drying temperature (40–50°C), airflow rate (0.6–1.1 m/s), apple slice thickness (4–12 mm), and relative humidity (25–28–40–45%); it was stated that the most important factor was found as slice thickness. The 3-fold increase in apple slice thickness increased the drying time by more than 500 min. In addition, researchers reported that, although the thickness is not important in the presence of free water to be removed at the beginning of drying, the importance of the thickness increases as the amount of water that will evaporate decreases [31].

Table 2 shows the model parameters of selected thin-layer drying models for the determination of the drying behavior of apple snacks. When Table 2 is examined, it is seen that all selected thin-layer models explain the drying behavior of apple chips with a high R^2 value (>0.972). The highest R^2 and lowest X^2 and RMSE values were generally obtained from the Page model. In addition, mathematical models that are simple and contain fewer terms are generally preferred to describe the drying behaviors of food materials. In this context, it is appropriate to choose the Page model. Similarly, in the literature, it is reported that the Page model could adequately describe the drying behavior of fluidized bed drying of apple cubes [32], and the hot air drying behavior of cylindrical apple slices at different temperatures, slice thicknesses, air velocities, and relative air humidities [31]. The drying (k, h^{-1}) and model (n, dimensionless) constants of the Page model generally increased with increasing temperature. Vega-Gálvez et al. [33] reported that the drying constant increased whereas the model constant of the Page model decreased depending on the increasing temperature. In addition, the drying constants of the Page model obtained for 1.5 mm thick samples are higher than that obtained for 5 mm. It is thought that the reason for this situation is that the apple slices dried faster at high

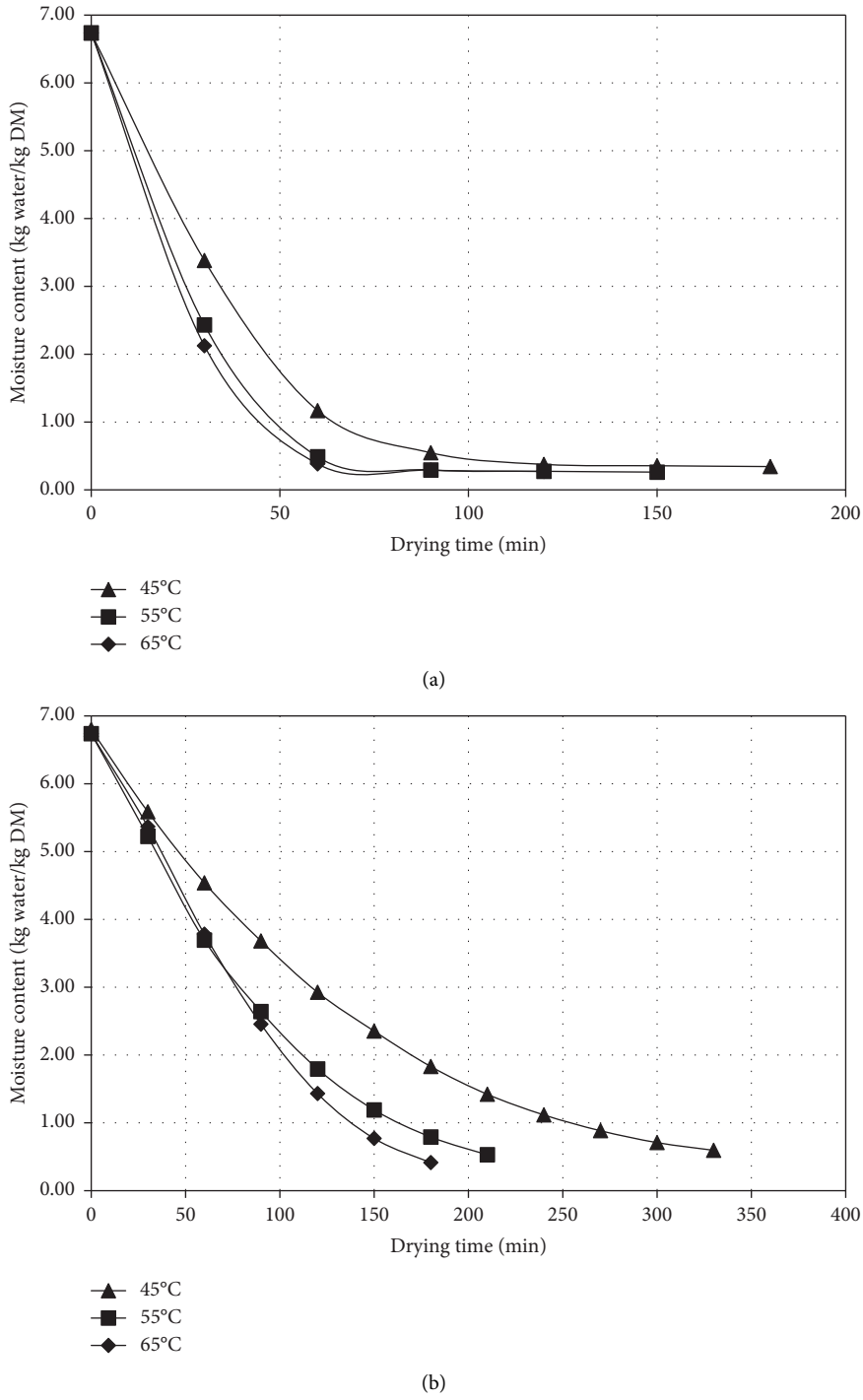

Figure 1: Changes in the moisture content values of apple slices during drying ((a) = 1.5 ± 0.5 mm thickness, (b) = 5 ± 0.5 mm thickness).

temperatures and low thickness due to the high evaporation rate. MR values that are calculated with the Page model versus experimental MR values are shown in Figure 2. MR values were generally gathered around a straight line. This shows that the Page model explains the hot air drying behavior of apple slices to a high extent.

The drying rates of apple slices were calculated and graphs were drawn of the drying rate versus moisture content (Figure 3). Although a temperature rise period was observed for the 5 mm thick apple slices that were drying at 55 and 65°C temperatures, the drying of all samples took place in the falling rate period. This is expected for biological materials. It shows that the moisture movement in the apple slices is mainly controlled by molecular diffusion [28]. In addition, with the increase in temperature, the evaporation rate of water increased and the drying rate increased. This is

Table 2: Thin layer mathematical models.

Models	Thickness (mm)	Drying air temperature (°C)	Model parameters			χ^2	RMSE	R^2
Page	1.5	45	$k = 1.566$	$n = 1.103$		0.0012	0.0287	0.992
		55	$k = 2.342$	$n = 1.175$		0.0009	0.0249	0.995
		65	$k = 2.533$	$n = 1.112$		0.0008	0.0220	0.996
Henderson and Pabis		45	$k = 1.540$	$a = 1.007$		0.0013	0.0299	0.992
		55	$k = 2.163$	$a = 1.003$		0.0011	0.0266	0.994
		65	$k = 2.397$	$a = 1.001$		0.0009	0.0229	0.996
Lewis		45	$k = 1.531$			0.0011	0.0300	0.992
		55	$k = 2.159$			0.0009	0.0266	0.994
		65	$k = 2.394$			0.0007	0.0229	0.996
Logarithmic		45	$k = 1.653$	$a = 0.987$	$b = 0.024$	0.0013	0.0270	0.993
		55	$k = 2.295$	$a = 0.985$	$b = 0.019$	0.0011	0.0240	0.995
		65	$k = 2.521$	$a = 0.986$	$b = 0.016$	0.0011	0.0210	0.997
Page	5	45	$k = 0.403$	$n = 1.072$		$1.48E-05$	0.0035	0.999
		55	$k = 0.588$	$n = 1.173$		$1.55E-05$	0.0034	0.999
		65	$k = 0.581$	$n = 1.413$		$3.11E-05$	0.0047	0.999
Henderson and Pabis		45	$k = 0.439$	$a = 1.016$		0.0001	0.0101	0.999
		55	$k = 0.664$	$a = 1.029$		0.0007	0.0226	0.995
		65	$k = 0.732$	$a = 1.054$		0.0035	0.0500	0.977
Lewis		45	$k = 0.431$			0.0002	0.0118	0.998
		55	$k = 0.645$			0.0008	0.0257	0.993
		65	$k = 0.695$			0.0035	0.0550	0.972
Logarithmic		45	$k = 0.400$	$a = 1.047$	$b = -0.040$	$5.18E-05$	0.0062	0.999
		55	$k = 0.538$	$a = 1.117$	$b = -0.104$	0.0002	0.0123	0.998
		65	$k = 0.423$	$a = 1.372$	$b = -0.350$	0.0009	0.0228	0.995

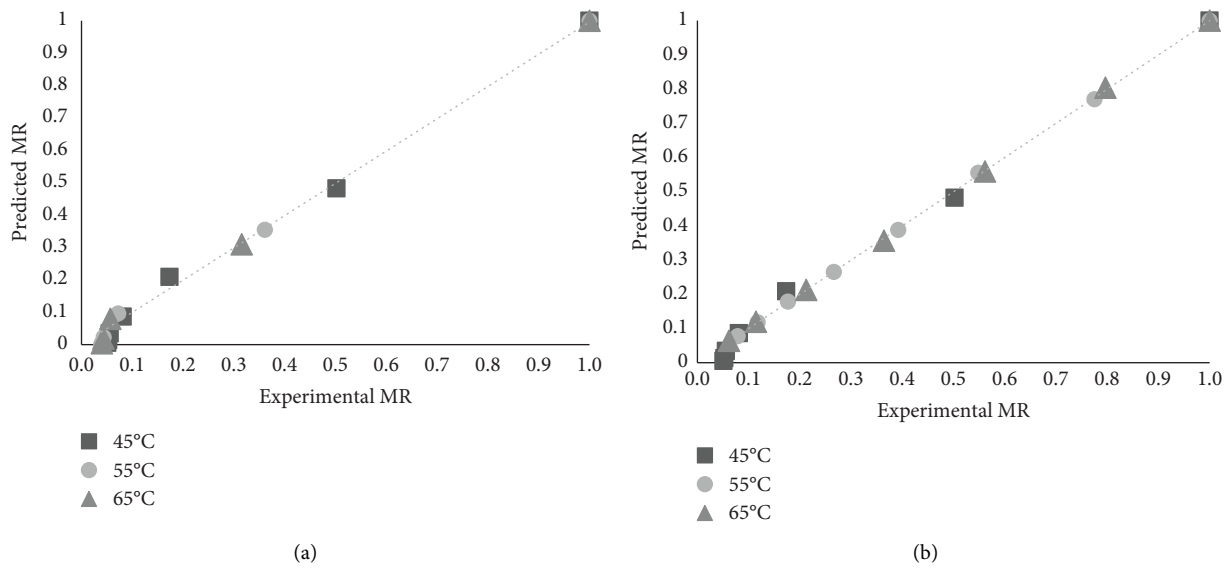

Figure 2: Predicted MR versus experimental MR ((a) = 1.5 ± 0.5 mm thickness, (b) = 5 ± 0.5 mm thickness).

an expected situation. It was also observed that there was an inverse relationship between the thickness and the drying rate. When the drying rates of apple slices were examined depending on the thickness, it can be said that the drying rates of 1.5 mm thick apple slices are approximately 3–4 times higher than those with a thickness of 5 mm. Similar findings were also obtained by Wang and Chao [34] and Sacilik and Elicin [27]. Wang and Chao [34] studied the effect of different thicknesses (3, 5, and 7 mm) and air temperatures (50, 60, and 75°C) on the drying rate of the Fuji apple slices, and the researchers stated that the drying rate increased with increasing drying temperature and decreasing slice thickness. The effective diffusion coefficient was calculated from the slope obtained by plotting the graph of ln MR versus ln t (min). D_{eff} values were calculated as $3.37E-07$ ($R^2 = 0.982$), $3.73E-07$ ($R^2 = 0.9335$), and $4.29E-07$ ($R^2 = 0.9405$) m^2/s for 1.5 mm slice thickness and $3.07E-06$ ($R^2 = 0.9458$), $3.12E-06$ ($R^2 = 0.9062$), and

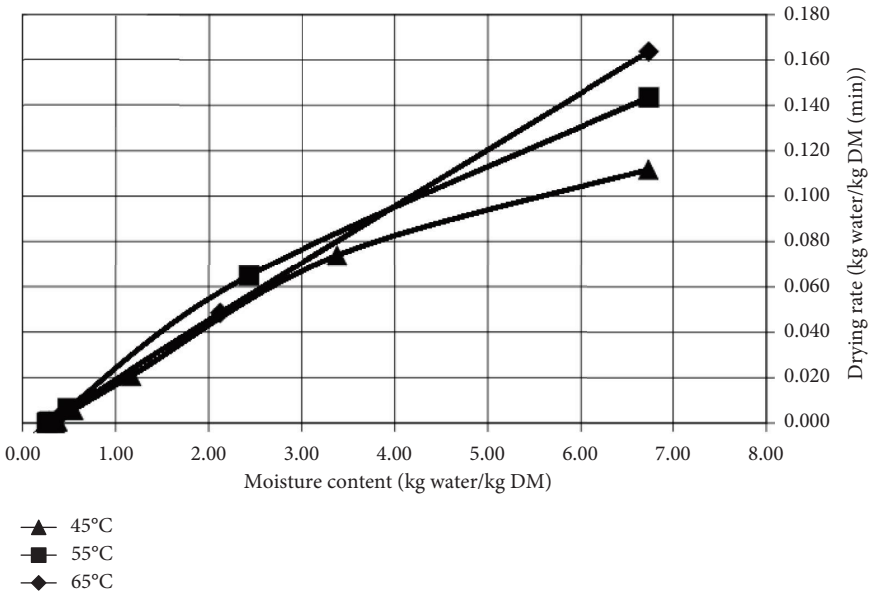

(a)

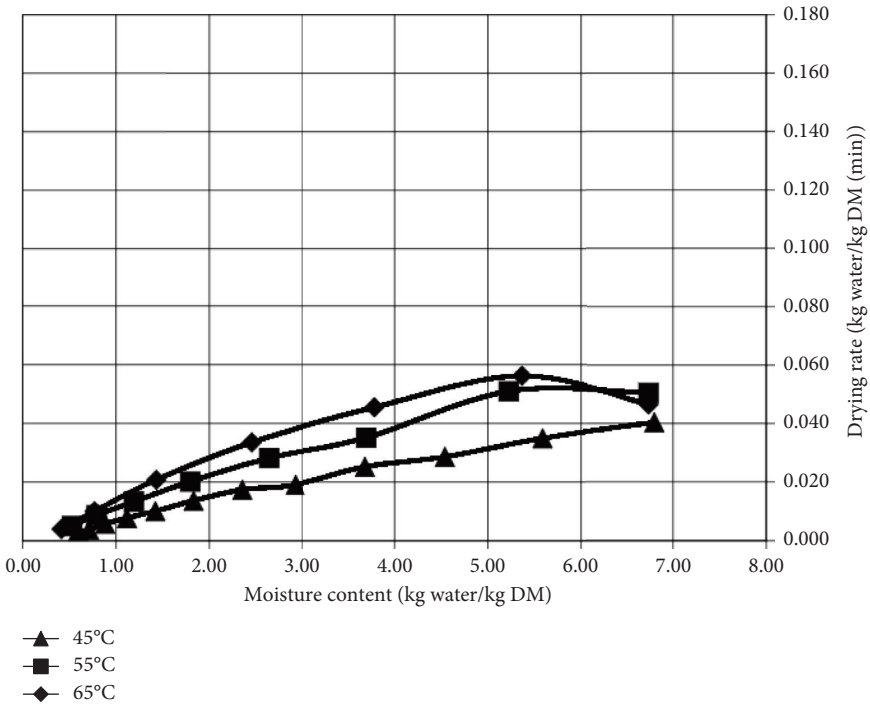

(b)

Figure 3: Changes in the drying rate of apple slices versus moisture content ((a) = 1.5 ± 0.5 mm thickness, (b) = 5 ± 0.5 mm thickness).

$4.31E-06$ ($R^2 = 0.9551$) m^2/s for 5 mm slice thickness at 45, 55, and 65°C temperatures. These values were found lower compared to the estimated values for apple slices. The D_{eff} values of hot air-dried apple slices were calculated as $4.85E-9\ m^2/s$ [35], $1.9E-10$ and $7.0E-10\ m^2/s$ [31], $2.27E-10$ and $4.97E-10\ m^2/s$ [27], $0.964E-09$ and $2.28E-09$ [36], $1.70E-09$-$4.45E-09\ m^2/s$ [37], $0.841E-9$-$2.060E-9\ m^2/s$ [38]. Different drying conditions (temperature, air flow rate, and so on) and slice thickness may be the reason for different values. The D_{eff} values increased depending on the increasing air temperature and slice thickness. Similar findings were also obtained by [4, 27, 31]. This is thought to be due to the fact that air temperatures accelerate moisture diffusion. In addition, Zhu et al. [35] reported that the temperature rising intensified the mobility of water molecules. Activation energy values were calculated as 10.56 kJ/mol and 14.70 kJ/mol for 1.5 mm and 5 mm sample thicknesses, respectively. It can be stated that 5 mm thick samples are more susceptible to temperature change compared to 1.5 mm thick samples. Higher E_a values such as

28.37 kJ/mol [39], 19.80 kJ/mol [28], 19.34 kJ/mol [36], and 113.018 kJ/mol [35] were observed for hot air-dried apple slices. It can also be stated that 5 mm thick samples are more susceptible to temperature change compared to 1.5 mm thick samples.

3.2. Desorption Isotherms. In order to determine the desorption isotherms of apple slices, the water activity values of samples were measured at half-hour intervals during drying, and the compatibility of these values with the models was examined and the results were given in Table 3. When Table 3 is examined that although χ^2 and RMSE values for GAB model are higher than BET and OSWIN models for 1.5 mm slice thickness, the highest R^2 values were obtained from the GAB model. The lowest R^2 values were obtained from the BET model. The BET model gives the most suitable results in water activity values between 0.05 and 0.45, however, our water activity values are not in this range. It may be the reason for low R^2 values [40]. For both thicknesses, it can be said that the GAB model is the best model for the determination of the desorption behavior of apple slices with the highest R^2 value. GAB model was also found the best model for representing the desorption isotherm 5 mm thick apple slices at 45°C [33]. According to the monolayer (C) values which ranged between 0 and 2 (except for the BET model for 1.5 mm thickness), it can be stated that all isotherms are J-Type [41]. It can be said that there is an increase in the k value depending on the temperature, but there is no trend for the monolayer (C) and monolayer moisture content (M_0) values. In addition, the k values calculated for 1.5 mm thick samples were higher than that calculated for 5 mm, and the opposite effect was observed for the C value.

3.3. Antioxidant Activity, Total Phenolic Compounds, and Color Values. The antioxidant activity and total phenolic compounds of fresh apple slices were found as 289.24 μmol Trolox equivalence/100 g DM and 957.63 mg Gallic acid equivalence/100 g DM, respectively. During the drying process, quality losses of dried foods occur depending on the drying conditions. For this reason, the changes in antioxidant activity, total phenolic compounds, and color values of apple chips during the drying process were investigated. While 1.5 mm thick samples lost 50% of their antioxidant activity in the first half-hour, 5 mm thick samples were lost in 1 hour. It was also observed that 90% of the antioxidant activity was lost as a result of the drying process for all thicknesses and temperature values. The antioxidant activity values of apple chips were measured as 32.37, 34.44, and 31.60 μmol Trolox equivalence/100 g DM for 1.5 mm thickness and 24.41, 31.45, and 25.79 μmol Trolox equivalence/100 g DM for 5 mm at 45, 55, and 65°C, respectively. According to the antioxidant activity values, it can also be said that the highest values were observed for 55°C temperature and 1.5 mm thickness. The drying times of the 5 mm thick sample were longer than the 1.5 mm thick sample. It may be the reason for lower antioxidant activity. Lower drying times result in higher quality in the dried product by minimizing undesirable changes [42, 43]. It is known that polyphenols and ascorbic acid contribute to the antioxidant activity of apples [2]. As a result of the drying process, approximately 55% decrease occurs in the total phenolic compounds of apples, while the loss of antioxidant activity is around 90%. It is known that ascorbic acid decomposes under the influence of heat, light, and metal. This is thought to be due to the loss of ascorbic acid.

The total phenolic compounds of the apple chips decreased depending on the increasing drying temperature and increasing thickness (411.90, 398.00, and 361.86 mg Gallic acid equivalence/100 g DM for 1.5 mm thickness and 368.45, 340.94, and 303.99 mg Gallic acid equivalence/100 g DM for 5 mm thickness at 45, 55, and 65°C, respectively). The phenolic compound loss is around 55%. Kidoń and Grabowska [42] reported that the initial total phenolic content of red flesh apple is 421 mg GAE/100 g DM and convective drying (60°C) and convective (60°C) + microwave vacuum (60 s at 1.0 kW, 60 s at 0.2 kW, 20 s without microwave radiation at 28 kPa) drying processes caused 20% reduction in the total phenolic content.

The color values of fresh apple slices were measured as $L = 72.41$, $a = 0.41$, and $b = 19.63$, respectively. The color values of 1.5 mm thick samples were $L = 70.49$, $a = 8.37$, and $b = 34.50$; $L = 65.35$, $a = 15.05$, and $b = 36.26$; $L = 73.52$, $a = 9.54$, and $b = 35.32$ for 45, 55, and 65°C, respectively. The color values of 5 mm thick samples were $L = 62.06$, $a = 13.65$, and $b = 38.68$; $L = 62.81$, $a = 10.28$, and $b = 34.42$; $L = 68.72$, $a = 10.21$, and $b = 39.99$ for 45, 55, and 65°C, respectively. According to the color values of the final product, it can also be said that the L value was generally found to be lower than the initial value (fresh apple), and the a and b values were found to be higher. Similar findings were also obtained for hot air-dried, freeze-dried, hot air + puffing dried, and hot air + CO_2 puffing dried apple slices [4], microwave + freeze-dried, microwave-vacuum + freeze-dried, freeze-dried, and hot air-dried apple slices [29]. Sacilik and Elicin [27] also reported that higher temperatures resulted in darker apple slices. Although the L value of the samples with a thickness of 5 mm was found to be lower than those with a thickness of 1.5 mm, generally higher a, and b values were obtained. In addition, a general decrease in color values was observed depending on the temperature. The heat effect and enzymatic and nonenzymatic browning reactions may be the reason for the formation of brown pigments that cause the lower and higher a, b, and ΔE values [42]. The ΔE values of apple slices were calculated as 16.97, 23.25, and 18.19 for 1.5 mm thickness and 25.40, 20.20, and 22.90 for 5 mm thickness at 45, 55, and 65°C, respectively. In light of these findings, it can be said that the total color change increases significantly as the thickness increases ($p < 0.05$). In addition, although the effect of temperature change in 1.5 mm thick samples was found to be statistically significant

Table 3: Desorption model parameters and statistical results.

Models	Thickness (mm)	Drying air temperature (°C)	Model parameters			χ^2	RMSE	R^2
		45	$k = 0.983$	$C = 4.885$	$M_0 = 0.316$	0.250	0.378	0.9992
GAB		55	$k = 1.162$	$C = 0.321$	$M_0 = 1.097$	1.871	3.270	0.9979
		65	$k = 2.001$	$C = 0.463$	$M_0 = 0.239$	0.641	0.506	0.9999
		45		$C = 13.587$	$M_0 = 0.258$	0.005	0.058	0.5706
BET		55		$C = 3.917$	$M_0 = 0.334$	1.164	0.881	0.5051
		65		$C = 81.090$	$M_0 = 0.272$	0.968	0.762	0.3014
		45	$k = 0.531$		$n = 0.754$	0.122	0.295	0.9112
Oswin	1.5	55	$k = 0.582$		$n = 0.829$	0.858	0.756	0.7934
		65	$k = 0.760$		$n = 0.715$	1.040	0.790	0.8920
		45		$C = 0.708$	$n = 0.020$	11.710	2.892	0.9662
Henderson		55		$C = 0.647$	$n = -0.168$	26.981	3.902	0.8536
		65		$C = 0.566$	$n = 0.607$	41.995	5.020	0.9128
		45		$C = 1.127$	$n = 1.012$	17.612	9.011	0.8940
Halsey		55		$C = 0.974$	$n = 1.022$	13.367	10.554	0.7582
		65		$C = 0.872$	$n = 0.870$	14.254	12.771	0.8757
		45	$k = 0.941$	$C = 1.209$	$M_0 = 0.665$	0.138	0.326	0.9992
GAB		55	$k = 0.979$	$C = 1.036$	$M_0 = 0.459$	0.643	0.671	0.9979
		65	$k = 0.991$	$C = 1.742$	$M_0 = 0.348$	0.324	0.450	0.9999
		45		$C = 4.238$	$M_0 = 0.331$	0.400	0.582	0.5706
BET		55		$C = 1.098$	$M_0 = 0.293$	0.849	0.824	0.5051
		65		$C = 1.335$	$M_0 = 0.271$	0.416	0.558	0.3014
		45	$k = 0.520$		$n = 0.839$	0.171	0.380	0.9112
Oswin	5	55	$k = 0.420$		$n = 0.906$	0.699	0.748	0.7934
		65	$k = 0.324$		$n = 0.964$	0.314	0.485	0.8920
		45		$C = 1.131$	$n = 0.562$	0.057	0.220	0.9662
Henderson		55		$C = 1.361$	$n = 0.426$	0.585	0.684	0.8536
		65		$C = 1.334$	$n = 0.491$	0.343	0.507	0.9128
		45		$C = 0.359$	$n = 1.020$	0.481	0.638	0.8940
Halsey		55		$C = 0.256$	$n = 0.756$	4.039	1.798	0.7582
		65		$C = 0.243$	$n = 0.850$	0.739	0.744	0.8757

Table 4: 0, 1st and 2nd order reaction kinetic constants.

Temperature (°C)		Thickness (mm)	0 order reaction kinetic constant (k_0)	R^2	1st order reaction kinetic constant (k_1)	R^2	2nd order reaction kinetic constant (k_2)	R^2
	45		74.25	0.7338	0.7182	0.9220	0.0097	0.9914
	55	1.5	85.60	0.6890	0.7863	0.8991	0.0100	0.9956
Antioxidant activity	65		117.81	0.7980	1.1067	0.9480	0.0149	0.9865
	45		44.98	0.8620	0.4792	0.9848	0.0074	0.9524
	55	5	70.88	0.9492	0.6101	0.9892	0.0080	0.8246
	65		82.68	0.8319	0.8090	0.9853	0.0120	0.9623
	45		191.03	0.9918	0.2941	0.9940	0.0005	0.9724
	55	1.5	222.42	0.9981	0.3432	0.9774	0.0006	0.9235
Total phenolic compounds	65		303.65	0.9958	0.4933	0.9807	0.0009	0.9357
	45		107.42	0.9794	0.1728	0.9966	0.0003	0.9957
	55	5	181.53	0.9682	0.3118	0.9905	0.0006	0.9848
	65		214.65	0.9721	0.3897	0.9931	0.0008	0.9699
	45		8.7268	0.9749	0.5902	0.9208	0.0426	0.8496
	55	1.5	8.1814	0.6736	0.1855	0.7320	0.0077	0.7603
Total color change (ΔE)	65		3.6072	0.8530	0.1625	0.8697	0.0100	0.8561
	45		0.7939	0.9976	0.0334	0.9969	0.0014	0.9959
	55	5	9.0028	0.9675	0.6317	0.9881	0.0520	0.9540
	65		11.309	0.7587	0.7099	0.8240	0.0542	0.8978

Table 5: Kinetic parameters of antioxidant activity and total phenolic compounds degradation of apple slices.

Temperature (°C)		Thickness (mm)	Q_{10} value	k (1/min)	$t_{1/2}$ (h)	E_a (kJ/mol)
Antioxidant activity	45	1.5	1.031	0.0097	0.36	19.02
	55			0.0100	0.35	
	65		1.490	0.0149	0.23	
	45	5	1.273	0.4792	1.45	23.39
	55			0.6101	1.14	
	65		1.326	0.8090	0.86	
Total phenolic compounds	45	1.5	1.164	191.03	2.50	20.65
	55			222.42	2.16	
	65		1.365	303.65	1.58	
	45	5	1.804	0.1728	4.01	36.53
	55			0.3118	2.22	
	65		1.250	0.3897	1.78	

($p < 0.05$), the effect of temperature on the total color values of 5 mm thick samples was found to be insignificant ($p > 0.05$).

3.4. Modeling Studies for Investigation of Bioactive Components and Total Color Changes. Their degradations were investigated using zero, first- and second-order reaction kinetic models, and the results are given in Table 4. The reaction kinetics, in which the highest R^2 values were obtained, was chosen as suitable. The total phenolic compounds of the 1.5 mm thick samples conformed to the 0^{th}-order reaction kinetics. Both the antioxidant activity and total phenolic compounds of the 5 mm thick samples were degraded in accordance with the 1st-order reaction kinetics. However, the antioxidant activities of 1.5 mm thick samples were degraded in accordance with the second-order reaction kinetics. Arora et al. [2] also reported that the degradation kinetic of the antioxidant activity and total phenolic content of apples after cutting followed the first-order reaction kinetics. It was observed that the ΔE values of the apple slices changed in accordance with the first-order reaction kinetics. Palazón et al. [44] reported that a higher correlation coefficient was obtained from the zero-order reaction kinetic model for L^*, a^*, b^*, and ΔE^* values of apple-based beikost samples stored at 37°C, whereas the higher correlation coefficient was obtained from 1^{st}-order reaction kinetic model for vitamin C and HMF. Saavedra et al. [45] reported that the pseudo-zero-order reaction kinetic model satisfactorily described the changes in ΔE^* values of apple cluster snacks stored at 18, 25, and 35°C.

It is important to determine the shelf life, which refers to the nutritional and sensory acceptability of foods [45]. Considering these reaction kinetics, Q_{10} value, half-life, and activation energy values were calculated and the results are given in Table 5. In all three reaction kinetics, the reaction rate constants increased with the increase in temperature and decreased as the thickness increased. For both antioxidant activity and total phenolic compounds, the Q_{10} value calculated for 65–55°C temperatures was found to be greater than that calculated according to 45–55°C temperatures. The half-life decreased with increasing temperature and increased with thickness. Higher activation energy values were calculated for 5 mm thick samples. In addition, it can be said that the activation energy values calculated for the total phenolic compounds are higher than those calculated for the antioxidant activity.

4. Conclusion

Nowadays, as the perception of living a healthy life has grown, there is an increase in the pattern of consumption of healthy snacks. One of the products frequently consumed within the scope of these snacks is apple chips. In this study, the changes in the quality characteristics of apple slices at different air temperatures and slice thicknesses were investigated during the production of apple slices consumed as a healthy snack. According to the findings of this study, it was concluded that during the drying process, approximately 45% of the total phenolic compounds and 10% of the antioxidant activity of apple chips were preserved. It is also concluded that the thinner samples (1.5 mm) were dried faster and the biochemical quality are better preserved than thick samples (5 mm). Although the drying temperature of 65°C is advantageous in terms of drying time and rate, it was observed that the antioxidant activity, phenolic compounds, and color of the samples dried at 45°C were better preserved. In this context, conditions, where the thickness and temperature are low, can be considered advantageous in terms of preserving the quality characteristics of apple chip snacks. It is predicted that the findings obtained from this study will shed light on the selection of drying conditions to preserve the quality properties of apple slices for scientific studies on the drying of apple slices. Furthermore, work will be carried out on the effect of different drying techniques such as freeze and puffing on the antioxidant activity and total phenolic compounds of the apple chip snacks.

Data Availability

The data that support the findings of this study are available from the corresponding author upon reasonable request.

Conflicts of Interest

The authors declare that they have no conflicts of interest.

References

[1] V. Rasooli Sharabiani, M. Kaveh, R. Abdi, M. Szymanek, and W. Tanaś, "Estimation of moisture ratio for apple drying by convective and microwave methods using artificial neural network modeling," *Scientific Reports*, vol. 11, no. 1, p. 9155, 2021.

[2] B. Arora, S. Sethi, A. Joshi, V. R. Sagar, and R. R. Sharma, "Antioxidant degradation kinetics in apples," *Journal of Food Science and Technology*, vol. 55, no. 4, pp. 1306–1313, 2018.

[3] N. P. Bondonno, C. P. Bondonno, N. C. Ward, J. M. Hodgson, and K. D. Croft, "The cardiovascular health benefits of apples: whole fruit vs. isolated compounds," *Trends in Food Science and Technology*, vol. 69, pp. 243–256, 2017.

[4] J. Zhu, Y. Liu, C. Zhu, and M. Wei, "Effects of different drying methods on the physical properties and sensory characteristics of apple chip snacks," *LWT - Food Science and Technology*, vol. 154, Article ID 112829, 2022.

[5] E. Betoret, N. Betoret, A. Arilla et al., "No invasive methodology to produce a probiotic low humid apple snack with potential effect against *Helicobacter pylori*," *Journal of Food Engineering*, vol. 110, no. 2, pp. 289–293, 2012.

[6] E. Betoret, E. Sentandreu, N. Betoret, P. Codoñer-Franch, V. Valls-Bellés, and P. Fito, "Technological development and functional properties of an apple snack rich in flavonoid from Mandarin juice," *Innovative Food Science and Emerging Technologies*, vol. 16, pp. 298–304, 2012.

[7] J. Moreno, J. Echeverria, A. Silva et al., "Apple snack enriched with L-arginine using vacuum impregnation/ohmic heating technology," *Food Science and Technology International*, vol. 23, no. 5, pp. 448–456, 2017.

[8] H. Wang, Q. Fu, S. Chen, Z. Hu, and H. Xie, "Effect of hot-water blanching pretreatment on drying characteristics and product qualities for the novel integrated freeze-drying of apple slices," *Journal of Food Quality*, vol. 2018, Article ID 1347513, 12 pages, 2018.

[9] W. P. da Silva, A. F. Rodrigues, C. M. D. P. S. e Silva, D. S. de Castro, and J. P. Gomes, "Comparison between continuous and intermittent drying of whole bananas using empirical and diffusion models to describe the processes," *Journal of Food Engineering*, vol. 166, pp. 230–236, 2015.

[10] S. V. Jangam, "An overview of recent developments and some R&D challenges related to drying of foods," *Drying Technology*, vol. 29, no. 12, pp. 1343–1357, 2011.

[11] D. I. Onwude, N. Hashim, R. B. Janius, K. Abdan, G. Chen, and A. O. Oladejo, "Non-thermal hybrid drying of fruits and vegetables: a review of current technologies," *Innovative Food Science and Emerging Technologies*, vol. 43, pp. 223–238, 2017.

[12] Z. Erbay and F. Icier, "A review of thin layer drying of foods: theory, modeling, and experimental results," *Critical Reviews in Food Science and Nutrition*, vol. 50, no. 5, pp. 441–464, 2010.

[13] G. E. Page, *Factors Influencing the Maximum Rates of Air Drying Shelled Corn in Thin Layers," ProQuest Dissertations and Theses*, Purdue University, West Lafayette, IN, USA, 1949.

[14] S. M. Henderson and S. Pabis, "Grain drying theory, I. Temperature effect on drying constant," *Journal of Agricultural Engineering Research*, vol. 6, pp. 21–26, 1961.

[15] W. K. Lewis, "The rate of drying of solid materials," *Journal of Industrial and Engineering Chemistry*, vol. 13, no. 5, pp. 427–432, 1921.

[16] A. Yagcioglu, "Drying characteristic of laurel leaves under different conditions," in *Proceedings of the 7th International Congress on Agricultural Mechanization and Energy*, pp. 565–569, Adana, Turkey, May 1999.

[17] C. Van Den Berg and S. Bruin, "Water activity and its estimation in food systems," *Theorical Aspects in Water Activity: Influence on Food Quality*, pp. 12–45, Academic Press, Cambridge, MA, USA, 1981.

[18] S. Brunauer, P. H. Emmett, and E. Teller, "Adsorption of gases in multimolecular layers," *Journal of the American Chemical Society*, vol. 60, no. 2, pp. 309–319, 1938.

[19] C. R. Oswin, "The kinetics of package life. III. The isotherm," *Journal of the Society of Chemical Industry*, vol. 65, no. 12, pp. 419–421, 1946.

[20] T. L. Thompson, R. M. Peart, and G. H. Foster, "Mathematical simulation of corn drying a new model," *Transaction of the ASAE*, vol. 11, no. 4, pp. 582–586, 1968.

[21] G. Halsey, "Physical adsorption on non-uniform surfaces," *The Journal of Chemical Physics*, vol. 16, no. 10, pp. 931–937, 1948.

[22] K. Thaipong, U. Boonprakob, K. Crosby, L. Cisneros-Zevallos, and D. Hawkins Byrne, "Comparison of ABTS, DPPH, FRAP, and ORAC assays for estimating antioxidant activity from guava fruit extracts," *Journal of Food Composition and Analysis*, vol. 19, no. 6-7, pp. 669–675, 2006.

[23] B. Cemeroglu, *Food analysis*, Food Technology Association Publications, Ankara, Turkey, 2 edition, 2010.

[24] P. B. Pathare, U. L. Opara, and F. A. J. Al-said, "Colour measurement and analysis in fresh and processed foods: a review," *Food and Bioprocess Technology*, vol. 6, no. 1, pp. 36–60, 2013.

[25] G. Jeevarathinam, R. Pandiselvam, T. Pandiarajan et al., "Design, development, and drying kinetics of infrared-assisted hot air dryer for turmeric slices," *Journal of Food Process Engineering*, vol. 45, no. 6, Article ID 13876, 2022.

[26] G. N. Roman, E. Rotstein, and M. J. Urbicain, "Kinetics of water desorption from apples," *Journal of Food Science*, vol. 44, no. 1, pp. 193–197, 1979.

[27] K. Sacilik and A. K. Elicin, "The thin layer drying characteristics of organic apple slices," *Journal of Food Engineering*, vol. 73, no. 3, pp. 281–289, 2006.

[28] M. Beigi, "Hot air drying of apple slices: dehydration characteristics and quality assessment," *Heat and Mass Transfer*, vol. 52, no. 8, pp. 1435–1442, 2016.

[29] Z. W. Cui, C. Y. Li, C. F. Song, and Y. Song, "Combined microwave-vacuum and freeze drying of carrot and apple chips," *Drying Technology*, vol. 26, no. 12, pp. 1517–1523, 2008.

[30] P. Jiang, W. Jin, Y. Liu et al., "Hot-Air drying characteristics of sea cucumber (*apostichopus japonicus*) and its rehydration properties," *Journal of Food Quality*, vol. 2022, Article ID 5147373, 9 pages, 2022.

[31] M. J. Royen, A. W. Noori, J. Haydary, and J. Haydary, "Experimental study and mathematical modeling of convective thin-layer drying of apple slices," *Processes*, vol. 8, no. 12, p. 1562, 2020.

[32] A. Kaleta, K. Górnicki, R. Winiczenko, and A. Chojnacka, "A Evaluation of drying models of apple (var. Ligol) dried in a fluidized bed dryer," *Energy Conversion and Management*, vol. 67, pp. 179–185, 2013.

[33] A. Vega-Gálvez, M. Miranda, C. Bilbao-Sáinz, E. Uribe, and R. Lemus-Mondaca, "Empirical modeling of drying process for apple (cv. *Granny smith*) slices at different air temperatures," *Journal of Food Processing and Preservation*, vol. 32, no. 6, pp. 972–986, 2008.

[34] J. Wang and Y. Chao, "Drying characteristics of irradiated apple slices," *Journal of Food Engineering*, vol. 52, no. 1, pp. 83–88, 2002.

[35] R. Zhu, S. Jiang, D. Li et al., "Dehydration of apple slices by sequential drying pretreatments and airborne ultrasound-assisted air drying: study on mass transfer, profiles of phenolics and organic acids and PPO activity," *Innovative Food Science and Emerging Technologies*, vol. 75, Article ID 102871, 2022.

[36] J. Srikiatden and J. S. Roberts, "Moisture loss kinetics of apple during convective hot air and isothermal drying," *International Journal of Food Properties*, vol. 8, no. 3, pp. 493–512, 2005.

[37] D. Velić, M. Planinić, S. Tomas, and M. Bilić, "Influence of airflow velocity on kinetics of convection apple drying," *Journal of Food Engineering*, vol. 64, no. 1, pp. 97–102, 2004.

[38] E. K. Akpınar, Y. Biçer, and A. Midilli, "Modeling and experimental study on drying of apple slices in a convective cyclone dryer," *Journal of Food Process Engineering*, vol. 26, no. 6, pp. 515–541, 2003.

[39] T. K. Tepe and B. Tepe, "The comparison of drying and rehydration characteristics of intermittent-microwave and hot-air dried-apple slices," *Heat and Mass Transfer*, vol. 56, no. 11, pp. 3047–3057, 2020.

[40] R. D. Andrade P, R. Lemus M, and C. E. Pérez C, "Models of sorption isotherms for food: uses and limitations," *Vitae*, vol. 18, no. 3, pp. 325–334, 2011.

[41] J. Blahovec and S. Yanniotis, "GAB generalized equation for sorption phenomena," *Food and Bioprocess Technology*, vol. 1, pp. 82–90, 2008.

[42] M. Kidoń and J. Grabowska, "Bioactive compounds, antioxidant activity, and sensory qualities of red-fleshed apples dried by different methods," *LWT - Food Science and Technology*, vol. 136, Article ID 110302, 2021.

[43] D. Witrowa-Rajchert, A. Bawoł, J. Czapski, and M. Kidoń, "Studies on drying of purple carrot roots," *Drying Technology*, vol. 27, no. 12, pp. 1325–1331, 2009.

[44] M. A. Palazón, D. Pérez-Conesa, P. Abellán, G. Ros, F. Romero, and M. L. Vidal, "Determination of shelf-life of homogenized apple-based beikost storage at different temperatures using Weibull hazard model," *LWT - Food Science and Technology*, vol. 42, no. 1, pp. 319–326, 2009.

[45] J. Saavedra, A. Córdova, L. Gálvez, C. Quezada, and R. Navarro, "Principal Component Analysis as an exploration tool for kinetic modeling of food quality: a case study of a dried apple cluster snack," *Journal of Food Engineering*, vol. 119, no. 2, pp. 229–235, 2013.

Hindawi
Journal of Food Quality
Volume 2023, Article ID 2811491, 12 pages
https://doi.org/10.1155/2023/2811491

Research Article

Microwave Drying Modelling of *Stevia rebaudiana* Leaves Using Artificial Neural Network and Its Effect on Color and Biochemical Attributes

Baldev Singh Kalsi, Sandhya Singh, Mohammed Shafiq Alam, and Surekha Bhatia

Department of Processing & Food Engineering, Punjab Agricultural University, Ludhiana, Punjab, India

Correspondence should be addressed to Baldev Singh Kalsi; baldev.kalsi94@gmail.com

Received 9 November 2022; Revised 16 December 2022; Accepted 20 March 2023; Published 11 April 2023

Academic Editor: Kaavya Rathnakumar

Stevia rebaudiana has grown in popularity and consumption across the world as an excellent natural sweetener due to its 300 times sweetness than sugar. Since Stevia leaves are often used in their dried state, the drying process has an inevitable effect on the attributes of finished product. In this study, Stevia leaves were microwave dried at five different levels of powers ranging from 180 to 900 W to evaluate the influence of power levels on moisture ratio (MR), drying rate and time, effective moisture diffusivity, specific energy consumption (SEC), color, and biochemical characteristics. Among the five selected thin layer models for evaluating the drying behavior, the semiempirical page model described the drying kinetics very well with $R^2 > 0.997$. The effective diffusivity increased from 3.834×10^{-11} to 1.997×10^{-10} m^2/s with increasing microwave power, while SEC first increased till 320 W to a value of 9.77 MJ/kg and then followed a decreasing trend. Furthermore, multilayer feed forward (MLF) artificial neural network (ANN) using backpropagation algorithm was used to predict the moisture ratio of Stevia leaves during microwave drying. The result showed that the ANN model with 15 neurons in 1 hidden layer could predict the MR with a high R^2 value (0.999). Thus, ANN modelling can successfully be used as an effective tool for predicting drying kinetics of samples. Furthermore, the color properties showed significant differences between fresh and dried samples except for the hue angle, and the variation in their values was not affected by the microwave dryer's power output. At 720 W power level, the highest content of stevioside (11.84 mg/g) and rebaudioside A (7.11 mg/g) along with maximum retention of ascorbic acid (~86%) was observed, while the highest total phenol content (56.98 mg GAE/g) and antioxidant capacity (74.22%) was reported in microwave dried samples at 900 W.

1. Introduction

Stevia rebaudiana Bertoni, belonging to the family of *Asteraceae* (Compositae), is a small perennial shrub which is indigenous to Paraguay, Brazil, and Argentina [1]. Stevia leaves, a natural sweetener, are seen as an alternative to artificial sweeteners because of its sweetness which is 300 times higher than sucrose with the added benefits of having no calories, no carbs, and without producing blood sugar spikes [2]. Stevia leaves can be eaten fresh or dried, and crushed or sweet components can be extracted from them. The dried leaves with moisture content of 10–13% are used to make commercial sweetener [3]. Depending upon the variety and growing conditions, the dried leaves have stevioside (sweet component) in the range of 4–20% [4].

Like other medicinal herbs, drying of Stevia leaves is necessary for storage and consumption. The drying involves the reduction of moisture to a limit which allows safe and long storage life. The moisture reduction during drying reduces the volume which minimizes the material required for packaging and space for storage and also reduces the cost of transportation [5]. Lately, microwave type of drying is favored because of short drying time period, uniformity in energy dissipation, enhancement of energy recovery, and quality of final product [6–8]. The microwave is an electromagnetic radiation having a frequency in the range of 300 MHz–300 GHz. The varying electric field causes the

rotation of polar particles, and collision of these particles cause friction which emits thermal energy [9, 10]. As a result, significant volumetric heat and gradient of internal vapour pressure are produced within the sample, which pushes moisture towards the surface of the sample from its core. This is the reason that microwave drying substantially completes in less time leading to improved quality of the food product and less energy consumption. This is in contrast to traditional drying, which transfers heat from the sample's surface to its core and lengthen the drying process [11–13].

Theoretical, semitheoretical, and empirical thin layer mathematical models are used to understand drying phenomena. Many of the models provide an acceptable regression to experimental drying data due to their empirical nature; however, they are only confined to processing situations [14]. Due to their learning capabilities and suitability for nonlinear processes, artificial neural networks (ANNs) have a number of advantages over traditional modelling methodologies [15–17]. They are able to model without making any assumptions about the characteristics of the underlying phenomenological mechanisms [14]. Recently, several studies have been reported the application of microwave radiation in drying of leaves of morisa xak (*Amaranthus caudatus*) [18], celery [19], coriander [19], *Laurus nobilis* [5], *Moringa oleifera* [20], and Kaffir lime [21]. The neural network as an approximation approach has been used for microwave drying of thyme leaves [22] and tea leaves [23]. Also, there are not many studies on microwave drying of Stevia leaves in the literature. Those investigations used only single microwave level power (700 or 800 W) [24, 25].

This study is the first (i) to examine how the microwave power level affects the kinetics of drying Stevia leaves and select the best model among five thin layer drying mathematical models, (ii) to determine the effective moisture diffusivity and specific energy consumption, (iii) to develop the ANN model for drying of Stevia leaves at different powers, and (iv) to study the effect of microwave powers on color and biochemical attributes.

2. Materials and Methods

2.1. Plant Material. Fresh leaves of *Stevia rebaudiana* Bertoni were harvested from a local greenhouse located in Ludhiana, Punjab, India. The leaves were meticulously detached from the stem and selected based on visual analysis to have nondestructive appearance and similar green color and size of leaves for the experiment. To preserve the original fresh quality, the plucked leaves were kept in a refrigerator at $5.0 \pm 2^{\circ}$C until they were utilized in drying trials. The determination of the initial moisture content of fresh leaves was carried out using the method described by the AOAC method [26]. Fresh Stevia leaves had an initial moisture content of 80.66% on a wet basis. The thickness of Stevia leaves were estimated by a calibrated digital caliper (Mitutoyo, model Absolute Digimatic, Japan) and was observed as 0.24 ± 0.005 mm.

2.2. Equipment and Procedure of Drying. The microwave drying of Stevia leaves was carried out using a domestic microwave oven (IFB Industries Limited, 34BC1, China) with maximum output power of 900 W at 2450 MHz. The oven has technical features of 230–240 V and 50 Hz. With a revolving glass plate with a diameter of 30 cm at the base of the oven, the drying chamber had a dimension of 376 mm × 498 mm × 500 mm. In addition, it had a digital control facility for modifying the processing time and could operate at various power levels.

For carrying out the drying trials, samples of 25 g of Stevia leaves were used which were weighed using a digital balance (SP J602, OAHUS Corporation, USA) with a precision of 0.01 g. The samples were dried at varying microwave power output from 180 to 900 W and at each of these power outputs, three replications were carried out. The experiments had a reproducibility of 5% or less. Weighing of samples was carried out at a defined time gap by shifting the glass plate, and in less than 10 seconds, each weighing process was finished. Drying was continued until the weight of the sample reduced to 0.1 g/g·db.

2.3. Moisture Ratio, Drying Rate, and Mathematical Modelling. By drying the fresh Stevia leaves in an oven for 24 hours at 105°C, the moisture content of the leaves was evaluated [26]. These moisture contents were utilised to estimate the moisture ratio using the formula and fitted into five popular thin layer drying models to determine the moisture ratio as a function of drying time, which are shown in Table 1.

The moisture ratio of Stevia leaves was determined using the following equation (1):

$$\mathrm{MR} = \frac{M_t - M_e}{M_0 - M_e}. \tag{1}$$

The drying rate was estimated with experimental moisture content data using following equation (2):

$$\mathrm{DR} = \frac{M_{t+dt} - M_t}{dt}, \tag{2}$$

where MR is the moisture ratio (dimensionless), DR is the drying rate (g water/g dry matter·min), M_0 is the initial moisture content (g/g db), M_e is the equilibrium moisture content (g/g db), M_t is the moisture content at the specific time, and M_{t+dt} is the moisture content (g/g·db) at $t + \mathrm{d}t$ [6].

2.4. Effective Moisture Diffusivity. The estimation of the rate of moisture movement during the drying process can be represented with effective diffusivity. Fick's second law of diffusion can be applied to proximate the mass transfer in a sample regardless of the sort of mechanism engaged in drying [27].

$$\mathrm{MR} = \frac{8}{\pi^2} \exp\left(-\frac{\pi^2 D_{\mathrm{eff}}}{4L^2}\right) t, \tag{3}$$

where L is the sample's half thickness (m), D_{eff} is the effective moisture diffusivity (m^2/s), and t is the drying time (s). The

Table 1: Statistical factors of different models fit of moisture ratio for microwave drying of Stevia leaves.

Model	Equation	Power (W)	Estimated coefficients	R^2	Adjusted R-square	χ^2	RMSE
Lewis	$MR = \exp(-kt)$	180	$k = 0.2153$	0.9690	0.9689	0.0030	0.0543
		360	$k = 0.3848$	0.9849	0.9848	0.0014	0.0373
		540	$k = 0.7508$	0.9974	0.9974	0.0002	0.0143
		720	$k = 1.7050$	0.9943	0.9943	0.0004	0.0204
		900	$k = 2.4763$	0.9992	0.9992	0.0001	0.0087
Page	$MR = \exp(-kt^n)$	180	$k = 0.10952$ $n = 1.39671$	0.9970	0.9969	0.0003	0.0169
		360	$k = 0.28767$, $n = 1.25896$	0.9989	0.9989	0.0001	0.0099
		540	$k = 0.75908$, $n = 0.01986$	0.9974	0.9974	0.0002	0.0143
		720	$k = 1.63719$, $n = 0.84917$	0.9993	0.9993	0.0001	0.0072
		900	$k = 2.41135$, $n = 0.95692$	0.9994	0.9994	0.0001	0.0075
Henderson and Pabis	$MR = a \exp(-kt)$	180	$k = 0.23591$, $a = 1.10368$	0.9784	0.9784	0.0021	0.0453
		360	$k = 0.41505$, $a = 1.08311$	0.9912	0.9911	0.0008	0.0285
		540	$k = 0.74052$, $a = 0.98617$	0.9975	0.9975	0.0002	0.0140
		720	$k = 1.65553$, $a = 0.97161$	0.9948	0.9948	0.0004	0.0195
		900	$k = 2.46346$, $a = 0.99417$	0.9992	0.9991	0.0001	0.0090
Logarithmic	$MR = a \exp(-k_1 t) + c$	180	$k = 1.15943$, $a = 1.1594$, $c = -0.0949$	0.9878	0.9877	0.0012	0.0341
		360	$k = 1.10756$, $a = 1.1075$, $c = -0.0458$	0.9941	0.9941	0.0005	0.0232
		540	$k = 0.99556$, $a = 0.9955$, $c = -0.0194$	0.9983	0.9983	0.0001	0.0116
		720	$k = 0.96565$, $a = 0.9656$, $c = -0.01243$	0.9955	0.9955	0.0003	0.0181
		900	$k = 0.99468$, $a = 0.9946$, $c = -0.00071$	0.9991	0.9990	0.0001	0.0095
Wang and Singh	$MR = 1 + at + bt^2$	180	$a = -0.1565$, $b = 0.0062$	0.9944	0.9943	0.0005	0.0231
		360	$a = -0.2747$, $b = 0.0191$	0.9905	0.9904	0.0009	0.0295
		540	$a = -0.4870$, $b = 0.058$	0.9486	0.9485	0.0041	0.0639
		720	$a = -0.8042$, $b = 0.1480$	0.7764	0.7764	0.0164	0.1279
		900	$a = -1.25736$, $b = 0.3622$	0.8723	0.8722	0.0124	0.1115

RMSE: root mean square error.

aforementioned equation (3) can be expressed as follows in logarithmic form:

$$\ln(\mathrm{MR}) = \ln\left(\frac{8}{\pi^2}\right) - \left(\frac{\pi^2 \times D_{\mathrm{eff}} \times t}{4L^2}\right). \quad (4)$$

Plotting experimental drying data as ln(MR) versus drying time (t) yields a straight line with a slope. The slope is further equated equal to $(\pi^2 \times D_{\mathrm{eff}})/4L^2$ and used to calculate the diffusion coefficient.

2.5. Specific Energy Consumption. Specific energy consumption (SEC) is defined as the amount of energy required to remove a unit mass of water from Stevia leaves and is estimated using mathematical formula given as follows[27]:

$$\mathrm{SEC} = \frac{P \times t \times 10^{-6}}{m_W}, \quad (5)$$

where m_w is the mass of water (kg) evaporated from the sample, P is the microwave power (W), t is the drying time, 10^{-6} is the conversion coefficient of J to MJ, and t is the drying time.

2.6. ANN Modelling. Different ANN models to predict the moisture ratio during microwave drying of Stevia leaves were designed and tested using MATLAB software (R2018a, MathWorks, USA). The most common renowned ANNs, multilayer feed-forward with backpropagation learning algorithm were selected. In the supervised training method used by this algorithm, the network weights and biases are firstly initialised at random. There are at least three layers (input-hidden-output) of nodes in MLF. The ANN contained two inputs (microwave power and time of drying) and one output variable (moisture ratio), as shown in Figure 1.

Before being divided into subgroups for training, validation, and testing, the experimental statistics was initially shuffled. For estimating the gradient along with training the network weights and biases, 70% of the data were used, while 15% were used for network evaluation and 15% were used for testing. Tansig was employed as the network transfer function in this study, with the Levenberg–Marquardt algorithm serving as the training function. Trial and error was utilised to calculate the number of neurons in the hidden layer in order to produce the optimum ANN model. Finally, three statistical criteria—mean square error (MSE), root mean square error (RMSE), and coefficient of determination (R^2)—were calculated to assess the performance of the ANN model as follows:

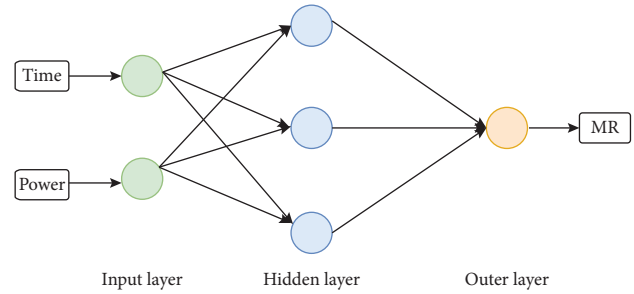

Figure 1: Configuration of artificial neural network model.

$$\mathrm{MSE} = \frac{1}{n}\sum_{i=1}^{n}\left(\mathrm{MR}_{\mathrm{predicted},i} - \mathrm{MR}_{\mathrm{real},i}\right)^2,$$

$$\mathrm{RMSE} = \left[\frac{1}{n}\sum_{i=1}^{n}\left(\mathrm{MR}_{\mathrm{predicted},i} - MR_{\mathrm{real},i}\right)\right]^{1/2}. \quad (6)$$

$$R^2 = 1 - \frac{\sum_{i=1}^{n}\left(\mathrm{MR}_{\mathrm{predicted},i} - \mathrm{MR}_{\mathrm{real},i}\right)^2}{\sum_{i=1}^{n}\left(\mathrm{MR}_{\mathrm{predicted,\,mean}} - \mathrm{MR}_{\mathrm{real},i}\right)^2}.$$

2.7. Color Characteristics. The different color values (L^*, a^*, and b^*) of the Stevia leaves were measured with a colorimeter (Konica Minolta CR-10 color reader, Japan). The value L^* is the measure of lightness which vary from zero for black to 100 for perfect white, value a^* measures redness when positive/greenness when negative, and value b^* measures yellowness when positive/blueness when negative. These values (L^*,a^*, and b^*) were converted into chroma [28] and hue angle [29] using following equations (7) and (8):

$$\mathrm{Chroma}\left(C^*\right) = \left(a^{*^2} + b^{*^2}\right)^{1/2}, \quad (7)$$

$$\mathrm{Hue\ angle}\left(h^*\right) = \tan^{-1}\left(\frac{b^*}{a^*}\right) \mathrm{when}\ a^* > 0\ \mathrm{and}\ b^* > 0, \quad (8)$$

$$\left(h^*\right) = 180^\circ + \tan^{-1}\left(\frac{b^*}{a^*}\right) \mathrm{when}\ a^* < 0\ \mathrm{and}\ b^* > 0\ \mathrm{or}\ b^* < 0, \quad (9)$$

$$\left(h^*\right) = 360^\circ + \tan^{-1}\left(\frac{b^*}{a^*}\right) \mathrm{when}\ a^* > 0\ \mathrm{and}\ b^* < 0. \quad (10)$$

2.8. Steviol Glycosides. The method of Ai et al. [30] was used to extract the steviol glycosides from Stevia leaves. A mixture of 0.2 g of powdered dried Stevia leaves and 10 mL of methanol-water solution (6 : 4 v/v) was sonicated (40 kHz,

250 W) at 60°C for 30 minutes followed by centrifugation for 5 min at 5000 × g. The resulting supernatant was diluted with 60% methanol to 50 mL. The repetition of extraction was carried out three times followed by filtration of extracts through a membrane filter (0.45 μm pore size) before being subjected to HPLC (high-performance liquid chromatography) analysis.

The determination of steviol glycoside was carried out using high-performance liquid chromatography (Agilent Technologies 1260, Wilmington, DE) equipped with an ODS2 column (4.6 mm × 150 mm, 5 μm particle size; Agilent Technologies) and fluorescence detector. The mobile phase was a mixture of acetonitrile and phosphate (32 : 68 v/v). The other parameters were as follows: column temperature 25°C, flow rate 1 ml/min, and injection volume 20 μl. The stevioside and rebaudioside A contents were quantified at 210 nm based on peak area, and results were expressed as mg per g sample.

2.9. Ascorbic Acid. The level of ascorbic acid in the samples of Stevia leaves was estimated using the 2, 6-dichloroindophenol titration method [26]. One gram of Stevia leaves sample was grounded with a mortar and pestle using 3% metaphosphoric acid followed by filtration through Whatman No. 1 filter paper. The ascorbic acid solution was titrated against dye solution (2, 6-dichloroindophenol using phenolphthalein as an indicator to an end-point of faint pink color which should persist for at least 15 s). Results were expressed in the form of mg/100 g of each sample.

2.10. Total Phenolic Content. The total phenolic content (TPC) was measured spectrophotometrically (Model: UV-2601 UV/VIS Double Beam, Rayleigh, China) at 765 nm using the Folin–Ciocalteu technique [31]. The calculation of total phenolics of leave samples was carried out using the linear equation generated from the calibration curve plotted by taking gallic acid as standard. The concentration of gallic acid solution was taken in the range of 5–25 μg/ml for preparing the standard curve. The TPC of Stevia leaves was expressed as equivalents of gallic acid/g (mg GAE/g) of dried leaves.

2.11. DPPH Radical Scavenging Activity. The antioxidant activity (AA) of the samples was estimated using 2,2-diphenyl-1-picrylhydrazyl (DPPH) assay according to the method described by Şahin et al. [32]. The proton-donating activity decreased the absorbance which was recorded at a wavelength of 517 nm and inhibition% was calculated using following formula:

$$\text{Inhibition } \% = \frac{A_0 - A_s}{A_0} \times 100, \tag{11}$$

where A_0 and A_s stand for the absorbance of control (methanol) and sample, respectively.

2.12. Statistical Analysis. Origin Pro 8.5 software was used to do the nonlinear regression analysis. The reduced chi-square (χ^2), root mean square error (RMSE), and coefficient of determination (R^2) were used to determine how well the drying curve fits performed. Higher R^2 values and lower χ^2 and RMSE values are regarded as indicators for a suitable model [33]. Statistical analysis was carried out using SPSS software version 20 for Windows. The means ± SD for triplicate assays of all parameters were examined for significance using ANOVA with t-test to determine any significant difference between the treatments at $p < 0.05$.

3. Results and Discussion

3.1. Moisture Ratio, Drying Rate, and Modelling of Drying Curves. Figure 2 displays the moisture ratio versus drying time for Stevia leaves dried in a microwave at various levels of microwave power. It is evident that when the microwave power level grew from 180 to 900 W, the drying durations of the leaves were drastically reduced to 2.5 minutes from 15 minutes. For Stevia leaves, it took 15, 9, 5.5, 4, and 2.5 min at 180, 360, 540, 720, and 900 W, respectively, to reach the final moisture level (<10% wet basis). As the level of microwave power raised four times, the average drying time dropped by 6 times. This suggests that mass movement within the leaves occurred faster under larger power level because generation of more heat takes place within the leaves and result in a huge vapour pressure differential between the product's center and surface due to the typical microwave volumetric heating [27]. Similar results have been reported in the literature for microwave drying of different leaves of *Pandanus amaryllifolius* [34], coriander [35], and *Ficus carica* Linn [11]. The drying rate versus time is depicted in Figure 3 for various microwave power levels. The current microwave drying experiment only shows a brief period of acceleration at the start, with no steady rate period. Moreover, it was observed that the increase in microwave power amplified the drying rate. These results are in accordance with findings for microwave drying of different food items such as parsley [36] and mango ginger [14].

The information of drying was used to explain the microwave drying kinetics of Stevia leaves. The nonlinear regression analysis was used to fit the experimental data with commonly used five model equations. The coefficient of determination (R^2), root mean square error (RMSE), and the chi-square (χ^2) between the experimental and projected moisture ratio values were used to assess the model's fitness. The statistical findings for Stevia leaves undergoing microwave drying from all models are displayed in Table 1. Analyzed parameter values included the R^2 value between 0.77643 and 0.9994, χ^2 value between 0.0001 and 0.0164, and RSME value between 0.0072 and 0.1279 for different models. The page model was found to be the most suitable one for all the experimental data with the value of coefficient of determination (R^2) greater than 0.997, root mean square error (RMSE) lower than 0.0003, and the chi-square (χ^2) lower than 0.01 in comparison to the statistical parameters obtained for other models selected for investigation (Table 1). Similar outcomes were noted when drying parsley leaves [36] and *Ficus carica* L. leaves [11] in the microwave. Comparison of experimental data with predicted page model is shown in Figure 2. It is observable that the value of the

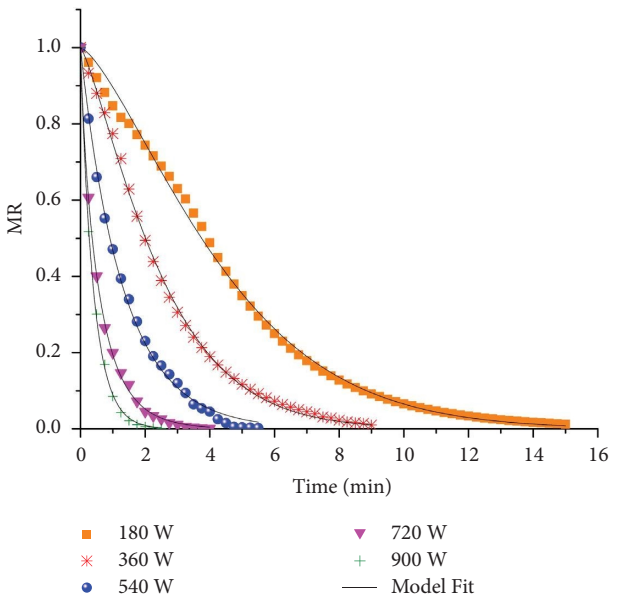

Figure 2: Variation of moisture ratio during microwave drying of Stevia leaves at different powers.

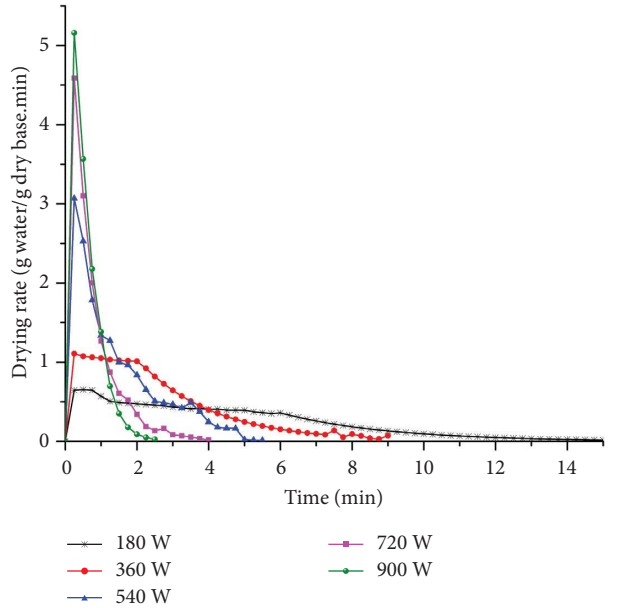

Figure 3: Variation of drying rate during microwave drying of Stevia leaves at different powers.

drying constant k rose together with the growth in the level of microwave power. This indicates that with the increase in microwave power the curve of drying becomes steeper signifying quicker drying of leaves [37].

3.2. Effective Moisture Diffusivity. The method of slopes, which involves graphing ln(MR) versus drying time (t) with regard to data acquired at various microwave power levels, was used to estimate moisture diffusivity. The effective moisture diffusivity values (D_{eff}) and corresponding values of coefficients of determination (R^2) at various power levels are shown in Table 2. In this investigation, D_{eff} values of Stevia leaves ranged from 3.009×10^{-11} to 2.636×10^{-10} m^2/s. Therefore, it was noted the D_{eff} values enhanced with increasing the power level which might be due to the development of a higher moisture gradient between the leaf samples and ambient along with an increment in the driving force of mass transfer and moisture diffusivity [38]. The microwave drying of leaves of purple basil [39] and *Ficus carica L.* [11] had comparable results. Moreover, values of effective diffusivity determined in the current investigation were within the general range 10^{-12} to 10^{-8} m^2/s for food items [27].

3.3. Specific Energy Consumption. The SEC values for various levels of microwave output power, which range from 6.78 to 9.77 MJ/kg water, are shown in the Table 2. This table shows that the final SEC of leaves enhances when microwave power increases from 180 to 360 W. Similarly, initial increase in SEC have been reported in microwave drying of onion slice [40]. In case of microwave drying of peppermint leaves, the SEC increased throughout the microwave power range of 200–600 W [38]. This might be explained by the last phases of the drying's decreased moisture content, which resulted in lower energy absorption by the samples and higher energy requirements for moisture removal [11]. However, The SEC of Stevia leaves decreased with an increase in power from 540 to 900 W which might be due to the decreasing drying time [41]. However, a minor fall in SEC between 540 and 720 W may be due to the fact that these powers (540 and 720 W) have quite closer drying time of leaves (330 and 240 sec, respectively).

3.4. ANN Modelling. Development of an artificial neural network (ANN) was carried out using multilayer feed forward topology and to determine the amount of hidden neurons, these topologies were evaluated. The MSE against the number of hidden neurons was plotted to provide insight into how the number of hidden neurons affects the performance of the artificial neural network, as shown in Figure 4. MSE is an average squared difference between outputs and targets, and lower values are considered for an optimal model. Among the different artificial neural networks, the best network was a three layered topology with 15 neurons in the hidden layer (2-15-1).

The comparison between the experimental and the best ANN model's predicted moisture ratio during the drying procedure is shown in Figure 5. Correlation coefficient (R) predicted by the ANN for training, validation, and testing was 0.99991, 0.99994, and 0.99996, respectively. Figure 6 displays the experimental MR as well as the projected MR by the best ANN for all microwave power levels. The outcomes demonstrated that the ANN is able to predict the drying kinetics of the Stevia leaves with high accuracy when they are dried using microwave energy. For the best ANN, it was discovered that the R^2, MSE, and RMSE values were 0.9999, 1.51×10^{-5}, and 0.039, respectively. Therefore, according to the results obtained in this investigation, a potentially

Table 2: Calculated effective moisture diffusivity values and specific energy consumption for microwave drying of Stevia leaves.

Microwave power level (W)	Effective moisture diffusivity				SEC (MJ/kg water)
	Slope	D_{eff} (m^2/s)	R^2	Adjusted R-square	
180	0.00516	3.834×10^{-11}	0.9920	0.9919	8.14 ± 0180^{c}
360	0.00828	4.470×10^{-11}	0.9920	0.9920	9.77 ± 0.29^{a}
540	0.01768	7.493×10^{-11}	0.9320	0.9319	8.94 ± 0.15^{b}
720	0.02681	1.106×10^{-10}	0.9859	0.9858	8.68 ± 0.21^{b}
900	0.04521	1.997×10^{-10}	0.9967	0.9966	6.78 ± 0.23^{d}

SEC: specific energy consumption and values with same superscript letters in the same column are nonsignificant at $p < 0.05$.

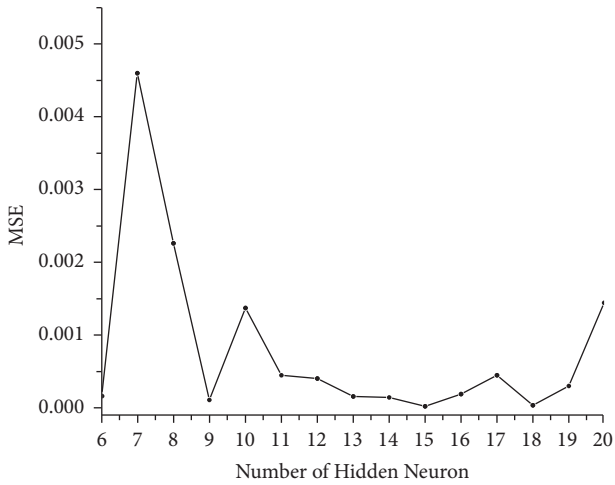

Figure 4: ANN performance evaluation based on the number of hidden neurons for microwave drying of Stevia leaves.

effective method for the prediction of drying kinetics of microwave drying Stevia leaves is ANN modelling.

3.5. Color Characteristics. The color parameters of dried Stevia leaves are depicted in Table 3. The microwave dried leaves showed a significant reduction ($p < 0.05$) in the values of L^*, b^*, and a^* in comparison to the fresh ones. Similarly, the values of chroma of Stevia leaves undergone microwave drying were significantly different from fresh leaves except the values of hue angle. The increase in the level of microwave power from 180 to 900 W did not demonstrate a significant influence ($p > 0.05$) on L^*, b^* and a^*, hue angle, and chroma values. This indicates that the change in parameters of color was not dependent on the level of microwave power. These findings are in good agreement with results of microwave-dried parsley leaves [36] and coriander leaves [35]. It is evident that a nice green tone was maintained even though microwave drying caused some darkening of the leaf color in comparison to the fresh Stevia leaves.

3.6. Steviol Glycosides. The effects of different microwave powers on the steviol glycoside content of Stevia leaves are shown in Table 4. The stevioside and rebaudioside A contents of dried leaves were significantly ($p < 0.05$) reduced in comparison to fresh leaves. The increase in power from 180 to 720 W significantly ($p < 0.05$) enhanced the stevioside and rebaudioside A content in dried leaves. This might be due to the reason that Stevia leaves contain steviol glycoside precursors, which when heated, undergo a chemical reaction to produce the matching sweeteners [42]. The highest content of stevioside (11.84 mg/g) and rebaudioside A (7.11 mg/g) was reported in samples dried at 720 W. Moreover, the increment of power level from 720 to 900 W decreased the content of stevioside and rebaudioside A to 9.01 mg/g and 6.44 mg/g, respectively. When the internal temperature of the material rises during drying, the occurrence of more enzymatic reactions takes place as a result of increased enzyme activity which might have resulted in the decrement of glycoside concentration [43].

3.7. Ascorbic Acid Content. Table 4 compares the ascorbic acid levels of samples of Stevia leaves exposed to different microwave power outputs in comparable to fresh leave sample. The ascorbic content of dried leaves was significantly reduced in comparison to fresh Stevia leaves, while power output also significantly affected the ascorbic acid content of leaves. The lowest value of the ascorbic acid (12.23 mg/100 g) was reported in case of 180 W microwave power which has the longest period of drying. The decline in the content of the ascorbic acid in microwave-dried samples was observed to be linked to the time of drying [44]. The ascorbic acid was retained maximum (~86%) in leaves dried at 720 W. Similar reduction in the values of the ascorbic acid with prolonging of microwave drying were reported for the microwave drying of collard leaves [45]. The ascorbic acid at 900 W was reported as 20.89 mg/100 g which is lesser than the value observed at 720 W. This might be due to the reason that though the drying time is short at 900 W, but the supply of heat is more, which might have led to the significant degradation of the ascorbic acid [46].

3.8. Total Phenolic Content. The total phenolic content of the Stevia leaves dried at different microwave power is depicted in Table 4. The fresh Stevia leaf sample initially estimated for the total phenolic content showed a value of 49.96 mg GAE/g. The total phenolic content of dried samples was significantly ($p < 0.05$) affected by the microwave power. The power of 180 and 360 W showed a significant decline in the content of total phenolics of about 15.55% and 10.58%, respectively, in comparison to that of fresh leaves. This might be due to the reason that phenolic content, being sensitive to the time of drying exposure, degraded at lower power (180 and 360 W) as a period of drying was larger at these powers.

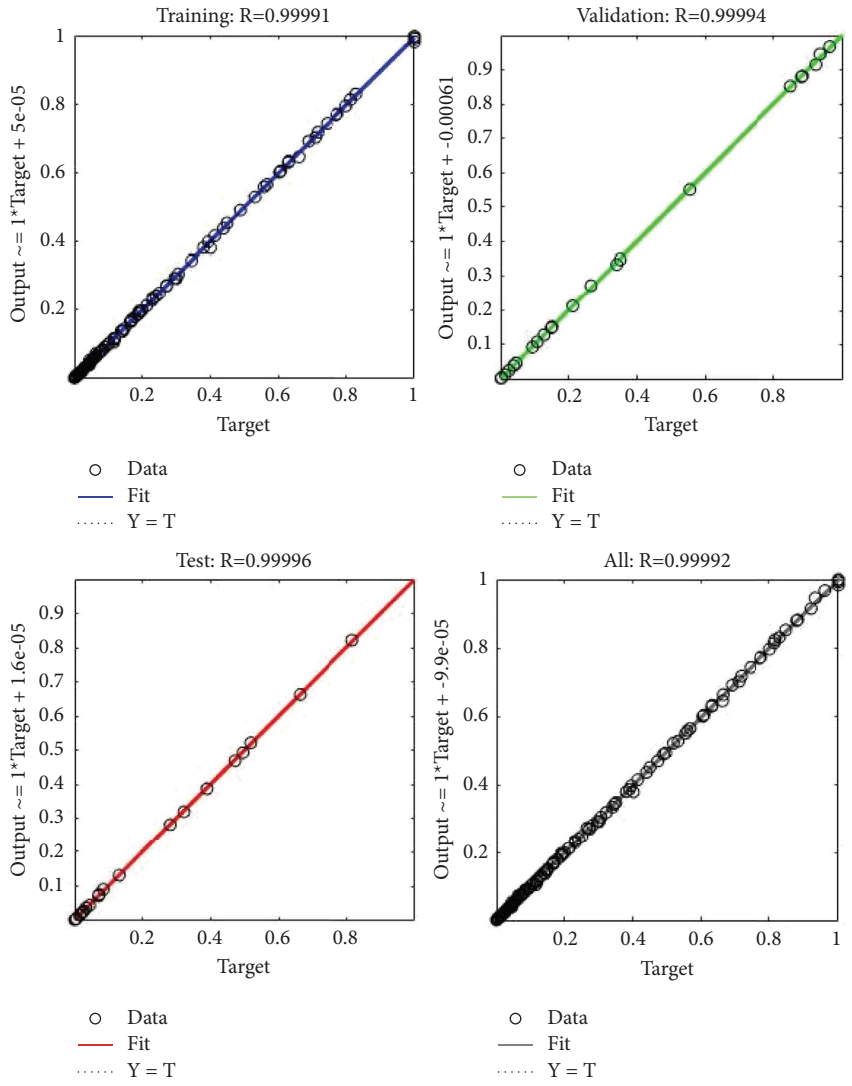

Figure 5: Comparison between experimental and predicted moisture ratios during training, validation, and testing of the best ANN model.

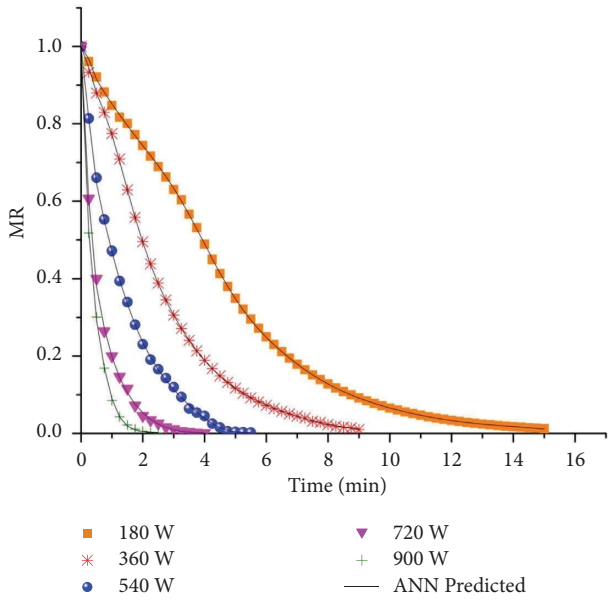

Figure 6: Best ANN model prediction and experimental data for microwave drying of Stevia leaves.

Table 3: Variation of color characteristics for the microwave drying of Stevia leaves.

Microwave power (W)	L^*	b^*	a^*	Hue angle	Chroma
Fresh leaves	41.30 ± 0.17^{a}	-11.10 ± 0.12^{e}	19.55 ± 0.53^{a}	119.60 ± 0.91^{a}	22.48 ± 0.42^{a}
180	38.20 ± 0.79^{b}	-10.20 ± 0.42^{d}	18.40 ± 0.79^{b}	119.01 ± 0.55^{ab}	21.03 ± 0.17^{b}
360	37.30 ± 0.50^{bc}	-9.50 ± 0.29^{cd}	17.90 ± 0.06^{bc}	117.95 ± 0.65^{bc}	20.26 ± 0.24^{bc}
540	36.50 ± 0.18^{cd}	-8.90 ± 0.01^{bc}	17.30 ± 0.28^{cd}	117.23 ± 0.38^{cd}	19.45 ± 0.06^{cd}
720	35.40 ± 0.84^{de}	-8.20 ± 0.25^{ab}	16.70 ± 0.13^{de}	116.15 ± 0.85^{d}	18.60 ± 0.18^{de}
900	34.20 ± 0.71^{e}	-7.90 ± 0.32^{a}	16.20 ± 0.50^{e}	115.99 ± 0.85^{d}	18.02 ± 0.18^{e}

Values with same superscript letters in the same column are nonsignificant at $p < 0.05$.

Table 4: Variation in biochemical parameters of Stevia leaves dried at different levels of microwave power.

Microwave power (W)	Steviol glycosides		Ascorbic acid (mg/100 g)	Total phenolic content (mg GAE/g)	Radical scavenging activity (inhibition %)
	Stevioside (mg/g)	Rebaudioside A (mg/g)			
Fresh leaves	12.56 ± 0.15^{a}	9.22 ± 0.29^{a}	25.30 ± 0.02^{a}	49.96 ± 0.09^{d}	79.09 ± 0.26^{a}
180	6.22 ± 0.21^{f}	4.97 ± 0.19^{f}	12.23 ± 0.48^{f}	41.19 ± 0.15^{f}	59.20 ± 0.13^{d}
360	7.71 ± 0.10^{e}	5.82 ± 0.11^{e}	15.35 ± 0.22^{e}	44.72 ± 0.36^{e}	50.14 ± 0.94^{e}
540	10.15 ± 0.53^{c}	7.11 ± 0.23^{c}	19.61 ± 0.70^{d}	52.54 ± 0.18^{c}	65.02 ± 0.70^{c}
720	11.84 ± 0.55^{b}	8.53 ± 0.01^{b}	21.75 ± 0.25^{b}	54.82 ± 0.09^{b}	69.55 ± 0.11^{bc}
900	9.01 ± 0.31^{d}	6.44 ± 0.24^{d}	20.89 ± 0.47^{c}	56.98 ± 0.03^{a}	74.22 ± 0.20^{b}

GAE: gallic acid equivalent and values with same superscript letters in the same column are nonsignificant at $p < 0.05$.

Similar findings related to the phenolic content degradation were reported for the microwave drying of kiwi slices [47]. With the increase of microwave power from 540 to 900 W, the total phenolic content increased from 52.54 to 56.98 mg GAE/g. This might be due to the reason that the increment in the microwave power generates high vapor pressure and temperature inside the tissue of plant which disrupts the polymer cell wall of plant and releases the phenolic components from cell walls along with bound phenolic compounds [48]. Similar trend of first decrease followed by an increase in the total phenolic content with increasing power was also observed in microwave drying of pineapple slices [49]. In another study on microwave drying of coriander leaves, the total phenolic content enhanced when the microwave was increased [50].

3.9. DPPH Radical Scavenging Activity. The change in the antioxidant capacity of the microwave-dried Stevia leaves obtained by using different microwave power is given in Table 4. The microwave drying significantly affected the radical scavenging activity of Stevia leaves. The DPPH inhibition percentages varied from 79.09 to 50.15%. Increasing the microwave power from 180 to 360 W led to the significant decrement in the radical scavenging activity of dried leaves in comparison to that of fresh leaves. The degradation of antioxidant compounds during drying is the cause of this decline. Similar decrement of antioxidant capacity was observed in the microwave drying of pineapples when microwave power was increased from 120 to 350 W [49]. In comparison to fresh Stevia leaves, the superior radical scavenging activity was observed at 900 W with a value of 74.22%. A nonsignificant difference was observed among the values of DPPH inhibition percentages at 540, 720, and 900 W. Similarly, the microwave drying of lemon myrtle leaves showed no significant difference for DPPH for three microwave power levels of 720 W, 960 W, and 1200 W [51]. For the microwave power above 360 W, the increase in the percentage of DPPH might be due to the growth of antioxidant characteristics of naturally formed components or products of the Maillard reaction with antioxidant activity [52].

4. Conclusion

Stevia leaves were dried in a microwave drier at different power levels (180, 360, 540, 720, and 900 W) to evaluate drying kinetics, effective moisture diffusivity, specific energy consumption, color changes, and biochemical attributes. The increase in the power levels led to the increment of dry rate and decrement of drying time. Regarding goodness of fit indices (R^2, χ^2, and RMSE), page model gave the best fit to the experimental data among five differently selected models. At all microwave power levels tested, this model predicted very well the moisture content as a function of drying time. The values of effective moisture diffusivity enhanced from 3.009×10^{-11} to 2.636×10^{-10} m^2/s with increment of the power level. Specific energy consumption (SEC) firstly increased and then decreased with increasing the power levels from 180 to 900 W. In order to describe microwave drying of Stevia leaves, a feed-forward artificial neural network using a backpropagation algorithm was also found to accurately predict the moisture content. The final selected model, 2-15-1 successfully showed the relationship between input and output parameters with $R^2 > 0.999$. The ANN has so demonstrated that it could be a viable substitute for Stevia leaves thin layer drying modelling due to its acceptable capabilities and simplicity. The color estimation demonstrated a significant ($p < 0.05$) change in color

parameters of microwave-dried leaves in comparison to fresh leaves, though a good green color was maintained. Moreover, color values of dried levels were not dependent on the power level. Stevia leaves dried at 720 W showed the highest content of stevioside (11.84 mg/g) and rebaudioside A (7.11 mg/g) and maximum (~86%) retention of ascorbic content. The highest total phenol content (56.98 mg GAE/g) and antioxidant capacity (74.22%) were observed in microwave-dried samples at 900 W.

Data Availability

All data pertaining to this work are available within the manuscript.

Conflicts of Interest

The authors declare that they have no conflicts of interest.

Authors' Contributions

Baldev Singh Kalsi was involved in investigation, conceptualization, methodology, formal analysis, software provision, writing of the original draft, data curation, and review and editing. Sandhya Singh was involved in conceptualization, methodology, supervision, project administration, validation, review, and editing. Mohammed Shafiq Alam was responsible for software provision, data curation, formal analysis, review, and editing. Surekha Bhatia was responsible for formal analysis, review, and editing.

Acknowledgments

The authors are thankful to AICRP (All India Coordinated Research Project) on Post-Harvest Engineering & Technology for financial assistance. The authors also like to thank the Punjab Agricultural University for facilities.

References

[1] P. Samuel, K. T. Ayoob, B. A. Magnuson et al., "Stevia leaf to stevia sweetener: exploring its science, benefits, and future potential," *The Journal of Nutrition*, vol. 148, no. 7, pp. 1186S–1205S, 2018.

[2] A. Periche, M. L. Castelló, A. Heredia, and I. Escriche, "Influence of drying method on steviol glycosides and antioxidants in Stevia rebaudiana leaves," *Food Chemistry*, vol. 172, pp. 1–6, 2015.

[3] M. Castillo Téllez, I. Pilatowsky Figueroa, B. Castillo Téllez, E. C. López Vidaña, and A. López Ortiz, "Solar drying of Stevia (Rebaudiana Bertoni) leaves using direct and indirect technologies," *Solar Energy*, vol. 159, pp. 898–907, 2018.

[4] A. Arslan Kulcan and M. Karhan, "Effect of process parameters on stevioside and rebaudioside A content of stevia extract obtained by decanter centrifuge," *Journal of Food Processing and Preservation*, vol. 45, no. 2, Article ID e15168, 2021.

[5] Y. K. Khodja, F. Dahmoune, M. Bachir bey, K. Madani, and B. Khettal, "Conventional method and microwave drying kinetics of *Laurus nobilis* leaves: effects on phenolic compounds and antioxidant activity," *Brazilian Journal of Food Technology*, vol. 23, 2020.

[6] S. Çelen, "Effect of microwave drying on the drying characteristics, color, microstructure, and thermal properties of trabzon persimmon," *Foods*, vol. 8, no. 2, p. 84, 2019.

[7] P. P. Potdar, P. Kaur, R. Zalpouri, and V. Ummat, "Convective and pulsed microwave drying of lemongrass (Cymbopogon citratus) shreds: kinetic modeling, retention of bio-actives, and oil yield," *Journal of Food Processing and Preservation*, vol. 46, no. 12, 2022.

[8] R. Pandiselvam, K. B. Hebbar, M. R. Manikantan, B. K. Prashanth, S. Beegum, and S. V. Ramesh, "Microwave treatment of coconut inflorescence sap (Kalparasa®): a panacea to preserve quality attributes," *Sugar Tech*, vol. 22, no. 4, pp. 718–726, 2020.

[9] P. Guzik, P. Kulawik, M. Zając, and W. Migdał, "Microwave applications in the food industry: an overview of recent developments," *Critical Reviews in Food Science and Nutrition*, vol. 62, 2021.

[10] R. Pandiselvam, Y. Tak, E. Olum et al., "Advanced osmotic dehydration techniques combined with emerging drying methods for sustainable food production: impact on bioactive components, texture, color, and sensory properties of food," *Journal of Texture Studies*, vol. 53, no. 6, pp. 737–762, 2022.

[11] P. Yilmaz, E. Demirhan, and B. Özbek, "Microwave drying effect on drying characteristic and energy consumption of Ficus carica Linn leaves," *Journal of Food Process Engineering*, vol. 44, Article ID e13831, 2021.

[12] A. Y. Aydar, T. Aydın, T. Yılmaz et al., "Investigation on the influence of ultrasonic pretreatment on color, quality and antioxidant attributes of microwave dried Inula viscosa (L.)," *Ultrasonics Sonochemistry*, vol. 90, Article ID 106184, 2022.

[13] N. Kutlu, R. Pandiselvam, I. Saka, A. Kamiloglu, P. Sahni, and A. Kothakota, "Impact of different microwave treatments on food texture," *Journal of Texture Studies*, vol. 53, no. 6, pp. 709–736, 2022.

[14] T. P. Krishna Murthy and B. Manohar, "Microwave drying of mango ginger (Curcuma amada Roxb): prediction of drying kinetics by mathematical modelling and artificial neural network," *International Journal of Food Science and Technology*, vol. 47, no. 6, pp. 1229–1236, 2012.

[15] J.-W. Bai, H.-W. Xiao, H.-L. Ma, and C.-S. Zhou, "Artificial neural network modeling of drying kinetics and color changes of ginkgo biloba seeds during microwave drying process," *Journal of Food Quality*, vol. 2018, Article ID 3278595, 8 pages, 2018.

[16] R. Pandiselvam, V. Prithviraj, M. R. Manikantan et al., "Central composite design, Pareto analysis, and artificial neural network for modeling of microwave processing parameters for tender coconut water," *Measurement: Food*, vol. 5, Article ID 100015, 2022.

[17] Y. Srinivas, S. M. Mathew, A. Kothakota, N. Sagarika, and R. Pandiselvam, "Microwave assisted fluidized bed drying of nutmeg mace for essential oil enriched extracts: an assessment of drying kinetics, process optimization and quality," *Innovative Food Science & Emerging Technologies*, vol. 66, Article ID 102541, 2020.

[18] P. K. Nayak, C. M. Chandrasekar, and R. K. Kesavan, "Effect of thermosonication on the quality attributes of star fruit juice," *Journal of Food Process Engineering*, vol. 41, no. 7, Article ID e12857, 2018.

[19] K. Mouhoubi, L. Boulekbache-Makhlouf, N. Guendouze-Bouchefa, M. L. Freidja, A. Romero, and K. Madani, "Modelling of drying kinetics and comparison of two processes: forced convection drying and microwave drying of

celery leaves (*Apium graveolens* L.)," *The Annals of the University Dunarea de Jos of Galati*, vol. 43, pp. 48–69, 2019.
[20] N. A. Samad, D. N. A. Zaidel, I. I. Muhama, Y. M. M. Jusoh, and N. A. Yunus, "Influence of microwave drying on the properties of Moringa oleifera leaves," *Chemical Engineering Transactions*, vol. 89, pp. 469–474, 2021.
[21] T. Pradechboon, N. Dussadee, Y. Unpaprom, and S. Chindaraksa, "Effect of rotary microwave drying on quality characteristics and physical properties of Kaffir lime leaf (Citrus hystrix D.C.)," *Biomass Conversion and Biorefinery*, pp. 1–10, 2022.
[22] A. Sarimeseli, M. A. Coskun, and M. Yuceer, "Modeling microwave drying kinetics of thyme (*thymus vulgaris* L.) leaves using ANN methodology and dried product quality," *Journal of Food Processing and Preservation*, vol. 38, no. 1, pp. 558–564, 2014.
[23] M. Fathi, S. Roshanak, M. Rahimmalek, and S. A. H. Goli, "Thin-layer drying of tea leaves: mass transfer modeling using semi-empirical and intelligent models," *International Food Research Journal*, vol. 23, pp. 40–46, 2016.
[24] M. A. A. Gasmalla, R. Yang, I. Amadou, and X. Hua, "Nutritional composition of *Stevia rebaudiana* Bertoni leaf: effect of drying method," *Tropical Journal of Pharmaceutical Research*, vol. 13, no. 1, pp. 61–65, 2014.
[25] R. Lemus-Mondaca, A. Vega-Gálvez, P. Rojas et al., "Antioxidant, antimicrobial and anti-inflammatory potential of Stevia rebaudiana leaves: effect of different drying methods," *Journal of Applied Research on Medicinal and Aromatic Plants*, vol. 11, pp. 37–46, 2018.
[26] Aoac, *Official Methods of Analysis of AOAC International - 20th Edition*, AOAC, Rockville, MD, USA, 20th edition, 2016.
[27] A. Surendhar, V. Sivasubramanian, D. Vidhyeswari, and B. Deepanraj, "Energy and exergy analysis, drying kinetics, modeling and quality parameters of microwave-dried turmeric slices," *Journal of Thermal Analysis and Calorimetry*, vol. 136, no. 1, pp. 185–197, 2018.
[28] K. Kaur, S. Kumar, and M. S. Alam, "Air drying kinetics and quality characteristics of oyster mushroom (Pleurotus ostreatus) influenced by osmotic dehydration," *Agricultural Engineering International: CIGR Journal*, vol. 16, pp. 214–222, 2014.
[29] B. S. Kalsi, S. Singh, and M. S. Alam, "Influence of ultrasound processing on the quality of guava juice," *Journal of Food Process Engineering*, Article ID e14163, 2022.
[30] Z. Ai, H. Ren, Y. Lin et al., "Improving drying efficiency and product quality of Stevia rebaudiana leaves using innovative medium-andshort-wave infrared drying (MSWID)," *Innovative Food Science & Emerging Technologies*, vol. 81, Article ID 103154, 2022.
[31] N. Hidar, M. Ouhammou, S. Mghazli et al., "The impact of solar convective drying on kinetics, bioactive compounds and microstructure of stevia leaves," *Renewable Energy*, vol. 161, pp. 1176–1183, 2020.
[32] S. Şahin, E. Elhussein, M. Bilgin, J. M. Lorenzo, F. J. Barba, and S. Roohinejad, "Effect of drying method on oleuropein, total phenolic content, flavonoid content, and antioxidant activity of olive (Olea europaea) leaf," *Journal of Food Processing and Preservation*, vol. 42, no. 5, Article ID e13604, 2018.
[33] M. Younis, D. Abdelkarim, and A. Zein El-Abdein, "Kinetics and mathematical modeling of infrared thin-layer drying of garlic slices," *Saudi Journal of Biological Sciences*, vol. 25, no. 2, pp. 332–338, 2018.
[34] K. Rayaguru and W. Routray, "Effect of drying conditions on drying kinetics and quality of aromatic Pandanus amaryllifolius leaves," *Journal of Food Science and Technology*, vol. 47, no. 6, pp. 668–673, 2010.
[35] A. Sarimeseli, "Microwave drying characteristics of coriander (Coriandrum sativum L.) leaves," *Energy Conversion and Management*, vol. 52, no. 2, pp. 1449–1453, 2011.
[36] Y. Soysal, "Microwave drying characteristics of parsley," *Biosystems Engineering*, vol. 89, no. 2, pp. 167–173, 2004.
[37] Y. Soysal, O. Serdar, and O. Eren, "Microwave drying kinetics of thyme," *International Journal of Food Science and Technology*, vol. 38, 2015.
[38] M. Torki-Harchegani, D. Ghanbarian, A. Ghasemi Pirbalouti, and M. Sadeghi, "Dehydration behaviour, mathematical modelling, energy efficiency and essential oil yield of peppermint leaves undergoing microwave and hot air treatments," *Renewable and Sustainable Energy Reviews*, vol. 58, pp. 407–418, 2016.
[39] K. Altay, A. A. Hayaloglu, and S. N. Dirim, "Determination of the drying kinetics and energy efficiency of purple basil (Ocimum basilicum L.) leaves using different drying methods," *Heat and Mass Transfer*, vol. 55, no. 8, pp. 2173–2184, 2019.
[40] M. Beigi and M. Torki, "Experimental and ANN modeling study on microwave dried onion slices," *Heat and Mass Transfer*, vol. 57, no. 5, pp. 787–796, 2021.
[41] E. Taghinezhad, M. Kaveh, A. Jahanbakhshi, and I. Golpour, "Use of artificial intelligence for the estimation of effective moisture diffusivity, specific energy consumption, color and shrinkage in quince drying," *Journal of Food Process Engineering*, vol. 43, no. 4, p. 2020, 2020.
[42] R. Lemus-Mondaca, K. Ah-Hen, A. Vega-Gálvez, C. Honores, and N. O. Moraga, "Stevia rebaudiana leaves: effect of drying process temperature on bioactive components, antioxidant capacity and natural sweeteners," *Plant Foods for Human Nutrition*, vol. 71, no. 1, pp. 49–56, 2016.
[43] X. Huang, W. Li, Y. Wang, and F. Wan, "Drying characteristics and quality of Stevia rebaudiana leaves by far-infrared radiation," *Lebensmittel-Wissenschaft und -Technologie*, vol. 140, Article ID 110638, 2021.
[44] I. A. Ozkan, B. Akbudak, and N. Akbudak, "Microwave drying characteristics of spinach," *Journal of Food Engineering*, vol. 78, no. 2, pp. 577–583, 2007.
[45] I. Alibas, "Microwave, vacuum, and air drying characteristics of collard leaves," *Drying Technology*, vol. 27, no. 11, pp. 1266–1273, 2009.
[46] M. A. Ali, Y. A. Yusof, N. L. Chin, and M. N. Ibrahim, "Effect of different drying treatments on colour quality and ascorbic acid concentration of guava fruit," *International Food Research Journal*, vol. 23, pp. S155–S161, 2016.
[47] N. Izli, G. Izli, and O. Taskin, "Drying kinetics, colour, total phenolic content and antioxidant capacity properties of kiwi dried by different methods," *Journal of Food Measurement and Characterization*, vol. 11, no. 1, pp. 64–74, 2016.
[48] I. Hamrouni-Sellami, F. Z. Rahali, I. B. Rebey, S. Bourgou, F. Limam, and B. Marzouk, "Total phenolics, flavonoids, and antioxidant activity of sage (salvia officinalis L.) plants as affected by different drying methods," *Food and Bioprocess Technology*, vol. 6, no. 3, pp. 806–817, 2012.
[49] N. Izli, G. Izli, and O. Taskin, "Impact of different drying methods on the drying kinetics, color, total phenolic content and antioxidant capacity of pineapple," *CyTA - Journal of Food*, vol. 16, no. 1, pp. 213–221, 2018.
[50] K. Mouhoubi, L. Boulekbache-Makhlouf, W. Mehaba, H. Himed-Idir, and K. Madani, "Convective and microwave drying of coriander leaves: kinetics characteristics and

modeling, phenolic contents, antioxidant activity, and principal component analysis," *Journal of Food Process Engineering*, vol. 45, no. 1, Article ID e13932, 2022.

[51] M. Saifullah, R. McCullum, A. McCluskey, and Q. Vuong, "Effects of different drying methods on extractable phenolic compounds and antioxidant properties from lemon myrtle dried leaves," *Heliyon*, vol. 5, no. 12, Article ID e03044, 2019.

[52] A. Ö. Karabacak, S. Suna, C. E. Tamer, and Ö. Çopur, "Effects of oven, microwave and vacuum drying on drying characteristics, colour, total phenolic content and antioxidant capacity of celery slices," *Quality Assurance and Safety of Crops & Foods*, vol. 10, no. 2, pp. 193–205, 2018.